

SAE Formula Powertrain

Design Report 2

**Marshall Fritz
Trent Greene
Jackson Nichols
Liam O'Connor
Aidan Willson**

Fall 2025-Spring 2026



Project Sponsors: Gore, Flagstaff Chevrolet, SFA Architects, JGGM Engineering

Faculty Advisor: Perry Wood

Instructor, Faculty Advisor: David Willy

Industry Advisor: Keith Wilson & David Kieke

DISCLAIMER

This report was prepared by students as part of a university course requirement. While considerable effort has been put into the project, it is not the work of licensed engineers and has not undergone the extensive verification that is common in the profession. The information, data, conclusions, and content of this report should not be relied on or utilized without thorough, independent testing and verification.

University faculty members may have been associated with this project as advisors, sponsors, or course instructors, but as such they are not responsible for the accuracy of results or conclusions.

EXECUTIVE SUMMARY

Northern Arizona University's SAE Formula team is currently designing an open wheeled race car to compete in the SAE race in May 2026. Throughout the course of this semester, we aim to finish most of the design work and end with a full frame welded by the start of next semester.

The powertrain sub team has evaluated several different approaches to the car this year. Instead of using the Honda CBR600 4-cylinder motor, we have elected to pick a lighter 2-cylinder engine. While we are purchasing an engine, there are several other design challenges to consider. Per FSAE rules, there is a 20 mm intake restrictor diameter that we must hit, which presents a host of factors to consider with our intake design. We also must design an exhaust system, chain and final drive, cooling, and fuel delivery.

We have purchased a Kawasaki Versys engine, which will aid the 2026 car in weight reduction. From there, we will be able to determine important exhaust and intake parameters that would simply be guesses in the current state of the project. We will be manufacturing a bell nozzle restrictor throat, have purchased a Taylor Mk2 differential and the subsequent sprockets with a mid-range ratio. We will purchase pre-fab axles that are already cut to size. We will likely purchase high compression pistons (13.5 CR) for increased power, as well as converting to a Kawasaki 650R head to increase performance. Going forward, there is a lot of research, calculations, and design work we must do before we can put the powertrain together.

We have begun to work with Keith Wilson of Wilson Manifolds and David Kieke of Taylor Race Engineering as industry advisors. These individuals and their respective companies have provided critical insight, and our team will continue to consult these advisors when necessary.

With Prototype Demo 2 approaching, we would like to begin to flow test 3D printed intake manifold prototypes and begin bench testing the Versys engine.

TABLE OF CONTENTS

Table of Contents

DISCLAIMER.....	1
EXECUTIVE SUMMARY.....	2
TABLE OF CONTENTS	3
1 BACKGROUND.....	1
1.1 PROJECT DESCRIPTION	1
1.2 DELIVERABLES	1
1.3 SUCCESS METRICS	2
2 REQUIREMENTS	2
2.1 CUSTOMER REQUIREMENTS (CRS).....	2
2.2 ENGINEERING REQUIREMENTS (ERs)	2
2.2 HOUSE OF QUALITY (HOQ)	3
3 RESEARCH WITHIN YOUR DESIGN SPACE	4
3.1 BENCHMARKING.....	4
3.2 LITERATURE REVIEW.....	4
3.3 MATHEMATICAL MODELING	12
3.3.1 <i>Theoretical Top Speed Calculations – Aidan Willson and Trent Greene</i>	12
3.3.2 <i>Intake Restrictor Max Flow Rate – Liam O’Connor</i>	15
3.3.3 <i>Intake Restrictor Geometry – Liam O’Connor</i>	17
3.3.4 <i>Intake Restrictor CFD Testing – Trent Greene</i>	19
3.3.5 <i>Engine Horsepower Restriction – Liam O’Connor</i>	22
3.3.6 <i>Exhaust System – Marshall Fritz</i>	23
3.3.7 <i>High Compression Piston Comparison – Aidan Willson</i>	27
3.3.8 <i>Axle Stress Calculations – Jackson Nichols</i>	30
3.3.9 <i>Fuel Tank Capacity – Jackson Nichols</i>	30
4 DESIGN CONCEPTS	31
4.1 FUNCTIONAL DECOMPOSITION.....	31
4.2 CONCEPT GENERATION	32
4.3 SELECTION CRITERIA.....	36
4.4 CONCEPT SELECTION	37
5 SCHEDULE AND BUDGET.....	38
5.1 SCHEDULE	38
5.2 BUDGET.....	40
5.3 BILL OF MATERIALS	41
6 DESIGN VALIDATION.....	41
6.1 FAILURE MODES AND EFFECTS ANALYSIS	41
6.2 INITIAL PROTOTYPING	44
6.2.1 <i>Engine Analyzer Pro Dynamometer Simulation</i>	44
6.2.2 <i>Intake Restrictor</i>	47
6.2.3 <i>3D Print of Eccentric Differential Mount</i>	48
6.3 ENGINEERING CALCULATIONS.....	50
6.3.1 <i>SolidWorks Differential Mount Variations</i>	50

6.3.2	<i>Tulip CV Joint Analysis</i>	56
6.3.3	<i>Radiator Fin Area</i>	58
6.3.4	<i>Exhaust Manifold Analysis</i>	62
6.3.5	<i>Camshaft Profile</i>	63
6.3.6	<i>SolidWorks Internal Flow Simulation</i>	66
6.3.7	<i>Motor Mount Tube Thickness</i>	69
6.4	70
7	REFERENCES.....	71
8	APPENDICES	75
8.1	APPENDIX A: FIGURES	75
8.2	APPENDIX B: TABLES.....	88
8.3	APPENDIX C: EQUATIONS	89
8.4	APPENDIX D: MATLAB.....	94

1 BACKGROUND

1.1 Project Description

The Society of Automotive Engineers Formula (FSAE) competition is a student-led event in which a team of mechanical and electrical engineering students design, build, and race an open wheeled car. The FSAE project gives students in-depth, hands-on experience with every level of automotive engineering. Written in the rules of the FSAE competition, there are countless design constraints that offer unique engineering challenges to be evaluated at the event.

The clients for this project include NAU's Sanghi College of Engineering, SAE, our sponsors, and our faculty advisors, David Willy and Perry Wood.

1.2 Deliverables

A short summary of Course, Customer, and Competition deliverables for the semester.

<u>Deliverables:</u>	<u>Due:</u>
Team Charter v1	4-Sep
Create Gantt Chart	30-Sep
Presentation 1	18-Sep
Peer Eval #1	19-Sep
Make Fundraising Flyer	19-Sep
Make Go Fund Me Post	22-Sep
Start Fundraising	Ongoing
Realis Picture, Email, and LinkedIn Post	26-Sep
Presentation #2 Calculations	7-Oct
Presentation #2	9-Oct
Competition Registration	24-Oct
Website Check #1	24-Oct
Buy Engine	31-Oct
Presentation #3	6-Nov
Prototype Demo #1	13-Nov
Peer Eval #3	14-Nov
Report #2	26-Nov
Prototype Demo #2	4-Dec
Final CAD and Final BOM	5-Dec
Project Management for 486C	6-Dec
Website Check #2	6-Dec
Peer Eval #4	7-Dec
Comp. Tech 26 Notice Form	8-Dec

1.3 Success Metrics

NAU FSAE's success in 2026 will be evaluated by, above all else, our ability to compete. The NAU team has been selected in the competition lottery, and the main goal is to pass the technical inspection at the event. In the competition, important metrics will be acceleration, top-end speed, handling, and durability. If we can be within 20% of the best time for each race, we would consider ourselves successful.

A longer-term goal beyond this year's project is to further the capabilities of NAU's FSAE for future teams. This means we will spend any extra cashflow toward outfitting the space in which we work to increase self-reliance and manufacturability. Furthermore, we will help future teams by having the 2026 team's struggles and successes documented and available within the NAU network.

2 Requirements

To ensure success and contentment among customers, the project must be broken down into goals tailored towards the customer's needs. These goals are then defined by specific and quantifiable engineering requirements chosen to give structure to the design process, making it more efficient and giving the design the best chance at being exceptional.

2.1 Customer Requirements (CRs)

The 2026 FSAE took the advice from 2025 team members and advisors to establish a list of customer requirements. These were mainly based on the pitfalls of the previous team, which could not compete at the Michigan International speedway due to a few design oversights.

- Pass Tech Inspection
- Reliable/Durable
- Safe
- Limited slip rear power delivery
- Ease of maintenance
- Drivability
- Standardized parts
- More accessible fuel fill
- Lightweight

2.2 Engineering Requirements (ERs)

These same requirements can be into quantifiable targets, shown below.

- Idle exhaust noise under 98 dbC. (103 is passing)
- Reduce weight of muffler (kg)
- Remove mass from intake manifold (kg)

- Minimize mechanical loss testing (hp)
- Decrease Distance of fuel fill to outermost frame rail (mm)
- Robust throttle cable with 50mm of adjustment (mm)

2.2 House of Quality (HoQ)

System QFD: Powertrain				Project: QFD Date: 09/14/25										
1	Engine noise less than 103 Dbc													
2	Reduce weight of muffler		+											
3	Remove mass from intake manifold													
4	Minimize mechanical loss testing		+	++										
5	Obtain LSD with smallest impact on budget													
6	Decrease distance from fuel fill to outermost frame rail													
7	Robust throttle cable with 50mm of adjustment			+										
		Legend A 2001 CBR600 F4i B 2012 Kawi Ninja 650R C 2014 Yamaha YZ450F												
		Technical Requirements						Customer Opinion Survey						
		Customer Weights (1-5)	Engine noise less than 103 Dbc	Reduce weight of muffler	Remove mass from intake manifold	Minimize mechanical loss testing	Obtain LSD with smallest impact on budget	Decrease distance from fuel fill to outermost frame rail	Robust throttle cable with 50mm of adjustment	1 Poor	2	3 Acceptable	4	5 Excellent
Customer Needs														
1	Pass Tech Inspection	5	9	1	1	9	1	1	9	ABC				
2	Reliable/Durable	4	1	1	3	9	3	1	9	B AC				
3	Safe	5	3	1	1	9	3	3	9	AB C				
5	Limited slip rear power delivery	3	1	1	1	9	9	1	1	ABC				
6	Ease of maintenance	3	1	3	3	1	1	3	3	A B C				
7	Drivability	3	1	3	3	3	9	1	9	AB C				
8	Standardized parts	4	3	1	1	1	3	1	3	ABC				
10	Make filling up fuel more accessible	5	1	1	3	1	1	9	1	A BC				
11	Lightweight car	3	1	1	9	1	1	1	1	ABC				
Technical Requirement Units			dbc	kg	kg	hp	\$	mm closer	mm					
Technical Requirement Targets			5	4	2	8	###	100	50					
Absolute Technical Importance			93	47	89	177	109	91	185					
Relative Technical Importance			11.8%	6%	11.3%	22%	14%	12%	23%					

Figure 2-1 - QFD

Based on the most important customer needs for the car, we applied engineering requirements that will ensure that each of the customers' requirements are satisfied. Each of the engineering requirements were then ranked with respect to the customer requirements to give a percentage of importance to each of the

engineering requirements. The top two engineering requirements came out to robust throttle cable with 50mm of adjustment and minimized mechanical loss testing. This helps us emphasize our efforts on the more important aspects of design, which will help ensure that the car is finished on time, and finished with the adequacy of the customer.

3 Research Within Your Design Space

3.1 Benchmarking

Engine	2001 Honda CBR600 F4i [1]	2012 Kawi Ninja 650R [2]	2014 Yamaha YZ450f [3]
<i>Stock Hp</i>	<i>110 Hp @ 12,500 rpm</i>	<i>72.1 Hp @ 8,500 rpm</i>	<i>58 Hp @ 9,900 rpm</i>
<i>Weight (lbs)</i>	<i>Heaviest</i>	<i>Medium</i>	<i>Lightest</i>
<i>Displacement (cc)</i>	<i>599</i>	<i>649</i>	<i>449</i>
<i>Peak Torque (lb-ft) (RPM)</i>	<i>48 lb-ft @ 10,500 rpm</i>	<i>48.6 lb-ft @ 7,000 rpm</i>	<i>35 lb-ft @ 7,300 rpm</i>

Table 3-1 - Engine Specifications

Differential	Taylor Race Engineering V2 [4]	Drexler V2/V3 [5]	Modified ATV [6]
<i>Cost</i>	<i>\$2,450</i>	<i>\$3,656</i>	<i>~\$500</i>
<i>Weight (lbs)</i>	<i>8.9</i>	<i>5.9</i>	<i>11-21</i>
<i>Further Drivetrain Support (Y/N)</i>	<i>Y</i>	<i>Y</i>	<i>N</i>

Table 3-2 - Differential Specifications

3.2 Literature Review

Aidan Willson

[1] SAE International, Formula SAE Rules 2025-v1, IC.1: “General Requirements”, VE.3: “Driver Equipment”, 31 Aug, 2025

-General engine requirements for designing powertrain, max displacement, driver requirements for safety equipment.

[2] T. D. Gillespie, S. Taheri, C. Sandu, and B. L. Duprey, *Fundamentals of Vehicle Dynamics*. Warrendale, PA: SAE International, 2021.

Book used for calculating: Chapter 2: Theoretical Mechanical Top Speed based on gear ratios.

[3] “2015 Kawasaki Ninja 650 6,” *Scribd*, 2015. <https://www.scribd.com/document/776296988/2015-Kawasaki-Ninja-650-6> (accessed Sep. 14, 2025).

-Kawasaki Ninja 650 Service manual for obtaining gear ratios used in calculations. Specific ratios for each gear in the transmission and final drive ratio.

[4] K. Lutenbacher, B. Mayeaux, and J. Waller, “FSAE Engine Selection: Four or One Cylinder.” Available: https://korilutenbacher.weebly.com/uploads/5/4/9/9/5499743/klutenbacher_bmayeaux_jwaller_me4633_fsa_report.pdf

-LSU Formula SAE engine selection from 2012, used as a reference for some basic calculations and their overall selection process for their drivetrain.

[5] MotorTrend Channel, “BIG Power from Small Block Engines! | Engine Masters | MotorTrend,” *YouTube*, Jul. 15, 2023. <https://www.youtube.com/watch?v=WAwXPMUe9JE> (accessed Sep. 10, 2025)

-YouTube Video about generating more power from smaller blocks such as a 4-cylinder engine. Useful for future modifications to our engine and ideal components to swap out.

[6] “Formula SAE 2025 Overall Results.” Accessed: Sep. 10, 2025. [Online]. Available: https://www.fsaeonline.com/CompResources/2025/c796a916-c2e8-4ce6-bae3-c79f36776556/FSAE_2025_MI5_results.pdf

-2025 formula results to benchmark (Not much out there), found some research from 2nd place Texas A&M but from 2005.

[7] B. Singh, “- Race Car Vehicle Dynamics Milliken Milliken,” *Scribd*, 2025. <https://www.scribd.com/document/858209436/Race-Car-Vehicle-Dynamics-Milliken-Milliken>

-Powertrain dynamics, more information on differentials and the various kinds we might select from for our design.

[8] V. R. J. Parikh, “Design and Analysis of Differential Mounts for K4,” [Online]. Available: <https://vrjparikh.github.io/data/eccentric.pdf>. [Accessed: Nov. 2, 2025].

-Design report of a differential mount that was beneficial to see what had previously been done and their process for solving for chain tensions and forces on the mount.

[9] "<Creating a differential holder for FSAE Cars>," YouTube, [Online]. Available: <https://www.youtube.com/watch?v=bhZukV4lAiw&t=573s>. [Accessed: Nov. 2, 2025].

-Helpful SolidWorks tutorial for the basic design process of a differential holder, obtaining pick up points for the frame, ultimately decided to mount to engine.

[10] S. K. Sahu and R. K. Sahu, "Design and Analysis of Eccentric Cam with Roller Follower," International Research Journal of Engineering and Technology (IRJET), vol. 7, no. 10, pp. 1830–1835, Oct. 2020. [Online]. Available: <https://www.irjet.net/archives/V7/i10/IRJET-V7I10283.pdf>. [Accessed: Nov. 3, 2025].

-Report for Eccentric design for differential of previous FSAE car from 2020. Gave some details on the locking of eccentric rings and their teams weight saving designs.

Liam O'Connor

[11] J. B. Heywood, "Chapter 14: Modeling Real Engine Flow and Combustion Processes," in *Internal Combustion Engine Fundamentals*, 2nd ed, McGraw Hill Education, 2018

-Background on methods for modeling engine flow

[12] SAE International, Formula SAE Rules 2026-Draft, IC.2: "Air Intake System" , 11 Aug, 2025

- Formula rules governing restrictor diameter

[13] F. Leach, "The scope for improving the efficiency and environmental impact of internal combustion engines - sciencedirect," ScienceDirect, <https://www.sciencedirect.com/science/article/pii/S2666691X20300063> (accessed Sep. 18, 2025).

- Engine Thermal Efficiency

[14] "Mass flow choking," NASA, <https://www.grc.nasa.gov/www/k-12/airplane/mflchk.html> (accessed Sep. 18, 2025).

- Max choked flow rate formula and calculation process

[15] R. Stone, "Chapter 6: Induction and Exhaust Processes," in *Introduction to Internal Combustion Engines*, 2nd ed, SAE Inc., 1993, pp. 231–274

- Internal Combustion Engine Compressible Flow basics

[16] D. Willy, "Formula SAE Restrictor Power Calculations." Northern Arizona University, Flagstaff, 2024

- Fundamentals for the max restrictor flow calculation

[17] R. Nakka, "Solid Rocket Motor Theory -- Nozzle Theory," Richard Nakka's Experimental Rocketry Site, https://www.nakka-rocketry.net/th_nozz.html (accessed Sep. 18, 2025).

- Theory for modeling ideal intake restrictor geometry based on a rocket nozzle.

[18] Kawasaki Versys Manual, Kawasaki Heavy Industries, 2007.

- Kawasaki Manual for engine specs

[19] *Introduction to Cams, Mechanical Reference*, [Online]. Available: <https://www.mechref.org/md/Cams/>. [Accessed: 25-Nov-2025].

- Camshaft profile fundamentals

[20] *SolidWorks Flow Simulation Transient Pressure Pulse, GoEngineer*, [Online]. Available: <https://www.goengineer.com/videos/solidworks-flow-simulation-transient-pressure-pulse>. [Accessed: 25-Nov-2025].

- Example for SolidWorks CFD simulation

Trent Greene

[21] "Figure 4: Drag and Lift coefficients of a FSAE car with different...", *ResearchGate*, 2024. https://www.researchgate.net/figure/Drag-and-Lift-coefficients-of-a-FSAE-car-with-different-aerodynamic-packages_fig13_320556659

Research from University of Southampton about drag and lift approximations for non-specific FSAE geometries.

[22] Caleb's Engineering Projects, "Calculate Top Speed and 0-60 of an Electric Racecar (FSAE)," *YouTube*, Sep. 08, 2020. <https://www.youtube.com/watch?v=pkWBeQO-0A8> (accessed Sep. 18, 2025).

Former FSAE Engineer series on the basics of design and calculations.

[23] Martin, "Engineering SPROCKET ENGINEERING DATA." Available: <https://www.martinsprocket.com/docs/catalogs/engineering/engineering%20catalog/sprocket-engineering-data.pdf>

Manufacturer catalog with specifications and standards for varying sprocket designs.

[24] Tsubaki, "The Complete Guide to Chain." Available: <https://www.ustsubaki.com/wp-content/uploads/the-complete-guide-1.pdf>

Manufacturer data on chain design, including force and standards specifications.

[25] E. Neumann, "Power Limited," *hpwizard.com*. <https://hpwizard.com/accelerating-power-limit.html>

Basic power limit theory equations and explanation pertaining to tire traction and aerodynamic performance.

[26]FSAE, “FSAE Rulebook 2026 T5,” *Fsaeonline.com*, 2025.

<https://www.fsaeonline.com/cdswb/gen/DownloadDocument.aspx?DocumentID=7ac1fb19-75d1-42d7-983d-ba9cd87fd092>

FSAE rule specifications about sprocket, chain, and splash guards.

[27]E. Oberg, F. Jones, H. Horton, H. Ryffel, C. Mccauley, and N. York, “Machinery’s Handbook 29 th Edition INDUSTRIAL PRESS,” 2012. Available:

<https://dl.icdst.org/pdfs/files4/80364b03673ba30eb5ccf1e27e119ffc.pdf>

Machinery handbook, used for chain and sprocket information.

[28] A. Schirn, “ASME B29.28-2015 (R2020): High-Strength Roller Chains - ANSI Blog,” *The ANSI Blog*, Sep. 08, 2023. <https://blog.ansi.org/ansi/asme-b29-28-2015-r2020-high-strength-roller-chains> (accessed Sep. 19, 2025).

ASME and ANSI chain standards.

[29] “All EPA Emission Standards | US EPA,” *US EPA*, Mar. 04, 2025. <https://www.epa.gov/emission-standards-reference-guide/all-epa-emission-standards>

[30] “J300_202405: Engine Oil Viscosity Classification - SAE International,” *Sae.org*, 2024. https://www.sae.org/standards/content/j300_202405/

[31]]Protolabs, “UL 94 Classification and Flame-Retardant Materials,” *Protolabs.com*, Apr. 14, 2017. <https://www.protolabs.com/resources/blog/flame-retardant-thermoplastics-and-ul-classifications> (accessed Sep. 19, 2025).

[32] ASTM International, ASTM D2700-22: Standard Test Method for Motor Octane Number of Spark-Ignition Engine Fuel, West Conshohocken, PA, USA: ASTM International, 2022

Marshall Fritz

[33] G. Blair, *Design and Simulation of Four-Stroke Engines*, SAE International, 1999.

Foundational textbook information on 4-stroke engine design. Provides a foundation in thermodynamics, combustion, and performance parameters to know the complete engine modeling for the NAU FSAE.

[34] A. Graham Bell, *Four-Stroke Performance Tuning*, 4th Edition, 2022.

Practical guide to tuning four stroke engines, intake and exhaust optimization strategies relevant to improving volumetric efficiency and torque in small racing engines.

[35] Y. Otobe, O. Goto, H. Miyano, M. Kawamoto, A. Aoki, and T. Ogawa, "Honda Formula One Turbocharged V6 1.5L Engine," SAE Technical Papers, Feb. 1989, doi: 10.4271/890877.

Technical document concerning a turbocharged Formula One engine. Provides analysis of high-performance exhaust and intake design principles relevant to compact FSAE engines.

[36] V. Sharma, S. Hittalamane, P. Gunjal, and G. Edison, "Exhaust Header Designing for Formula SAE Car," 2017.

Approaches for designing FSAE exhaust headers. Includes computations for runner diameter, length, and wave tuning. Applies directly to the NAU FSAE exhaust runner design.

[37] D. Kennedy and G. Woods, "Development of a New Air Intake and Exhaust System for a Single Seat Race Car," ITRN, 2011.

Describes the development of intake and exhaust systems for a small race car, focusing on volumetric efficiency and eliminating back pressure. Provides information to guide design development of runner sizing.

[38] S. Mangukiya and R. Shah, "Enhancing the Performance of Single Cylinder Motorcycle Engine for Formula Student Vehicle by Optimizing Intake and Exhaust System," JETIR, Vol. 5, Issue XX.

Discusses the optimization of intake and exhaust for a single-cylinder motorcycle engine and provides engineering techniques to size and balance airflow relative to the NAU FSAE exhaust design.

[39] A. Sayyed, "Air Flow Optimization through an Intake System for a Single Cylinder Formula Student FSAE Race Car," IJERT, Vol. 6, Issue 01.

Focuses on airflow optimization relating to intake aspect of exhaust design process. Provides information to maximize engine performance and efficiency.

[344] P. H. Smith and J. C. Morrison, *Scientific Design of Exhaust and Intake Systems*, 3rd ed., R. Bentley, 1971.

Important work created on exhaust and intake system design. Provides a detailed methodology to calculate runner lengths, diameters, and tuning with pressure wave action. Useful for both diameter and length calculations in NAU FSAE exhaust and intake systems.

[35] B. J. McBride, M. J. Zehe, S. Gordon, and Glenn Research Center, Cleveland, Ohio, "NASA Glenn Coefficients for Calculating Thermodynamic Properties of Individual Species," Sep. 2002. [Online]. Available: <https://ntrs.nasa.gov/api/citations/20020085330/downloads/20020085330.pdf>

Reference for NASA polynomial coefficients with respect to determining specific heat, gas constant, and

specific heat ratio of the exhaust gases. Critical to coefficient accuracy associated with the exhaust system when determining runner length and speed-of-sound based design specifications.

Jackson Nichols

[36]“Engine - fswiki.us,” Fswiki.us, 2022. https://fswiki.us/Engine#Motorcycle_engines (accessed Sep. 18, 2025).

Used to increase familiarity in the world of FSAE. Two cylinders are smoother than one, and more simple than four

[37]M. Streeter, “The Suzuki RE-5 Was Supposed To Be The Future Of Motorcycles, Now It’s An Example Of A Past Failure - The Autopian,” The Autopian, May 04, 2023. <https://www.theautopian.com/the-suzuki-re-5-was-supposed-to-be-the-future-of-motorcycles-now-its-an-example-of-a-past-failure/> (accessed Sep. 16, 2025).

Used when considering using rotary engine

[38]World Nuclear Association, “Heat Values of Various Fuels - World Nuclear Association,” world-nuclear.org, 2020.<https://world-nuclear.org/information-library/facts-and-figures/heat-values-of-various-fuels>

Used in calculations of max hp for choked flow

[39]M. J. Moran, H. N. Shapiro, D. D. Boettner, and M. B. Bailey, Fundamentals of engineering thermodynamics, 8th ed. Hoboken, Nj: Wiley, 2014.

Thermodynamics text. Used for review and ultimately excluded from calculations.

[40] SAE International, Formula SAE Rules 2026-Draft, T.5: “Powertrain” , 29 Aug, 2025

Used for getting informed about restrictions in FSAE.

[41] F. M. White and H. Xue, Fluid Mechanics, 9th ed. New York, NY, USA: McGraw-Hill, 2021.

Used for review of compressible nozzle flow.

[42] R. G. Budynas and J. K. Nisbett, Shigley’s Mechanical Engineering Design, 11th ed. New York, NY, USA: McGraw-Hill, 2019. ISBN 978-0-07-339821-1.

Used while discussing gear forces in the drivetrain.

- [41] F. M. White and H. Xue, Fluid Mechanics, 9th ed. New York, NY, USA: McGraw-Hill, 2021.
- [42] R. G. Budynas and J. K. Nisbett, Shigley's Mechanical Engineering Design, 11th ed. New York, NY, USA: McGraw-Hill, 2019. ISBN 978-0-07-339821-1.
- [43] A. Pandit and V. K. Chawla, "Design and manufacturing of a fuel tank for formula SAE vehicle," Materials Today: Proceedings, vol. 43, pt. 1, pp. 148–153, 2021, doi: 10.1016/j.matpr.2020.11.251.
- [44] "Engine - fswiki.us," Fswiki.us, 2022. https://fswiki.us/Engine#Motorcycle_engines (accessed Sep. 18, 2025).
- [45] M. Streeter, "The Suzuki RE-5 Was Supposed To Be The Future Of Motorcycles, Now It's An Example Of A Past Failure - The Autopian," The Autopian, May 04, 2023. <https://www.theautopian.com/the-suzuki-re-5-was-supposed-to-be-the-future-of-motorcycles-now-its-an-example-of-a-past-failure/> (accessed Sep. 16, 2025).
- [46] World Nuclear Association, "Heat Values of Various Fuels - World Nuclear Association," world-nuclear.org, 2020. <https://world-nuclear.org/information-library/facts-and-figures/heat-values-of-various-fuels>
- [47] M. J. Moran, H. N. Shapiro, D. D. Boettner, and M. B. Bailey, Fundamentals of engineering thermodynamics, 8th ed. Hoboken, Nj: Wiley, 2014.
- [48] SAE International, Formula SAE Rules 2026-Draft, T.5: "Powertrain" , 29 Aug, 2025
- [49] F. M. White and H. Xue, Fluid Mechanics, 9th ed. New York, NY, USA: McGraw-Hill, 2021.
- [50] Kawasaki Versys Manual, Kawasaki Heavy Industries, 2007.
- [51] *Introduction to Cams, Mechanical Reference*, [Online]. Available: <https://www.mechref.org/md/Cams/>. [Accessed: 25-Nov-2025].
- [52] J. B. Heywood, *Internal Combustion Engine Fundamentals*, 2nd ed. New York, NY, USA: McGraw-Hill, 1988.
- [53] *SolidWorks Flow Simulation Transient Pressure Pulse, GoEngineer*, [Online]. Available: <https://www.goengineer.com/videos/solidworks-flow-simulation-transient-pressure-pulse>. [Accessed: 25-Nov-2025].
- [54] M. F. Harrison and A. Dunkley, "The acoustics of racing engine intake systems," *Journal of Sound and Vibration*, vol. 271, no. 3–5, pp. 959–984, Apr. 2004, doi: 10.1016/S0022-460X(03)00773-9.
- Research on acoustic harmonic for air intake systems in formula style race cars.
- [55] S. P. R. Chennadi, "Design and tuning of intake manifold by inertial and acoustic resonance effects," *International Journal for Research in Applied Science and Engineering Technology (IJRASET)*, vol. 8, no. VIII, pp. 884–890, Aug. 2020, doi: 10.22214/ijraset.2020.30884.
- Used mainly for commentary on inertial ramming effects and how to design for them.

3.3 Mathematical Modeling

In the following sections, the mathematical modeling for the FSAE powertrain was limited by the lack of software in our possession. We identified “independent” subsystems that could be modeled with basic inputs.

3.3.1 Theoretical Top Speed Calculations – Aidan Willson and Trent Greene

To set up further and more advanced calculations. We can take the gear ratios and peak engine performance characteristics of a specific engine such as the Yamaha YZ450F or Kawasaki Ninja 650R. The motorcycle owner’s manual [10] and online engine specification tables were used to find specific gear ratios, peak torque and peak power values, as well as corresponding rpm for each peak value. With these specs obtained, I used these equations below from the Fundamentals of Vehicle Dynamics [9].

$$\omega_e = N_t * N_f * \omega_w \quad \frac{\omega_e}{(N_t * N_f)} = \omega_w$$

$$V_x = \omega_w * r$$

Equation 3-1 - Speed Equations

Using equation (6) and manipulating to obtain the wheel speed based on engine speed (ω_e), dividing by current gear ratio (N_t) multiplied by final drive ratio (N_f). Further using this value and a few conversions along the way to find the Velocity (8) in miles per hour for a specific engine and its gear/torque/power characteristics. These equations were all implemented into MATLAB for ease of modification if we need to compare engines. Additionally, you can edit the tire size in the code to test different selections for diameter. Below are the results of the program based on the inputs of rpm, front and rear sprocket teeth. These results can be further used to create a heatmap of various sprocket variations that we are considering.

```
Enter the max rpm value: 8500
Enter the number of teeth on the front sprocket: 17
Enter the number of teeth on the rear sprocket: 36
Top Speed in 1st gear: 78.37 mph
Top Speed in 2nd gear: 111.47 mph
Top Speed in 3rd gear: 143.33 mph
Top Speed in 4th gear: 171.97 mph
Top Speed in 5th gear: 197.79 mph
Top Speed in 6th gear: 224.25 mph
```

Figure 3-2

The two heatmaps display top speed based on peak torque rpm and peak power rpm. From these, we can obtain ideal ratios and peak top speed based on these ratios.

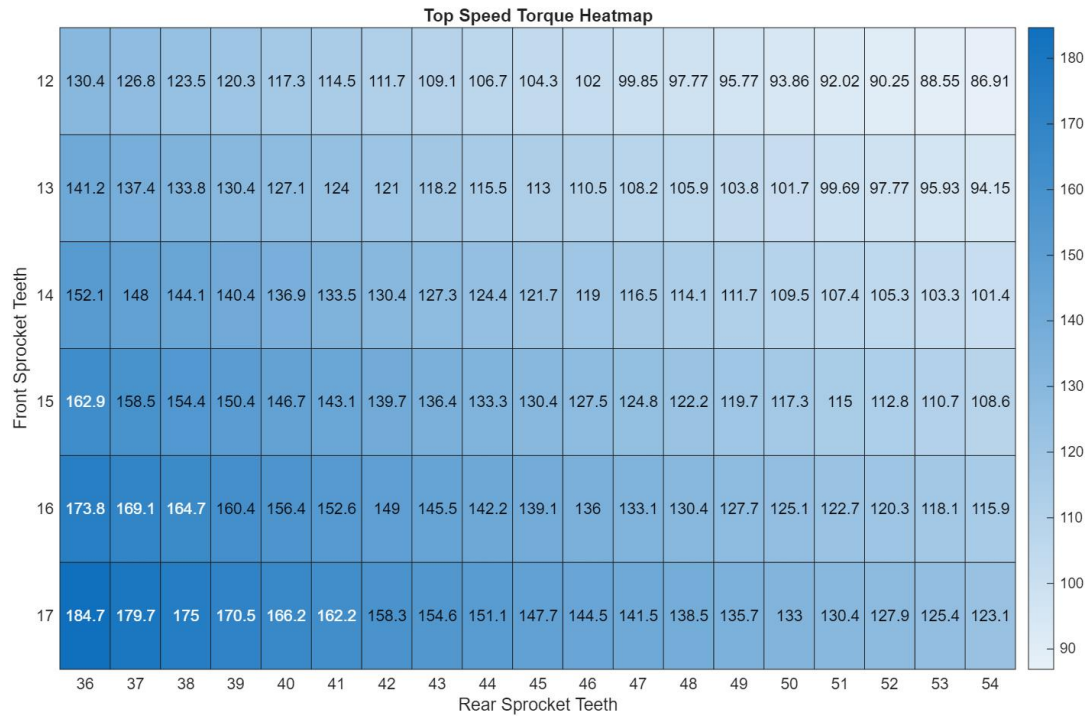
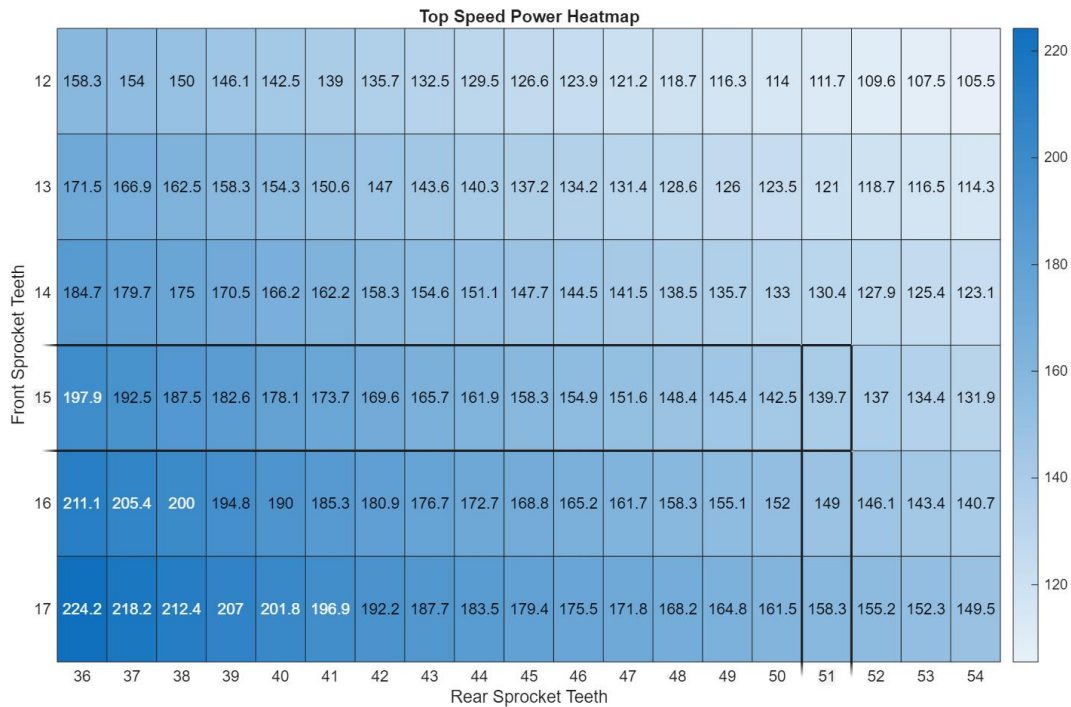


Figure 3-3-1: Theoretical Top Mechanical Speeds



Based on the heatmap data, we can see our highest top speed of 224.2 mph comes from a 17, 36 sprocket ratio and can plan accordingly to incorporate the results.

As a starting point for engine selection calculations, theoretical top speeds depending on engine power and gear ratios could be used to get estimates on basic expected performance and rule out certain gear ratios. The equation below was used, sourced from Erik Neumann of hpwizard.com. [33]

From equation (1) and [equation \(1b\) from the accelerating page](#), we get: [\(more\)](#)

$$v_{max} = \sqrt[3]{\frac{q}{2} + \sqrt{\frac{q^2}{4} + \frac{p^3}{27}}} + \sqrt[3]{\frac{q}{2} - \sqrt{\frac{q^2}{4} + \frac{p^3}{27}}} \quad (9)$$

Where:

$$q = \frac{P_t}{0.5\rho (C_{D^A} - f_r C_{L^A})} \quad (9.1)$$

$$p = \frac{f_r mg}{0.5\rho (C_{D^A} - f_r C_{L^A})} \quad (9.2)$$

Equation 3-2- Top Speed with Resistance

As the aero package has not yet been manufactured for the new car, rough estimates for drag and lift coefficients were made using the University of Southampton's guide based on non-specific aerodynamic package types [29]. This yielded a coefficient of drag estimate of 0.68 and a coefficient of lift of -2.68. Standard atmospheric air pressure was used, and a rolling resistance coefficient of 0.02 was assumed, as we are planning to use slick tires. For engine power inputs, the resulting graph below used a Kawasaki 650R, which after a mechanical loss overestimate, makes around 64 horsepower. However, this could be changed to input any engine we would want to test for.

To parametrize this equation to account for final drive, we factored in an estimate on mechanical loss and varying gear ratios from Taylor Racing Engineering's sprocket catalog for FSAE vehicles. This includes a sprocket A count of twelve to seventeen, and a sprocket B count of thirty-six to fifty-four. The highest possible speed with resistance was divided by the highest possible mechanical speed to create a resistive coefficient (about 36.17%) that could be applied to all the mechanical speeds to estimate top speeds at each gear ratio. The resulting table is shown below.

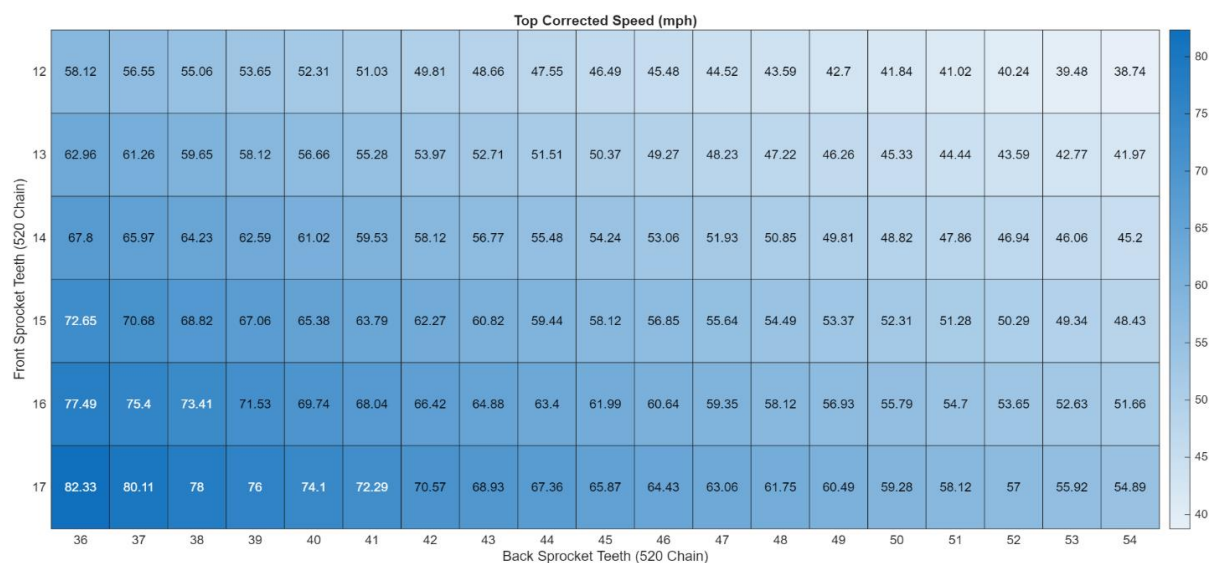


Figure 3-2: Top Corrected Speed in mph, with resistance

From this estimation, we see that in the lowest gearing, 82.3 miles per hour is the maximum possible speed. We can also rule out the highest gear ratios, where top speeds do not even hit 45 miles per hour.

3.3.2 Intake Restrictor Max Flow Rate – Liam O'Connor

Objective

This analysis is meant to calculate the maximum possible flow rate of air through the intake air restrictor for FSAE engines. This allows you to get a baseline of how much horsepower an engine can make when using the restrictor, before the engine's power is impacted by the restrictor.

Assumptions

- Atmospheric Pressure at inlet
- Isentropic-Compressible flow

- Ideal gas
- Velocity of Mach 1 at throat
- 20 mm diameter at throat (FSAE rules [5])

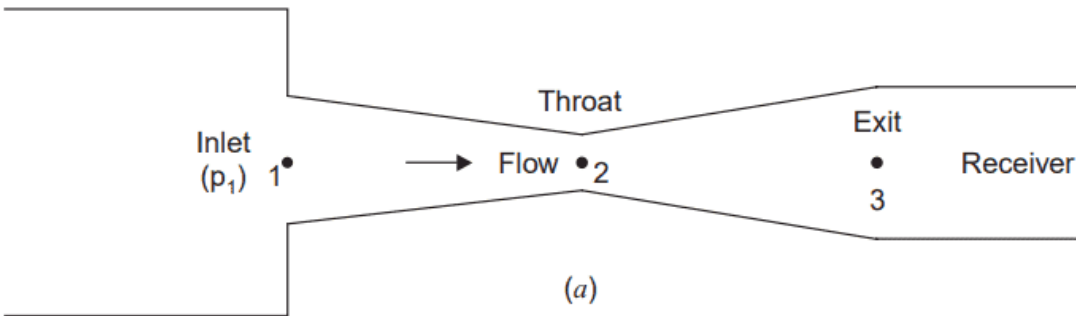


Figure 3-3 - Air Restriction Diagram

Based on the assumptions made above you can use equation 3-1 to solve for the maximum possible flow rate of air. This is based on the values used below.

- $A^* = 314.15 \text{ mm}^2$ (area at throat)
- $T_0 = 300\text{K}$ (temp at inlet)
- $\gamma = 1.4$ (specific heat ratio)
- $R = 287 \frac{\text{J}}{\text{kgK}}$ (gas constant)
- $p_0 = 101,325 \text{ Pa}$ (atmospheric pressure)

$$\dot{m} = \frac{p_o A^*}{\sqrt{T_o}} \sqrt{\frac{\gamma}{R} \left[\frac{2}{\gamma + 1} \right]^{\frac{\gamma+1}{\gamma-1}}}$$

Equation 3-4 - Choked Flow Rate Formula

When plugging these values into equation 3-1 you get a maximum flow rate of 74.3 grams per second of air through the restrictor. This value is mostly useful for a baseline on a flow rate, which may not actually be achievable in real life, as this equation is only a function of the diameter, which means that the boundaries of the restrictor do not impact the final flow rate at all, which is not realistic for a real-life scenario. This number can be further modified by adding a coefficient of discharge, where a number is chosen by typical values associated with nozzle type. The goal for this is to design a restrictor that has the highest discharge coefficient, minimizing the boundary effects on the flow of the restrictor.

3.3.3 Intake Restrictor Geometry – Liam O'Connor

Objective

Develop a restrictor geometry that optimizes the air flow to the maximum possible given the FSAE diameter limit. This will subsequently minimize the power loss on the engine that is directly a result of the intake restrictor.

Assumptions

- Isentropic flow
- $k=1.4$
- Velocity of Mach 1 at throat
- Rocket nozzle geometry will perform optimally

By using formulas for rocket nozzle geometry, we know we'll be able to achieve the highest possible flow rate, as we know that rocket nozzles amplify velocity to the point of creating thrust, which should also work the best when used as an intake geometry.

$$\frac{A}{A^*} = \frac{1}{M} \left(\frac{1 + \frac{k-1}{2} M^2}{1 + \frac{k-1}{2}} \right)^{\frac{k+1}{2(k-1)}}$$

Equation 3- - Area Ratio for Rocket Nozzle

The above equation 3-2 calculates the area ratio with respect to Mach number and the specific heat ratio. This ratio is the cross-sectional area at any point x over the cross-sectional area at the throat of the nozzle. Because the throat diameter is known by FSAE rules (20mm), and the Mach number is assumed to be 1 at that point, we can use that to make a plot of Mach number with respect to radius of the nozzle. This gives you a plot that tells the radius of the nozzle based on the Mach number of the flow, which is important for figuring out exit sizes for the nozzle that will work the best.

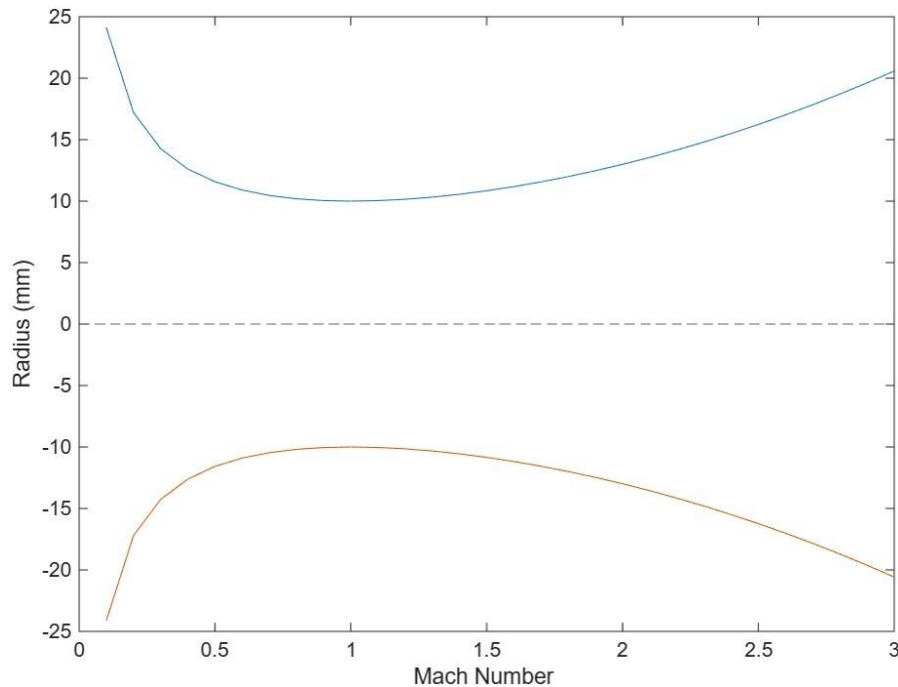


Figure 3-4 - Radius Vs. Mach Number

This plot shows the specific radius with exit Mach Number. With this you can figure out a suitable exit diameter for the restrictor and use that Mach number with the method of characteristics to get a suitable geometry.

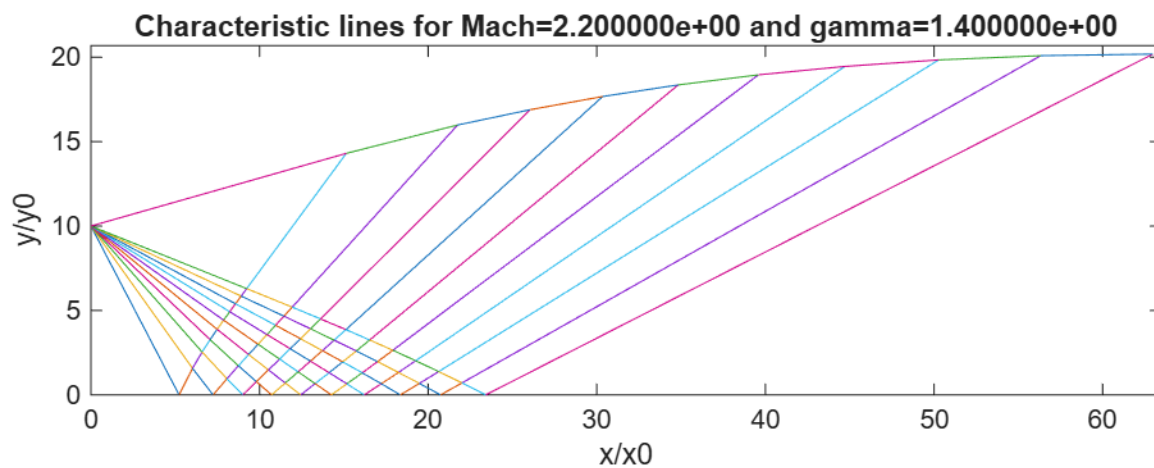


Figure 3-5 - Method of Characteristics Divergent Section

Using existing MATLAB code made by Shubham Maurya, a method of characteristics plot was created. This code takes user inputs of radius, exit Mach number, specific heat ratio, and number of characteristic lines to create this graph. With this you now have a full usable geometry that you can use to make CAD models for the diverging section of a bell nozzle. Theoretically this type of diverging section should be the most optimal for use as an intake restrictor.

3.3.4 Intake Restrictor CFD Testing – Trent Greene

Objective

This analysis sought to find the best intake throat shape using the above method of characteristics models (bell nozzles) and various de-Laval throat nozzles. Between the two styles, angles and lengths of the divergent section were changed to maintain the same overall shape. The goal was to achieve the lowest pressure drop possible and limit turbulence to achieve the best conditions for the plenum, as we are attempting to approach a steady-state, effectively infinite air supply.

Model Description

We used the described de-Laval and Bell nozzles in an ANSYS Discovery Simulations. Typically, de-Laval nozzles are the simplest to manufacture, but Bell nozzles tend to be more efficient. We used air gas as the volume and 6061-T6 aluminum for the structure. The inlet velocity was set at 25 m/s with no induced pressure (0 Pa) at the exit. This was a rough approximation of being at cruising speed in the vehicle. The main assessment criteria was finding which had the lowest pressure drop, not actual pressure values, at the 25 m/s inlet is an ideal case. All convergent geometry was the same across all models. We can, however, normalize the conditions across all models to assess which is the best performing. The model characteristics for each are shown below, as are the tested pressure drops from the simulations.

Table 3-3

Name	Length of Divergent section (mm)	Type	Max Pressure Drop (Pa)
Strt_throat_1	104	De-Laval	466
Strt_throat_2	77	De-Laval	569
Strt_throat_3	89	De-Laval	532
Strt_throat_4	153	De-Laval	444
Strt_throat_5	208	De-Laval	471
MOC_throat_1	63	Bell	786
MOC_throat_2	153	Bell	412

We first modeled one Bell type option and five options for de-Laval type restrictor. After running these simulations, we found that the 63mm was efficient for its short length, but in general, the longer de-Laval lengths did better. However, the 208 mm throat was too long, as pressure drop began to increase again after the 153 mm throat. Using this information, we created a second Bell nozzle using method of characteristics that was limited to a 153 mm length. This was the best performing nozzle. Creating more Bell nozzles to test would simply be too time consuming.

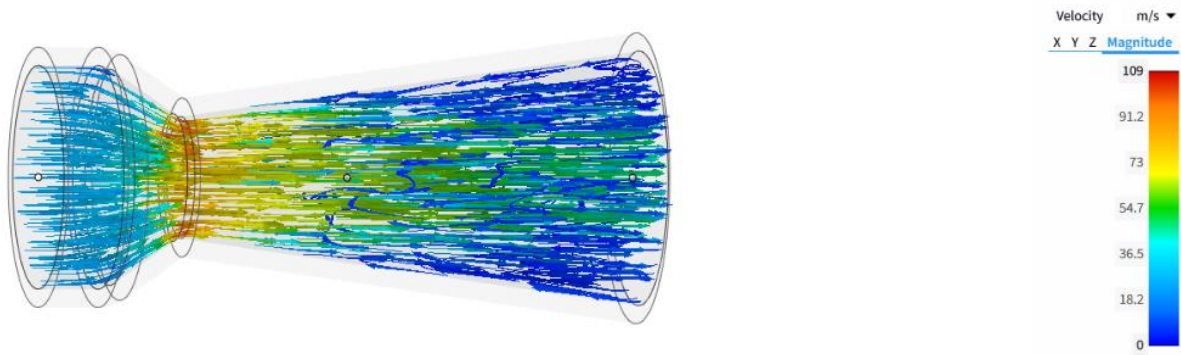


Figure 3-3-6; 77 mm de Laval Nozzle

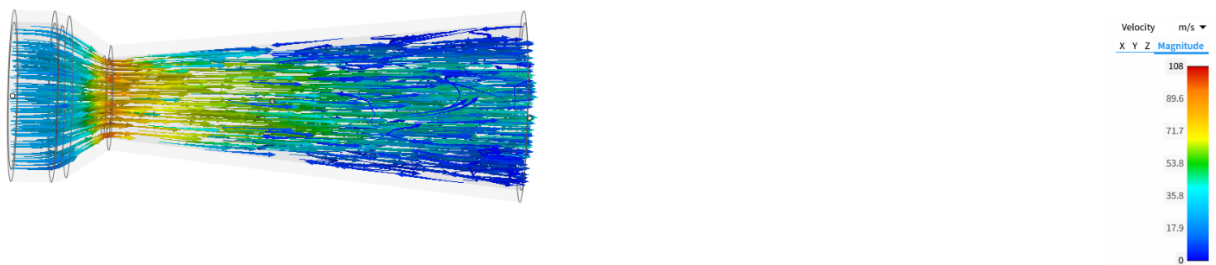


Figure 3-7; 89 mm de-Laval Nozzle

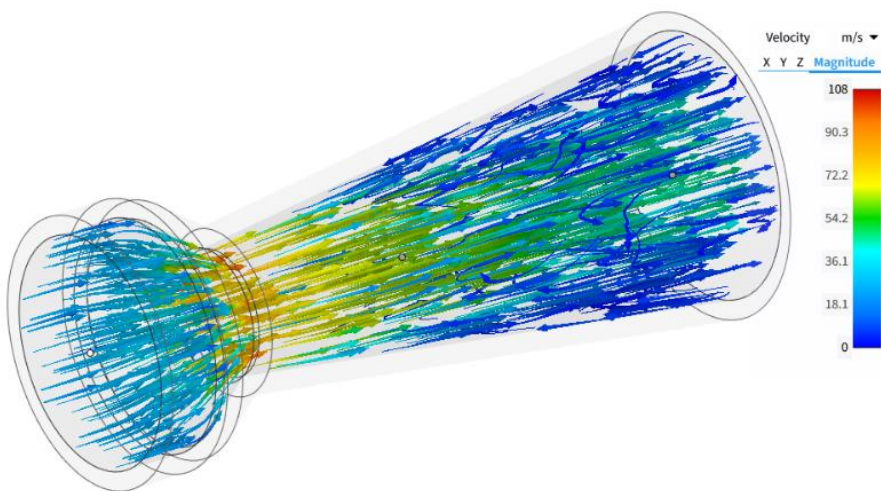


Figure 3-3-8; 104 mm de-Laval Nozzle

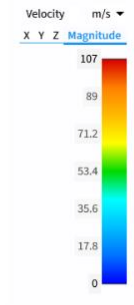
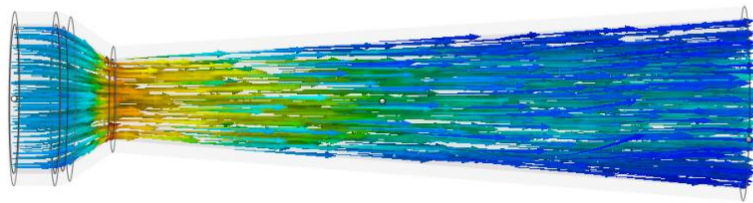


Figure 3-3-9; 153 mm de-Laval Nozzle

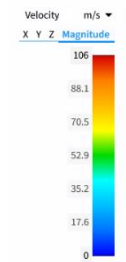
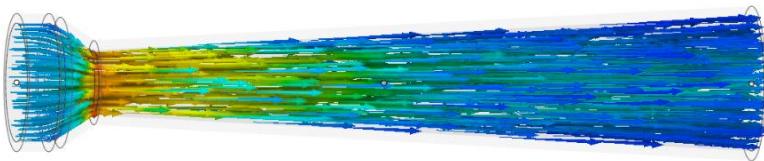


Figure 3-10; 208 mm de-Laval Nozzle

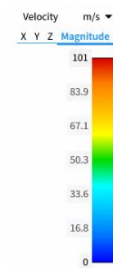
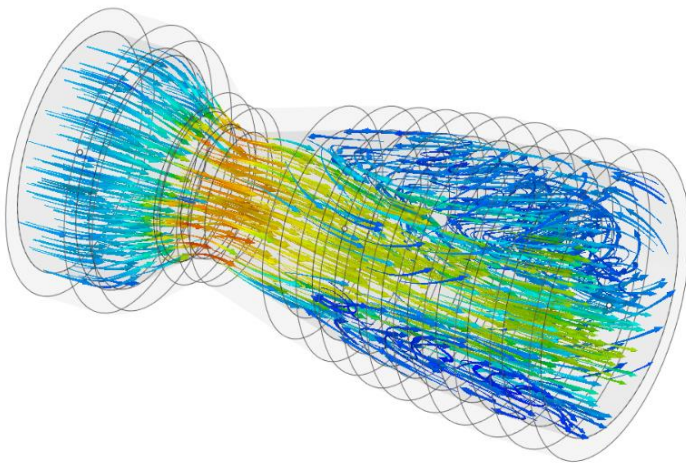


Figure 3-11; 63mm Bell Nozzle

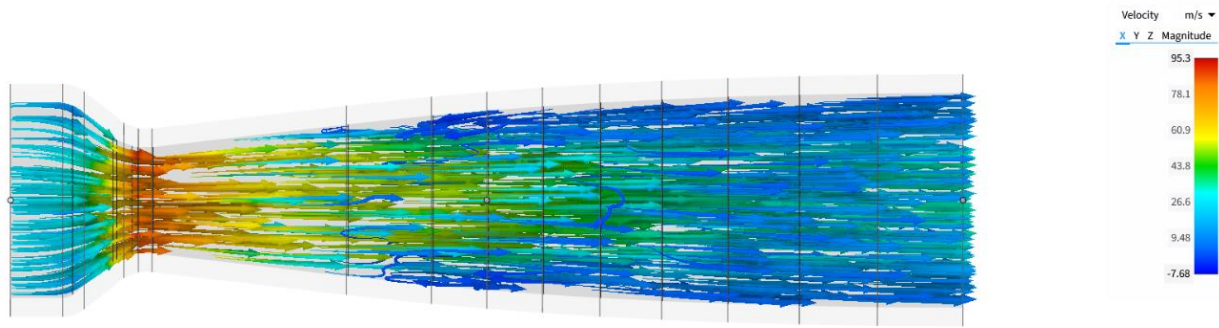


Figure 3-12; 153 mm Bell Nozzle

3.3.5 Engine Horsepower Restriction – Liam O'Connor

Objective

Calculate the threshold, in terms of horsepower, in which the engine will be choked off by the intake restrictor. This will help in choosing an engine, because it will help find an engine that will be affected minimally by the restrictor, strictly in terms of horsepower.

Assumptions

- Ideal Gas
- $\eta = 0.25$ (thermal efficiency)
- $AFR = 14.7$ (air fuel ratio)
- $LHV = 44 \frac{MJ}{kg}$ (low heating value)

Using a thermal efficiency of 0.25 is meant to underestimate horsepower possibilities, as lots of engines hover around 30% thermal efficiency. Using an air fuel ratio of 14.7 represents the ideal stoichiometric ratio for an internal combustion engine. It's likely that the real engine won't be at stoichiometric ratio, it helps to use it because it limits calculation errors associated with using a richer AFR, which will overestimate an engine's possible power output, when using the formula from this section. An LHV of 44 is a standard number based on 93 octane, which is a standard fuel likely to be used with the chosen engine.

$$\dot{m}_{fuel} = \frac{Power}{LHV * \eta_{thermal}}$$

Equation 3-6 - Power Formula

The above equation 3-6 uses power, LHV, and thermal efficiency to calculate the mass flow rate of fuel. Switching this equation around, you can use a known mass flow rate of fuel to calculate the power instead. Based on the max mass flow rate of air going through the restrictor from section 3.3.2, you can calculate the mass flow rate of fuel by dividing the max air flow rate by the AFR. With that you can then calculate the horsepower threshold.

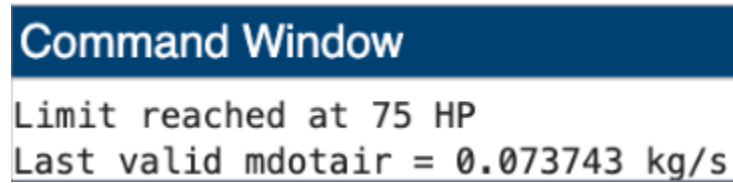


Figure 3-13 - Horsepower Threshold

Using a MATLAB code to find the threshold, the threshold came out to 75 horsepower. This helps us by giving us a metric to compare stock engines to find one that's as close as possible to the threshold. This will give us an engine that theoretically shouldn't be affected by the intake restrictor very much, meaning power loss will be minimal. Then we can effectively choose an engine that gets as close as possible to the threshold, while also being the lightest possible, which will give us a clear winner for the optimal engine.

3.3.6 Exhaust System – Marshall Fritz

Runner / Collector Diameter

Objective

This analysis aimed to find the most appropriate exhaust runner and collector diameters for the Formula SAE powertrain based on flow assumptions created from the Ideal Gas Law. The motivation for this calculation was to evaluate that the velocity of the exhaust gases remains suitable for design purposes, high enough to scavenge the cylinders, but low enough to reduce the amount of backpressure.

Model Description

A computational MATLAB model was developed to find exhaust dimensions based upon the function of engine parameters and gas properties. The model assumes:

- Steady, compressible flow with negligible losses across small distances using short exhaust runners.
- Ideal gas behavior for intake and exhaust flow conditions.
- Constant pressure and temperature at the exhaust outlet for each engine cycle.

Key user-defined inputs include:

- Engine displacement V_T [cc]
- Engine speed N [rpm]
- Volumetric efficiency V_E
- Cylinder count n_{cyl}
- Intake and exhaust temperatures T_i, T_e [°C]

- Atmospheric pressure P_{atm} [atm]
- Exhaust port diameter D_{port} [mm]
- Target mean exhaust velocity v [m/s]

Governing Equations

Analysis begins with the volumetric flow rate of air per intake stroke of a four-stroke engine:

$$Q_{t,intake} = \frac{V_T \cdot N}{2 \cdot 60} \cdot V_E$$

Equation 3-3 - Intake Volumetric Flow Rate

From ideal gas law, air density is taken to be defined by (11) and the total mass flow rate of the engine is:

$$\rho_i = \frac{P}{R \cdot T_i}$$

Equation 3-4 – Intake Air Density

$$\dot{m}_{air} = \rho_i \cdot Q_{t,intake}$$

Equation 3-5 – Intake Mass Flow Rate

At the exhaust, assuming negligible fuel mass from combustion and ideal gas characteristics, the total exhaust volumetric flow rate is denoted by:

$$Q_{t,exhaust} = \frac{\dot{m}_{air} \cdot R \cdot T_e}{P}$$

Equation 3-6 – Exhaust Volumetric Flow Rate

Flow rate is then divided by the number of cylinders (14) and the area of the runner is calculated by dividing by the target exhaust velocity, giving the area which can be easily converted into a diameter:

$$Q_{c,exhaust} = \frac{Q_{t,exhaust}}{n_{cyl}}$$

Equation 3-7 – Volumetric Flow Rate per Cylinder

$$A_r = \frac{Q_{c,exhaust}}{v_{target}}$$

Equation 3-8 – Runner Area

The MATLAB outputs for runner diameter, collector diameter, and total exhaust flow rate. The outcome allows correct exhaust geometric sizing referenced against thermodynamic and fluid flow constraints. Aiming for an exhaust gas velocity of approximately 50–70m/s is typically a good range for optimizing scavenging and reducing backpressure for small displacement FSAE engines. Likewise, the model could

be used parametrically to model and evaluate alternative design conditions, engine sizes, or target performance. Further refinement might involve:

- Incorporating modeling of exhaust pulse timing and wave reflections.
- Using CFD to validate flow uniformity and pressure losses through the collector.

At the target engine speed of 7000 rpm and a volumetric efficiency of 0.9, the analysis of the exhaust flow yielded a total volumetric flow rate for the 650cc twin-cylinder engine of 0.113 m³/s. The design mean exhaust velocity of 60 m/s dictated an approximate runner diameter of 34.7 mm, which is closely aligned with the 35 mm exhaust port diameter, showing that the flow should maintain consistent continuity. The collector diameter of 49.0 mm provides sufficient cross-sectional area to combine both runner streams together without excessive backpressure. These outcomes indicate that the exhaust geometry is a satisfactory balance between flow and back pressure to promote efficient gas removal and maintain performance at target engine speeds.

Header Runner Length

Objective

The purpose of this model is to evaluate the ideal exhaust runner length for the FSAE engine based on its exhaust gases' thermodynamic properties and pressure wave propagation. A proper runner length can help maximize scavenging, yields more torque, and improves volumetric efficiency.

Model Description

The model utilizes a quasi-one-dimensional organ pipe inspired analysis of exhaust gas dynamics, which includes air-fuel ratio, exhaust temperature, and exhaust composition. The following assumptions have been made:

- Exhaust gas is an ideal gas mixture.
- Combustion products are limited to CO₂, H₂O, N₂, O₂, and CO.
- The runner length is adjusted for pressure wave reflections and the operational RPM of the engine to allow for resonance at the desired speed.

Key user-defined inputs include:

- Exhaust temperature T_c [°C]
- Air-fuel ratio and equivalence ratio ϕ
- Engine speed N [RPM]
- Fuel stoichiometry and chemical composition for 93-octane gasoline

Governing Equations

Analysis starts with defining the equivalency ratio from the defined air fuel ratio (AFR):

$$\phi = \frac{AFR_{stoich}}{AFR}$$

Equation 3-9 – AFR Equivalency Ratio

Mole fractions are computed for each combustion product and specific heat at constant pressure is obtained through NASA Glenn polynomial coefficients:

$$y_i = \frac{n_i}{\sum n_i}, \quad i = CO_2, H_2O, O_2, N_2, CO$$

Equation 3-10 – Mole Fraction of Exhaust

$$C_{p,mix} = \sum_i y_i \cdot C_{p,i}(T)$$

Equation 3-11 – NASA Glenn's Polynomials

The gas constant for the exhaust is required to find the specific heat ratio both are calculated using the following equations:

$$R_{mix} = \frac{R_u}{MW_{mix}}$$

Equation 3-12 – Gas Constant

$$\gamma = \frac{C_{p,mix}}{C_{p,mix} - R_{mix}}$$

Equation 3-13 – Specific Heat Ratio

Speed of sound is a function of the gas constant, specific heat ratio, and temperature. This speed changes the rate of pressure wave propagation and is a major part in determining the desired length. The final runner length is also dependent on the revolutions and exhaust valve duration:

$$a = \sqrt{\gamma \cdot R_{mix} \cdot T}$$

Equation 3-14

$$L = \frac{a \cdot 120}{N}$$

Equation 3-15

Results

The MATLAB program provides:

- Speed of sound a in the exhaust gas [m/s]
- Exhaust runner length L [m]

These are first order approximations that may be useful in designing runners in general to tune pressure waves and improve engine performance.

The runner length is an important variable for engine performance in high-speed racing applications. Runners that are properly sized:

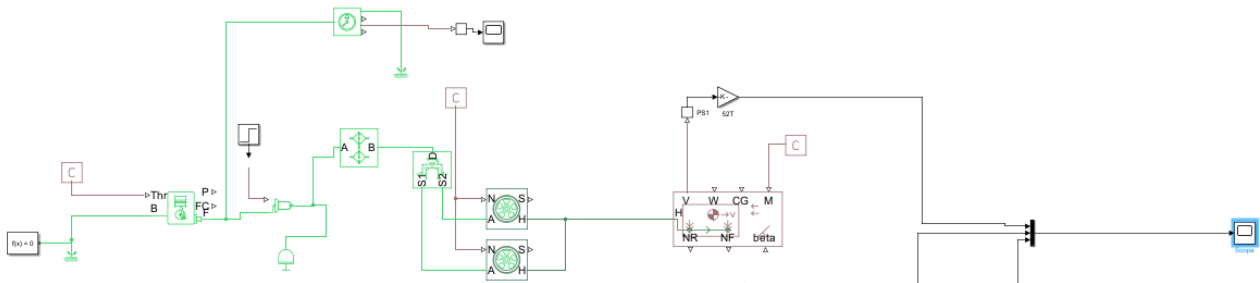
- Improve low to mid-range torque via pressure wave scavenging.
- Reduce exhaust backpressure, thus allowing for more volumetric efficiency.

- At an exhaust gas temperature of 700 °C, an AFR of 13.2, and an engine speed of 7000 RPM, the speed of sound in the exhaust was calculated to be 607.2 m/s, resulting in the optimal runner length of 0.8675 m (2.85 ft).

3.3.7 High Compression Piston Comparison – Aidan Willson

Validate whether it will be useful to incorporate a high compression piston kit into the power train design. Using MATLAB Simulink modeling to obtain velocity vs time and RPM vs time curves that compare the compression.

A Simulink model using powertrain components was created with driveline blocks provided in the Simulink software. It uses component models such as engine, transmission, chain drive, differential and wheels to output the Velocity vs RPM. Modify the components to simulate a specific engine performance curve and use this data to confirm the performance increase if a higher compression ratio is used.



The stock Kawasaki ninja 650R has a compression ratio of 10.8:1 and a peak power of 53.7 kW. Using a higher compression ratio increases the volume size between the top dead center and bottom dead center of the cylinder. This model will be analyzing a new compression ratio of 13.5:1. Based on another model that Liam created, we obtained a potential power increase of ~1kW gained based on the new ratio. But there is High chance the estimation is flawed and does not give accurate results. Most likely a higher power gain from the higher compression ratio is obtained. To offset this error, we will use a theoretical 10% power gain to accurately estimate and compare the power when using high compression pistons. The resulting power increase would be ~5.37 kW gained, and this gives a new peak power of 59.07 kW.

For this model we will compare the stock compression ratio power, the calculated higher compression ratio yielding ~1 kW of power gained, and a theoretical higher compression ratio yielding a 10% power gain. All three can be viewed on the Velocity vs Time and RPM vs Time graphs below.

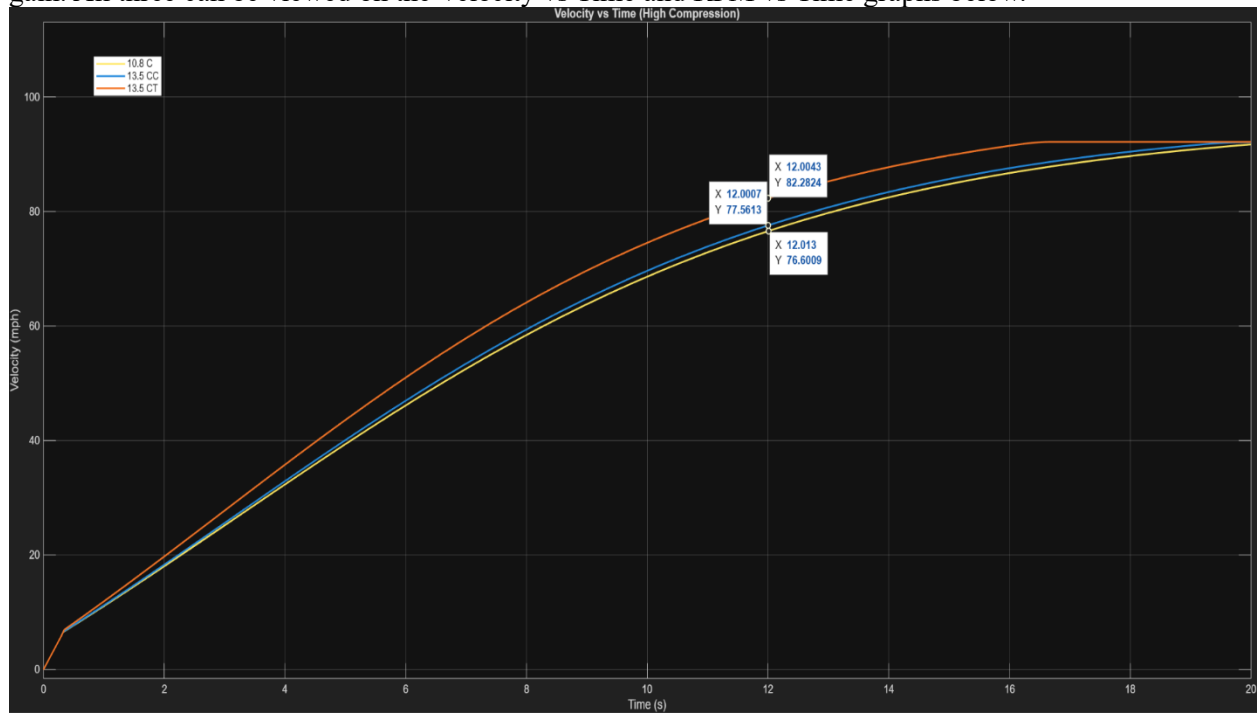


Figure 3-16 Velocity vs Time for Various Compression ratios

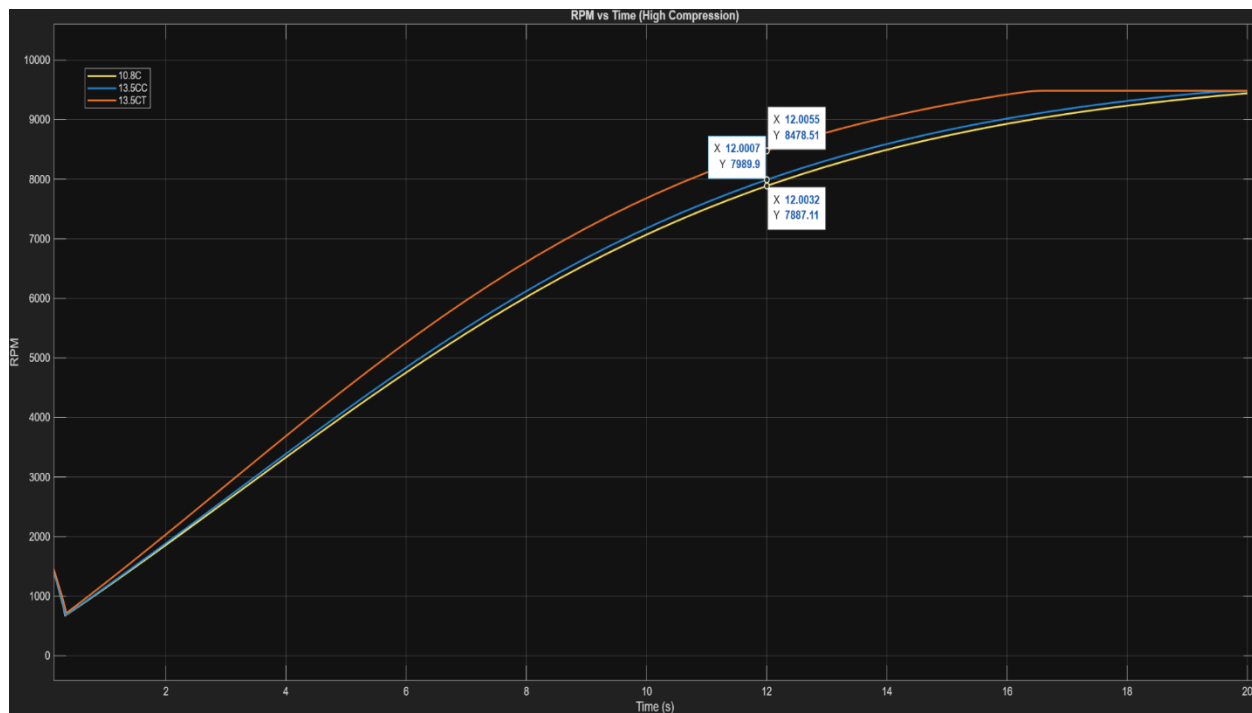


Figure 3-17 RPM vs Time for Various Compression ratios

Results:

Looking closer at the graphs of each compression ratio variation, we can observe the minimal increase in performance if the actual power gain is only ~1 kW. Only increasing top speed from 76.6 mph at 12 seconds to 77.56 at the 12 second mark. We can see the theoretical higher compression ratio that gives a power increase of 10% results in a much more promising velocity and rpm curve. A potential increase in top speed from 76.6 mph to 82.28 mph at the same 12 second mark. A large potential increase in RPM at 12 seconds from 7887 rev/min to almost 8500 rev/min. An overall increase of 5.68 mph and the rpm curve show a significant increase as well.

Discussion:

Our compression ratio can be fairly easily modified using a high compression piston kit. The question is if the increased compression ratio would be a valuable and effective design purchase. If the power increase is in fact only a ~1 kW increase, then based on our results the high compression kit would not be effective or worth the money. Based on the results of a theoretical 10% power increase using 13.5:1 high compression piston kit, the increase in velocity and peak rpm would be very beneficial for maximizing the performance of our engine. If we do decide to go that route, JE pistons make an affordable 13.5:1 compression piston kit for the Kawasaki 650R at a price of \$525 [36] and is easily accessible via their website. The increased compression ratio would also mean that we need to increase the fuels' octane. With additional resources from an online forum [37], the chart below can be used to verify the correct octane to be used.

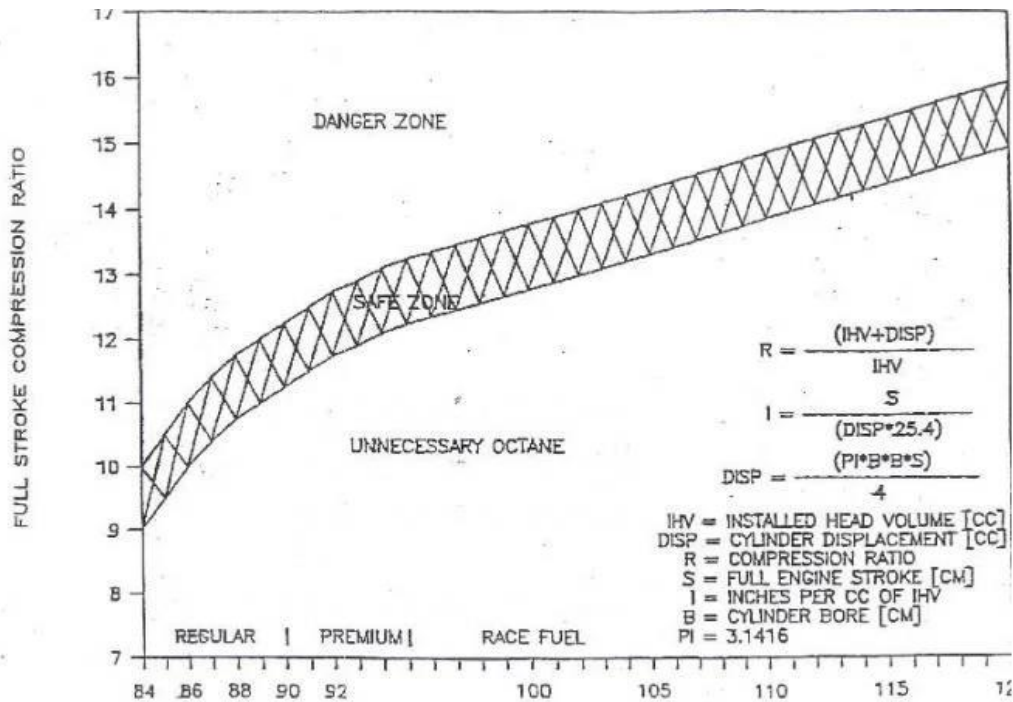


Figure 3-10 - Octane Vs. Compression Ratio

Based on the chart, a compression ratio of 13.5:1 would fall into the 100-octane range. This works out well because the fuel order form for Formula Competition provides fuel of up to 100-octane.

3.3.8 Axle Stress Calculations – Jackson Nichols

To calculate the stress the team's half shafts will endure, combined stress analysis was performed given the chosen engine's torque.

The von Mises equation,

$$\sqrt{\left(\frac{\sigma_x - \sigma_y}{2}\right)^2 + \tau_{xy}^2}$$

Equation 3-16

was selected for this purpose as half shafts are mostly made of SAE 4130 or SAE 4140 ductile steels.

Comparing the allowable stress to the actual stress experienced, the minimum diameter of the shafts then converged to 15.9 mm.

3.3.9 Fuel Tank Capacity – Jackson Nichols

As shown in section 3.3.5, the maximum possible horsepower given our intake restrictor was 75 horsepower. Plugging this value back into the Power Formula (equation 33), the mass flow rate of fuel can be found. At 0.0051 Kg/s, the mass fuel rate is rated for fuel usage at the rpm of the engine, where it

makes the most power. For our selected engine this is about 8,000 RPM.

Fuel tank capacity was then calculated based off of the endurance loop race time of SAE Formula 2025. This is the longest race in the event and so is used as the most fuel necessary for the 2026 car. Also included was a factor of safety of 1.1. The team determined this to be sufficient as the car will cycle through max power RPMs opposed to doing the entire race at this engine speed.

Fuel tank capacity then, was determined to be 2.7 gallons. This calculation is checked by the average FSAE tank being 1.3-2.6 gallons [43]. Purchase of the engine and load testing will enable a more precise measurement of AFRs and temperatures which will enable more precise calculations in this area.

4 Design Concepts

4.1 Functional Decomposition

For the functional decomposition diagram, only subsystems that we must make design decisions for where included. For example, the extent to which we are making decisions for with the engine are strictly air management and compression ratios. Beyond those two subsystems of the engine, we will keep the engine stock.

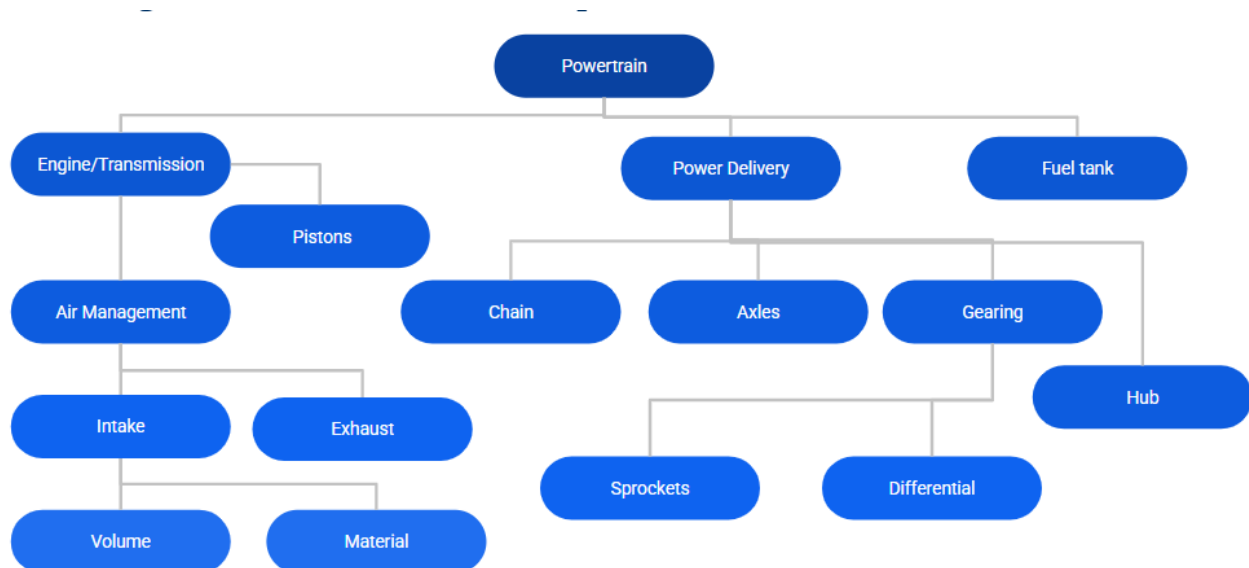


Figure 4-1

4.2 Concept Generation







	Solution		
Subsystem	1	2	3
Engine			
	Yamaha 450F	Kawasaki 650R	Honda CBR 600
Differential			
	Drexler	Taylor V2	ATV OE

Figure 4-2: Morphological matrix of Engine and Differential Options

Engine

- Yamaha 450F
 - Pros :
 - Lightest of our options
 - Good power to weight
 - Compact
 - Cons :
 - Low power, comparatively (58 hp)
 - Would require very large intake
 - Acoustic harmonics are not ideal
- Kawasaki 650R
 - Pros:
 - Good power to weight

- More power than Yamaha
 - Intake does not need to be as large; takes in more air per cycle
 - Lowest powerband
- Cons:
 - Unbalanced
 - Air intake is still not near steady state
 - Not as much power as CBR (72 hp)
- Honda CBR 600
 - Pros:
 - Most power (110 hp)
 - Closest to steady state air intake
 - Balanced
 - Cons:
 - Very heavy
 - High powerband

Differential

- Taylor Mk2
 - Pros
 - Cheap (\$2400)
 - Lightweight
 - Works with 520 chain and expected loads, high quality LSD
 - Cons
 - Must use Taylor specific sprockets
- Drexler
 - Pros
 - High quality LSD
 - Light
 - Commonly used in formula
 - Cons
 - Expensive (\$3500)
- ATV OEM
 - Pros

- Durable
- Cons
 - Heavy
 - Difficult to integrate

Motor Mounts			
	Solid	High Stiffness Silicone	Standard
Cooling			
	Fan over radiator	No fan	No Fan with aero Package

Figure 4-1 showing radiator and motor mount options

Intake Material			
	Aluminum	Plastic	Composite Printed Plastic w/ Strengthening
Fuel Tank			
	Stainless	Plastic	Aluminum

Figure 4-4; Intake and Fuel Tank Morphological Matrix

Intake Material

- Aluminum
 - Pros
 - High quality surface (low roughness)
 - Good heat resistance
 - Cons
 - Heavy
 - Expensive, for both materials and manufacturing
- Plastic
 - Pros
 - Light
 - Cheap
 - Easy to manufacture

- Cons
 - Poor heat resistance and durability
 - Surface roughness is not as good
- Composite
 - Pros
 - Good surface roughness is achievable
 - Super lightweight
 - Good heat resistance
 - Cons
 - Very expensive and difficult to manufacture


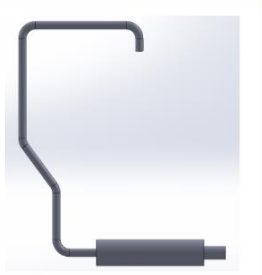
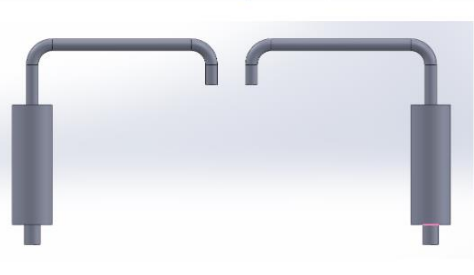
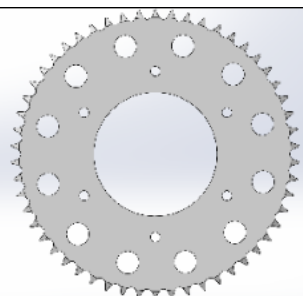
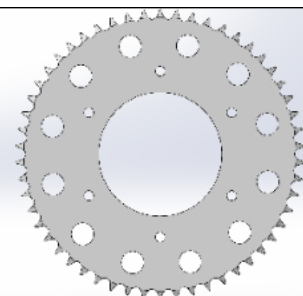
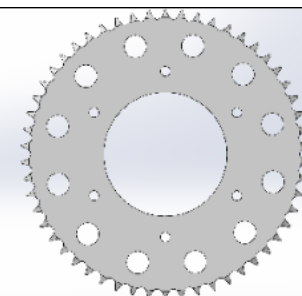
Exhaust						
	Side Exit		Rear Exit		Dual Side Exit	
Rear Sprocket Count						
	36-42		42-48		48-54	

Figure 4-5; Morphological Matrix with Every Part Choice

4.3 Selection Criteria

Selection criteria differed for each component of the power train. In general, methods that prioritized weight and cost reduction were selected. In this thinking, the powerhouse of the powertrain, our engine, must be able to reach the maximum possible horsepower given the intake restrictions while being as light as possible. Based on the horsepower threshold calculation in section 3.3.5, the Kawasaki is the closest in horsepower to the calculated 75 horsepower threshold, indicating that it makes the most horsepower while still being low enough to have little horsepower loss. Even though the Honda CBR has quite a bit more power, we know that it will be severely limited by the restrictor, likely dropping it down to similar

numbers as the Kawasaki. Since the Kawasaki is only 2 cylinders, it is much lighter than the Honda, making it a better overall choice for both acceleration and top speed. Compared to the Yamaha, the Kawasaki is heavier than the Yamaha, but the power and torque discrepancy between them makes the Yamaha a poor choice. The Kawasaki also has better opportunity to make horsepower through high compression pistons, where the Yamaha and Honda are already high compression engines, with little to gain in that respect. Lastly, the torque is a major deciding factor in which engine is best for Formula. Speeds are fairly low in each event, meaning that the emphasis should be on having the best acceleration. Of all three engines, the Kawasaki makes its torque lowest in the rpm range, which will yield better acceleration than the other engines. The Kawasaki also makes the most peak torque, further highlighting it as the best choice.

For the differential, the cheapest option that provided limited slip power delivery was to be selected. For the material used in motor mounts, comfort and performance were to be balanced, since the price difference between high quality aftermarket and OEM options is not substantial enough to be a selection criterion. The selection criteria for the cooling system were again to minimize cost. Furthermore, simplicity was valued for reliability here. In the case of intake, selection for size and shape must maximize the engine's ability to receive air for any given stage of the power cycle. The material of the intake was to be selected to maximize weight loss and strength. Again, the price difference between methods and materials was not substantial enough to be considered. Axles had the selection criteria for being made of SAE 4130 or SAE 4140 steel. They also must've withstood the calculated stresses specific to the engine chosen. The method of chain tensioning was determined based on simplicity, measured by number of moving parts, and ease of maintenance. The exhaust system was to be selected based off of its ability to flow and properly scavenge exhaust gases. This was determined to use simulation software. Finally, the size of the rear sprocket was selected to balance top speed and acceleration. It was shown in speed and acceleration curves that it would be optimal to have a mid-range gear ratio using a small front sprocket to reduce the envelope on the transmission

4.4 Concept Selection

The parallel twin Kawasaki engine and Taylor Race Engineering Mk 2 differential proved to the team to be the cheapest while still hitting our horsepower and stress requirements. Thus, these two components were selected by the process of elimination. For the exhaust, the rear exit design was selected for it's increased scavenging, lower sound output, and simpler fabrication. These properties were determined by CAD software and this layout had the best of these properties out of all three exhaust systems modeled. The cooling system was picked to be a water cooled engine with aero components to aid in it's cooling. After a conversation with the aero group, this was determined to be possible, and also fulfilled the requirements for simplicity on the powertrain side of things. Further components selected for the design of the car were high stiffness silicone motor mounts, aluminum intake material with a large internal volume, prefabricated axels cut to size (Taylor Race Engineering), an aluminum fuel tank, and a solid chain guide/ tensioner.

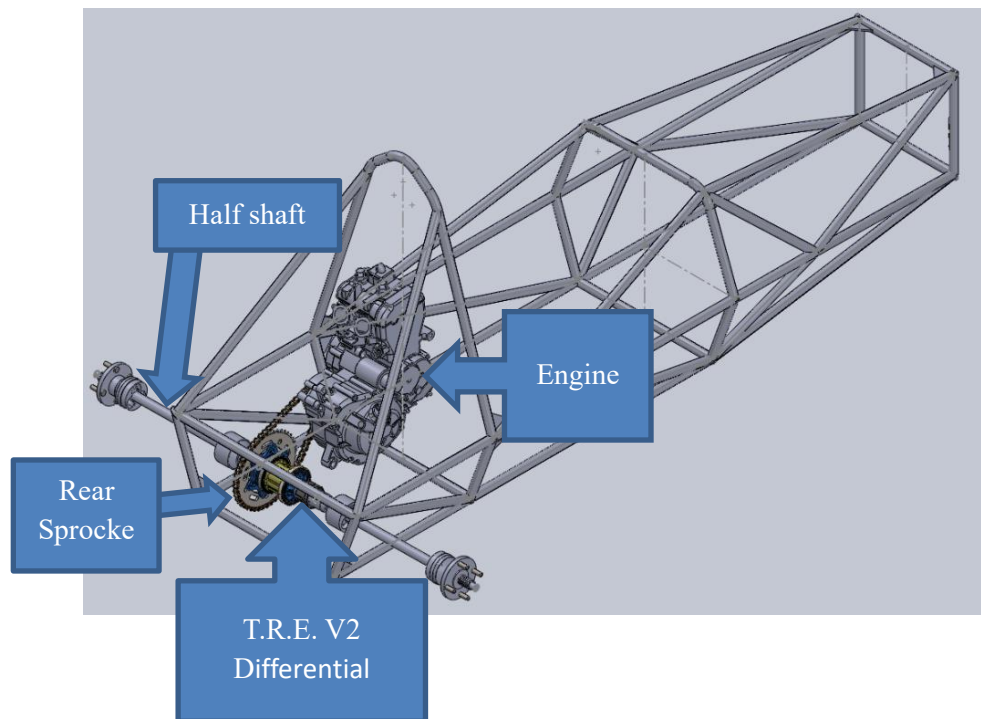


Figure 4-6; CAD Model as of now

5 Schedule and Budget

5.1 Schedule

Fall Semester Gantt Chart

Task	Start	Due	Finish State	24-Aug	31-Aug	7-Sep	14-Sep	21-Sep	28-Sep	5-Oct	12-Oct	19-Oct	26-Oct	2-Nov	9-Nov	16-Nov	23-Nov	30-Nov	7-Dec
Team Charter V1.0	3-Sep	4-Sep																	
Create Gantt Chart	3-Sep	30-Sep																	
Presentation 1	15-Sep	18-Sep																	
Peer Eval #1	19-Sep	19-Sep																	
Make Fundraising Flyer		19-Sep																	
Make Go Fund Me Post		22-Sep																	
Start Fundraising																			
Realis Picture, Email, and LinkedIn Post	21-Sep	26-Sep																	
Presentation #2 Calculations	2-Oct	7-Oct																	
Presentation #2	23-Sep	9-Oct																	
Competition Registration	9-Oct	24-Oct																	
Buy Engine	5-Oct	31-Oct																	
Website Check #1		24-Oct																	
Presentation #3	19-Sep	6-Nov																	
Prototype Demo #1	9-Oct	13-Nov																	
Peer Eval #3		14-Nov																	
Report #2		26-Nov																	
Prototype Demo #2		4-Dec																	
Final CAD and Final BOM		5-Dec																	
Project Management for 486C		6-Dec																	
Website Check #2		6-Dec																	
Peer Eval #4		7-Dec																	
Comp. Tech 26 Notice Form	24-Oct	8-Dec																	

Finish States		Legend	
Not Complete		Team Set Objectives	
Complete		Capstone Course Deliverables	
In Progress		Formula SAE Deliverables	
Ongoing			

Spring Semester Gantt Chart

Task	Start	Due	Finish State	12-Jan	19-Jan	26-Jan	2-Feb	9-Feb	16-Feb	23-Feb	2-Mar	9-Mar	16-Mar	23-Mar	30-Mar	6-Apr	13-Apr	20-Apr	27-Apr
Manufacture Motor Mounts	1-Jan	14-Jan																	
Print intake geometries	1-Jan	14-Jan																	
Team welding certifications	1-Dec	12-Jan																	
Test fit motor with mounts and differential	19-Jan	22-Jan																	
Manufacture differential mounts - alum.	22-Jan	8-Feb																	
Manufacture exhaust	2-Feb	23-Mar																	
Manufacture/ purchase fuel tank	2-Feb	2-Mar																	
dyno testing	2-Mar	6-Apr																	
shakedown testing	30-Mar	24-Apr																	
Competition	14-May	17-May																	

For this upcoming semester, the team will need to complete all tasks on the Gantt chart as well as other, unforeseen challenges. The predicted tasks are as follows: the motor mounts will need to be manufactured out of steel. To accomplish this task, they will need to be cut to size, coped, and welded together. They should fit on the frame as they mainly attach to the cockpit cage. Different intakes will need to be printed so that they can be visualized by the team and retrofitted on the engine so that dynamometer testing can take place. The team needs to be certified to weld at the machine shop so that the frame can be pieced together and tabs may be welded to the frame easily. The differential and motor need to be placed in the rear of the frame so that the frame team can see if the rear cage is large enough to accommodate all powertrain components. The exhaust will need to be fabricated with ample time to test the decibel reading and make any corrections necessary. The fuel tank will need to be manufactured/ purchased in a similar timeline to allow complete dyno and shakedown testing.

5.2 Budget

Budget					
Income to date			Expensies to date		
Date	Funds	Sponsor	15-Nov	\$1,176	Tooling, prototyping
25-Aug	\$5,000	Gore	4-Nov	\$2,500	Engine/Bike
9-Oct	\$5,000	Flagstaff Chevy	29-Oct	\$2,900	Registration
25-Oct	\$2,500	Seabury Fritz	Total:	\$1,914	
1-Nov	\$1,000	JGJM			
3-Nov	\$4,520	GoFundMe			
4-Nov	\$500	Midtown Clinic			
Anticipated Expensies					
Date	Cost	Part			
31-Oct	\$2,875	Differential			
15-Nov	\$300	Sprockets			
15-Nov	\$200	Chain			
15-Nov	\$800	Exhaust			
20-Dec	\$800	Intake			
30-Nov	\$800	Pistons			
30-Nov	\$400	Fuel Tank			
30-Nov	\$80	Fuel Lines			
30-Nov	\$300	CV axles			
31-Dec	\$1,500	Excess			
14-May	\$1,975	Food + Travel			

5.3 Bill of Materials

Projected BOM: Powertrain rev. 2			
Materials:	Cost HIGH:	Cost LOW:	Chosen:
Differential	\$ 2,450.00	\$ 2,450.00	Taylor Racing Mk2
Engine/transmission	\$ 2,500.00	\$ 2,500.00	Kawasaki Versys
Sprockets	\$ 200.00	\$ 100.00	Taylor Racing A-12t B-48t
Chain	\$ 150.00	\$ 50.00	520 Chain
Exhaust	\$ 200.00	\$ 100.00	TC Bros Exhaust kit
Intake	\$ 800.00	\$ 500.00	Aluminum Custom
New head	\$ 600.00	\$ 300.00	E-bay
Fuel Tank	\$ 300.00	\$ 100.00	Speedway Aluminum
Fuel Lines	\$ 80.00	\$ 50.00	-
CV axles	\$ 650.00	\$ 400.00	Taylor Racing Tripod and CV
Excess	\$ 1,500.00	\$ 500.00	-
Muffler	\$ 300.00	\$ 100.00	-
	HIGH	LOW	
Total Cost:	\$ 9,730.00	\$ 7,150.00	

6 Design Validation

6.1 Failure Modes and Effects Analysis

A failure modes and effects analysis was run and is shown below. This exercise was achieved by anticipating problems with each subsystem that is expected to be either designed or tampered with. As there is not currently an operable car, this is all merely speculation. Detection and recommended action for structural components would not be possible within our budget, so detection scores are high. This FMEA will be used to prioritize different components of our design.

Product Name	Development team							Page No
System Name	NAU FSAE 26							
Subsystem Name	Powertrain							
Component Name								
Part # and Functions	Potential Failure Mode	Potential Effect(s) of Failure	Severity (1-10)	Potential Causes and Mechanisms of	Occurrence	Detection	Recommended Action	RPN

				Failure				
Differenti al	Sheared off internal gears	Non moving condition of car	10	Materials defect/ Fluid level/type /condition	2	9	temperatur e readout	180
Engine	Force and/or temperatu re induced deformati on	Non moving condition of car	10	Low Oil Level due to leak or failure	3	5	check engine light	150
Sprockets	High- cycle Fatigue	Broken Sprocket. Possible failure of chain.	7	Material Defect	3	7		147
Chain	High- cycle Fatigue	Flying, broken chain	8	Insufficen t maintenec e	3	9		216
Exhaust	Corrosion	holes in exhaust	4	Exposure to road condition s	4	5	sensor	80
Intake	Ductile Rupture	Catastrop hic engine failure, explosion	10	Material defects, gasket failure, preignitio n, detonatio n	1	7	sensor	70
Pistons assembly	Cracks	Catastrop hic engine failure	9	Material defects, preignitio n, detonatio n	2	5	check engine light	90

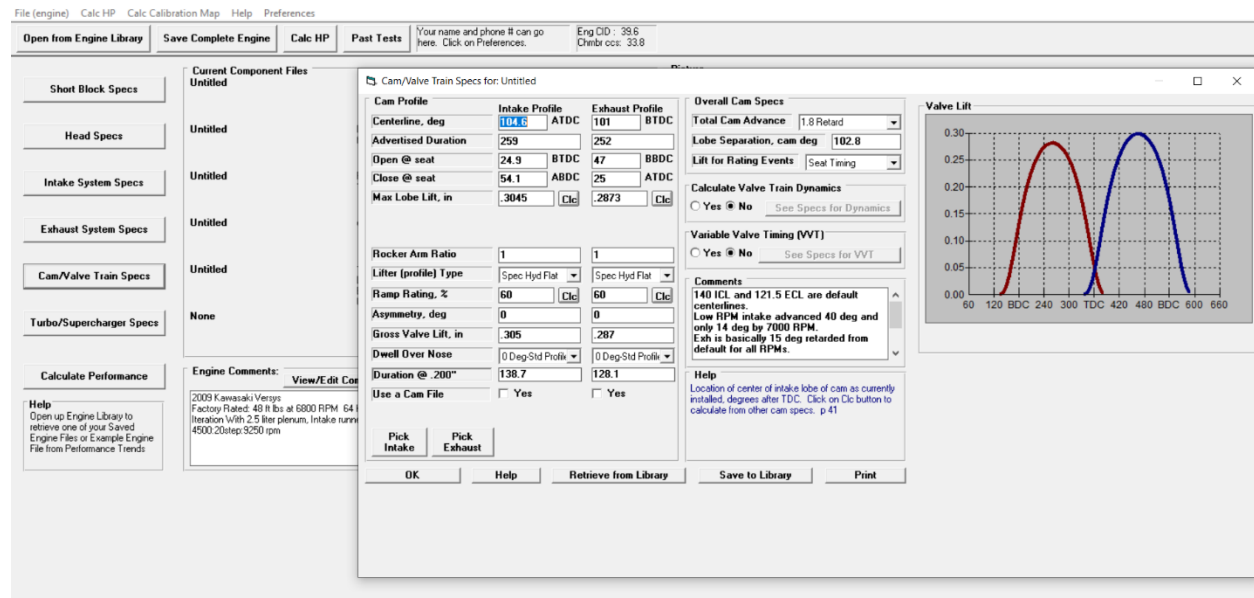
Fuel tank	Leak	Leak, fire/explosion	10	Welding or material defect	3	10	pressure sensor/gauge for lines	300
Fuel Lines	Leak	Leak, fire/explosion	10	Material defects, preignition, detonation	3	10	pressure sensor/gauge for lines	300
CV axels	Leak or tooth shear	Leak or no power to wheel, loss of control	7	Material defects,	5	8		280
Muffler	blows packing out	Too loud (tech failure)	4	Exhaust velocity too high	4	3		48
Engine Mounts	Fracture	Engine not supported, misalignment and unbalance	7	Material defects, poor welds/ fasteners, unexpected and sudden load change, extreme vibrations	3	10		210
Differential Mounts	Fracture	Misalignment	7	Material defects, poor welds/ fasteners, unexpected and sudden load change, extreme vibrations	3	10		210

6.2 Initial Prototyping

6.2.1 Engine Analyzer Pro Dynamometer Simulation

Engine Analyzer Pro's dynamometer simulation was used to approximate horsepower and torque figures at certain rotational velocities. This simulates engine values only and excludes any downstream mechanical losses. The goal of these simulations is to observe the effects of modifying several design variable that are within our control to modify and identify which decisions would be appropriate without a physical dynamometer.

The inputs for the simulation were fixed camshaft geometry based on physical data collected from the Kawasaki Versys engine, plenum volume, intake runner lengths, cylinder and injector data, and compression. The cam and valve setup information is shown below.



Figure

A dynamometer simulation was ran for varying plenum volumes. Runner length was kept at 16 inches for all volume simulations, and stock compression is shown. We see very little variation between runs, signifying that the volume is likely ample for all volumes shown. A 2.5 liter plenum was used as the baseline size, as this is approximately four times the displacement volume of the stock engine, which was guessed using interpolation based on research conducted on four and one cylinder engines and corresponding plenum volumes[54].

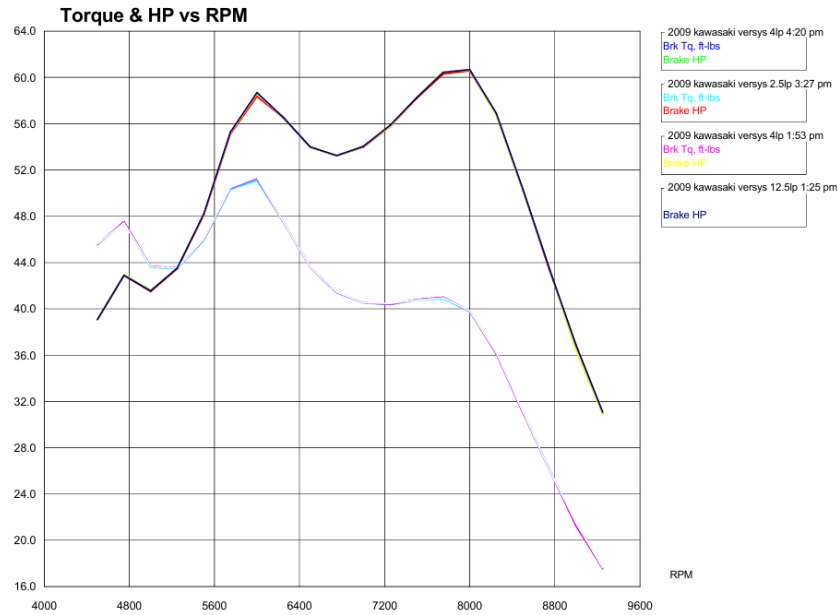


Figure 6-2: Parametric Plenum Volume Dynamometer Simulations

It is reasonable to surmise that physical data testing will be necessary on prototype intake manifolds to accurately model airflow and its effects on the running engine.

Figure 6-3, shown below, shows simulations ran with variable runner lengths. The purpose of this test was to determine whether a longer or shorter runner length would be optimal for an FSAE car. We observe that with decreased runner length, peak power increases and peak torque decreases. The most important result to note is the shifting of the power band. Increased runner length “moves” the power band to a lower RPM range, meaning the max torque and power are achieved at lower engine speeds.

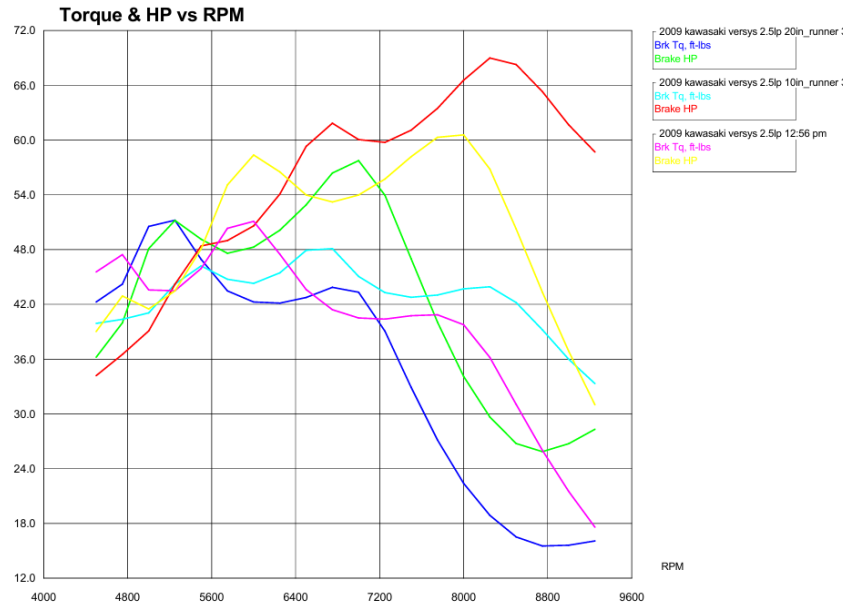
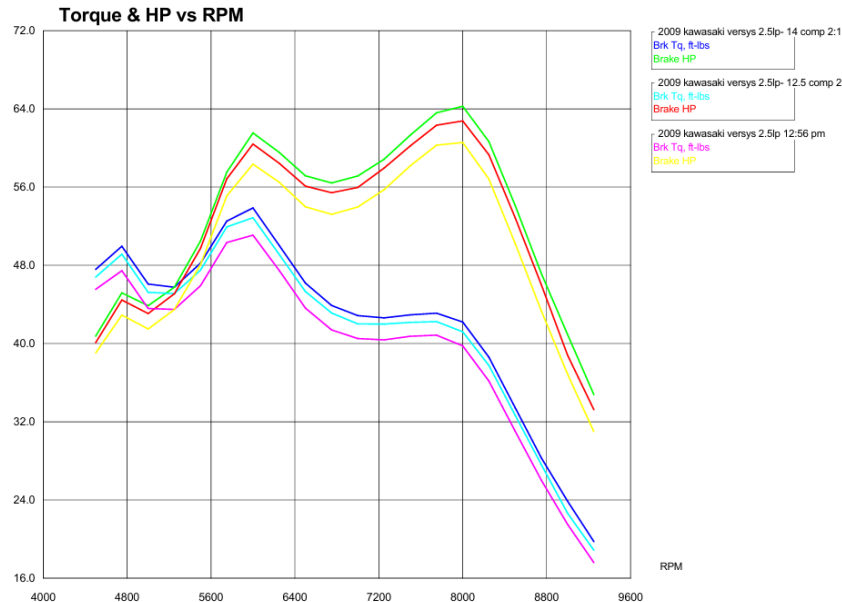


Figure 6-3 Parametric Runner Length Dynamometer Simulations

In Figure 6-3, we see that decreasing the runner length to 10 inches increases the maximum power to just under 70 horsepower, but brings the power band to between 6800 to 8400 rpm. The 16 inch runner length, calculated based on acoustic harmonics equations [54], achieve a maximum power of above 60 horsepower while maintaining a powerband that is between 6000 and 8000 rpm, which is much more desirable for a short track racing application with tight turns. Increasing the runners to 20 inches would drop the maximum power below the desired horsepower. This test reaffirms the validity of using the 16 inch runner length from acoustic harmonics.

Figure 6-4 below shows dynamometer simulations varying different compression ratios. The stock compression is 10.6:1, and a 12:1 and 14:1 were simulated. These ratios could be achieved by purchasing high compression pistons or by shaving the head down. We observe that increasing compression simply increases the torque and power of each simulation, without moving the powerband along the RPM range.



Figure

The obvious route is to increase the compression to optimize performance. There are limiting factors as far as implementation, though, including honing and replating cylinder walls and budgeting concerns. This is a clear decision that will simply have to wait until budgeting is concrete.

6.2.2 Intake Restrictor

For the intake restrictor prototype, the primary goal was to determine the manufacturability of the nozzle and mounting flange. For optimal performance, the intake restrictor must utilize complex geometry, so it was necessary to find if the geometry could be easily manufactured. By using a 3D printer to print a CAD model for the restrictor. We found that the printer was excellent for printing complex geometry in a short period of time. It was also able to do this while staying within an acceptable tolerance. Because of the speed, we were also able to find that it will be essential for physical flow testing multiple geometries in order to find the best performing nozzle. Going forward we plan to print more designs to do experimental testing and find the best design.



Figure 6-4- Restrictor 3D Print



Figure 6-5- Bend Flange Print



Figure 6-6- Bell Nozzle Print

6.2.3 3D Print of Eccentric Differential Mount

The 2nd iteration of the mount was 3D printed into 4 separate pieces with the help of Seth Jones, an EE on the Boeing team. Pieces were super glued together and dried to get a better visualization for the alignment to the engine mounts. Once assembled, a bolt and nut were added to the clamped end pieces. With the pieces together next to the engine, we will be able to see if the prototype is an accurate representation for the size of the mount and placement of the mounting points.



Figure 63 - Differential Mount 3D Print

Below is the mount attached to 1 of the mounting points on the engine. The rough measurements that I used for the CAD model were not the most accurate and that is prevelant in the prototype. The angle is not quite correct for the sprocket to sit at the right angle. This give good insight for the next variation of the mount and how to adjust the positioning. Additionally, the bottom bracket was not aligned with bottom mount. Once we acquired the engine CAD model this process becomes much easier.

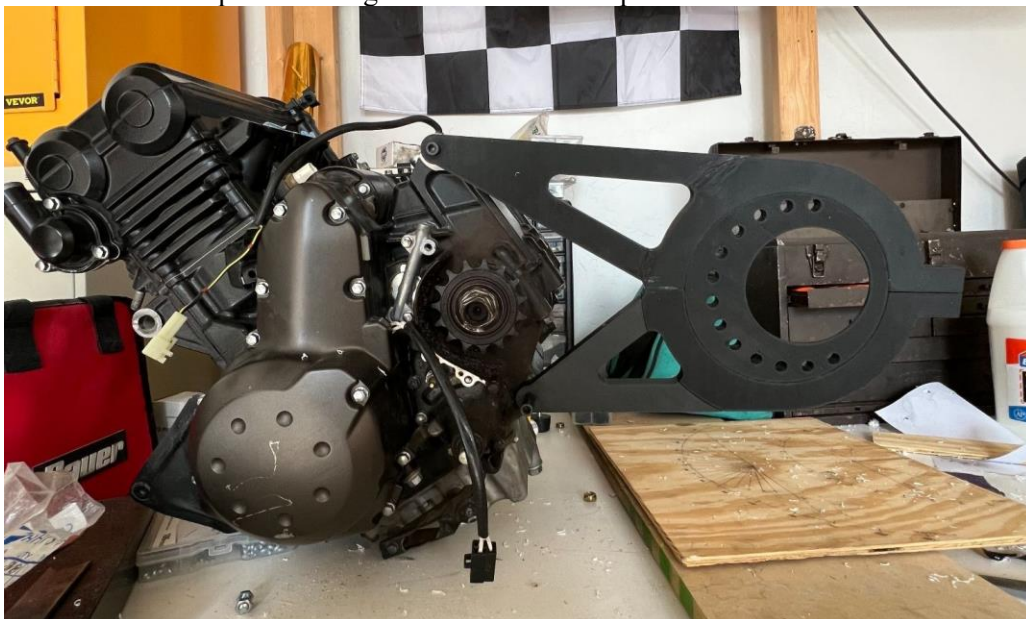


Figure 64 - Mount Attached to the Engine

Based on the first prototype model, some modifications are needed to ensure a proper design for the eccentric differential mount. This was very useful for the next iterations to know exactly what needed to be altered.

6.3 Engineering Calculations

6.3.1 SolidWorks Differential Mount Variations

To house the limited-slip differential, an eccentric mount design was selected and created in SolidWorks. The eccentric mount provides an easy tension for the chain. Before starting the SolidWorks model, some force calculations and dimensions are needed. The dimension sheet for the MK2 Single drive differential from Taylor Race engineers was useful for starting the CAD model and obtaining bearing sizes for the eccentric pieces.

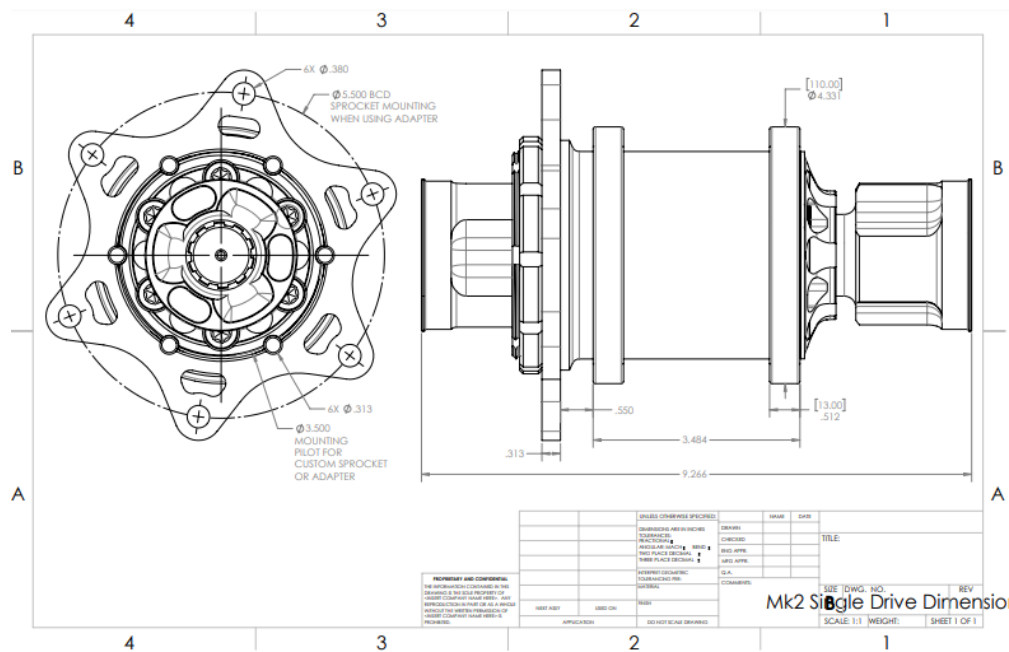


Figure 65 - Taylor Racing Mk2 LSD Dimensions

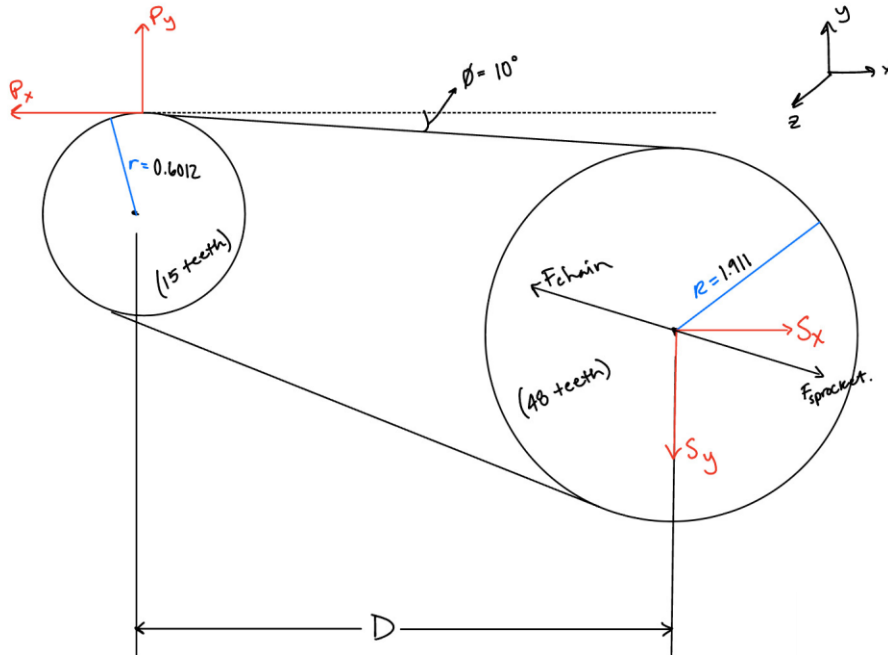


Figure 66 - Sprocket Force Drawing

Engine Torque \rightarrow 61 Nm or 45 lb-ft

Pitch \rightarrow 520 ($\frac{5}{8}$ - 0.625)

Pitch radius Where N is # of teeth

$$\text{front} = \frac{P}{2 \sin(\frac{180}{N})} = \frac{0.625}{2 \sin(\frac{180}{15})} = \frac{1.503 \text{ in}}{12 \text{ in}} = 0.125 \text{ ft}$$

$$\text{rear} = \frac{P}{2 \sin(\frac{180}{N})} = \frac{0.625}{2 \sin(\frac{180}{48})} = \frac{4.778 \text{ in}}{12} = 0.398 \text{ ft}$$

45 lb-ft Primary Reduction: 2.095

Final Reduction: 3.067
1st Gear: 2.438

$$704.93 \text{ lb-ft} = F_{\text{chain}}(r)$$

$$F_{\text{chain}} = 5639.44 \text{ lb}$$

$$S_{\text{sprocket}_x} = F_{\text{chain}} \cos(10^\circ)$$

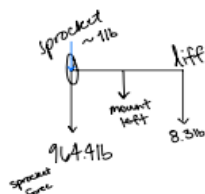
$$S_x = 5553.76 \text{ lb-ft}$$

$$S_{\text{sprocket}_y} = S_x \sin(10^\circ)$$

$$S_y = 964.4 \text{ lb-ft}$$

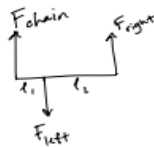
$$F_{\text{chain}} = \sqrt{5553.76^2 + 964.4^2} = 5636.87 \text{ lb}$$

$$M_{\text{chain}} = 5636.87(0.398 \text{ ft}) = 2,243.47 \text{ lb-ft}$$



$$\sum F_y = 0$$

$$-1 \text{ lb} - 964.4 \text{ lb} - 8.3 \text{ lb} = -973.7 \text{ lb}$$



$$l_1 \approx 2 \text{ in} \rightarrow 0.166 \text{ ft}$$

$$l_2 \approx 8.75 \text{ in} \rightarrow 0.729 \text{ ft}$$

$$F_{\text{left}} > F_{\text{right}}$$

Figure 67 - Differential Mount Force Calculation

A hand calculation was made to find the x and y loads on the mounting points of the differential mount, as well as the torque that occurs on the inner ring of the mounts. Starting with engines peak torque value of ~45 lb-ft and multiplying by the 1st Gear ratio, Primary and Final Reductions ratios to obtain a torque value of 705 lb-ft. Based on these calculations, for the sprocket a X load of 5553.76 lbf and Y load of 964.4 lbf was used in the FEA simulations. On the mounting points in the x-direction a force of 2277 lbf and in the x-direction about 400 lbf. A CAD model was then created for the eccentric differential mount on the left-hand side. FEA was performed in SolidWorks to obtain the following simulated results for the Von Mises Stresses on the mount and the rotating eccentric piece. The material selected for these parts was Aluminum 7075 due to its high strength while still reducing weight. If cost becomes an issue, a substitute such as Aluminum 6061 could be used as well.

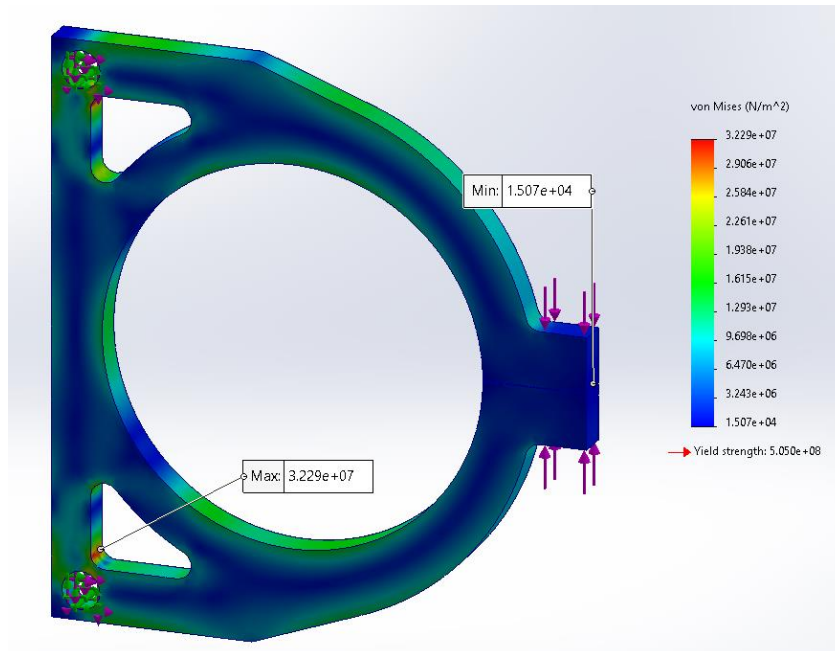


Figure 68 - FEA Simulation of Diff. Mount

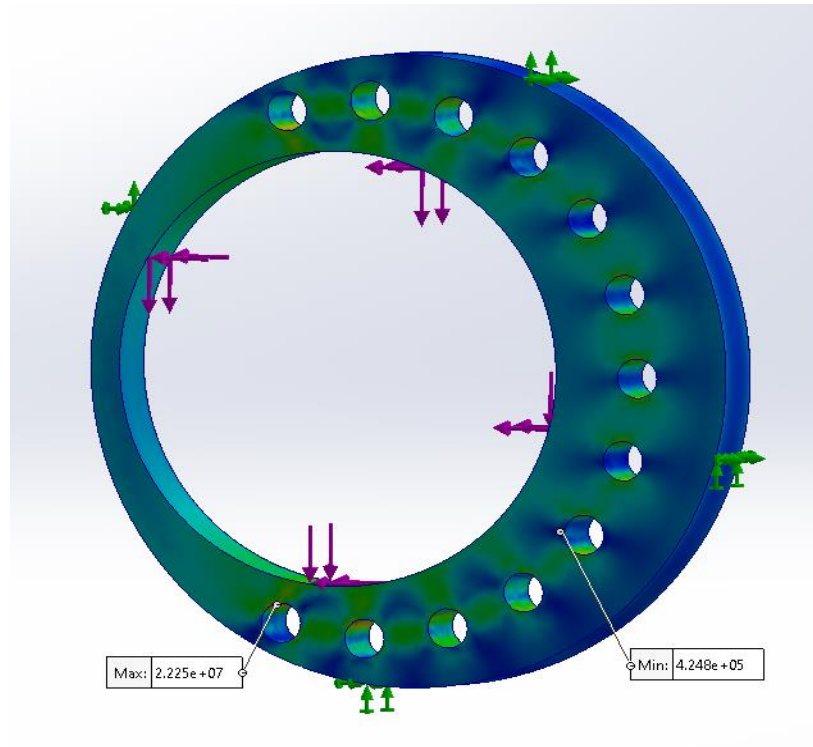


Figure 69 - FEA Simulation on Eccentric Disk

From the results above, we can observe a slight weak point on the differential mount around the mounting holes. Other than the peak stress of $3.3e7 \text{ N/m}^2$ at this point, the design should hold up to the force of the engine and support the loads on the mounts. After further discussion the Mount geometry was changed from the current design that is mounting to the rear of the frame. To an engine mounted orientation instead. The design was produced in SolidWorks and 3D printed for prototype presentation #1.

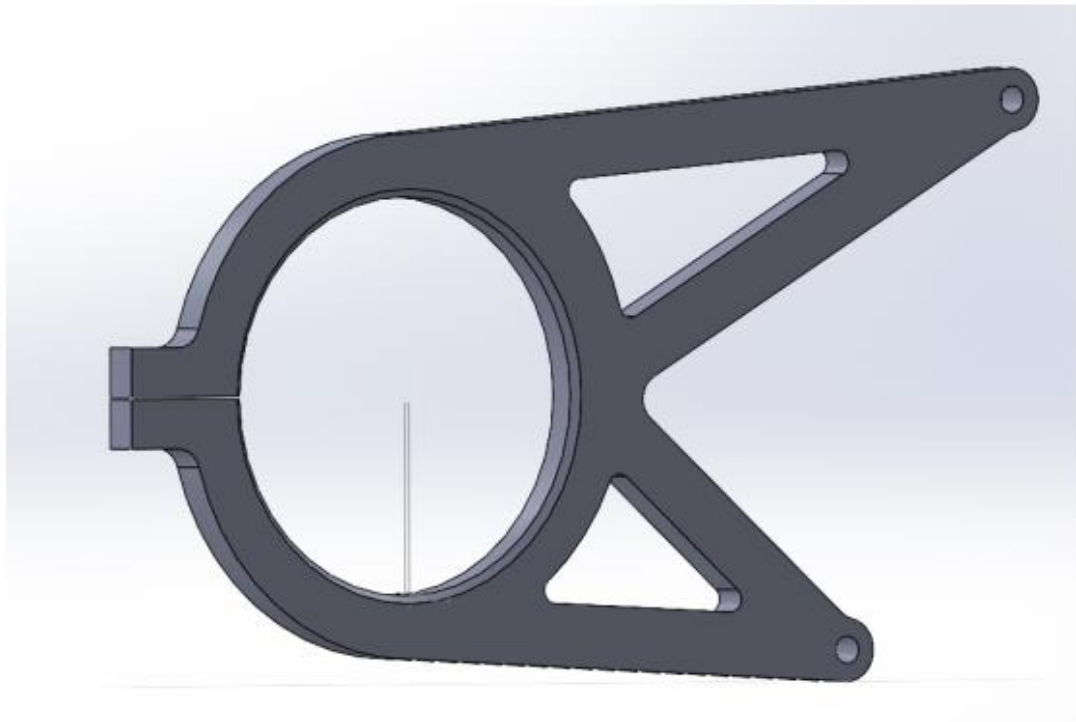


Figure 70 – Second Iteration for Eccentric Diff. Mount

The redesigned shape also features a small chamfer around the center ring for smooth fitment of the inner eccentric piece. This design was 3D printed but the measurements for mounting points on the engine were rough measurements taken by hand. Once the Kawasaki 650 versys engine scan was acquired from ASU's Formula Team, the mount could use the actual dimension directly in solid works. The design also did not have any support to ensure the clamping side would not deform to the side.

This new iteration was also not properly aligned to account for the -10 degree slop on the chain and sprocket design, for the Final CAD model this will be altered. Two designs were made for an end plate to prevent any motion of the clamped end pieces.

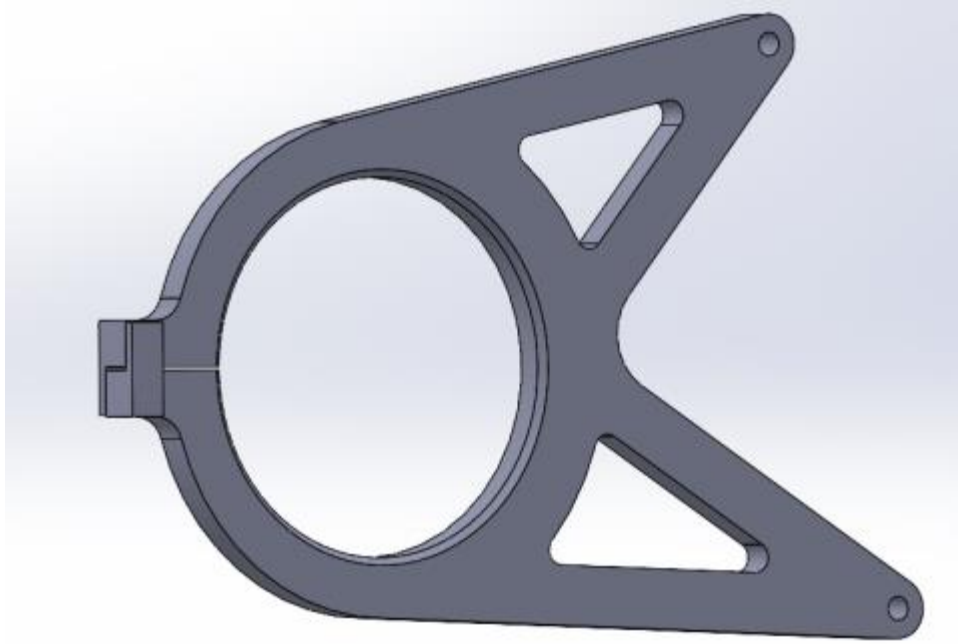


Figure 71 – Third Iteration for Eccentric Diff. Mount

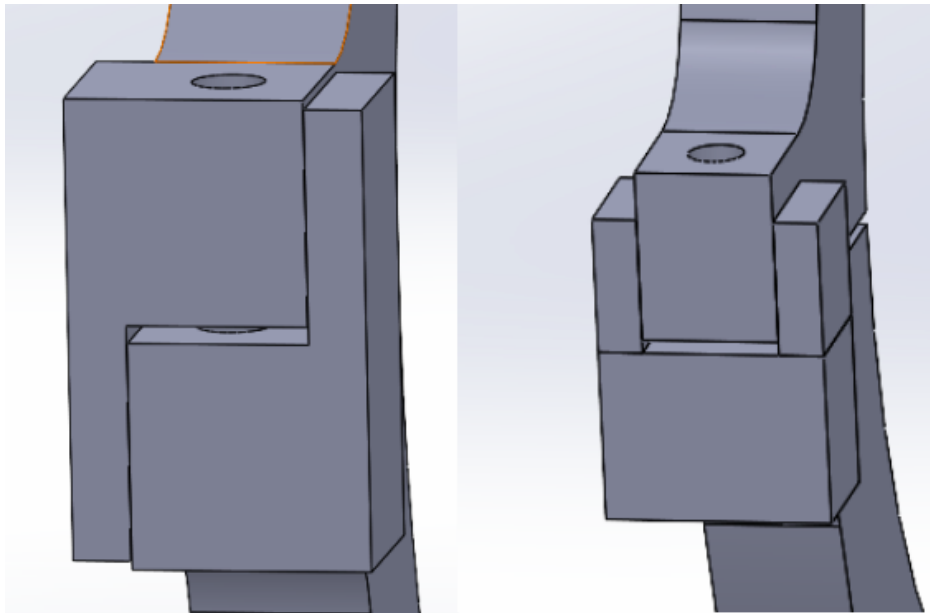


Figure 72 – End Plates for Clamped side of Mount

The design on the right will be used going forward due to its rigid geometry; the first design doesn't resist any of the horizontal force on the ends.

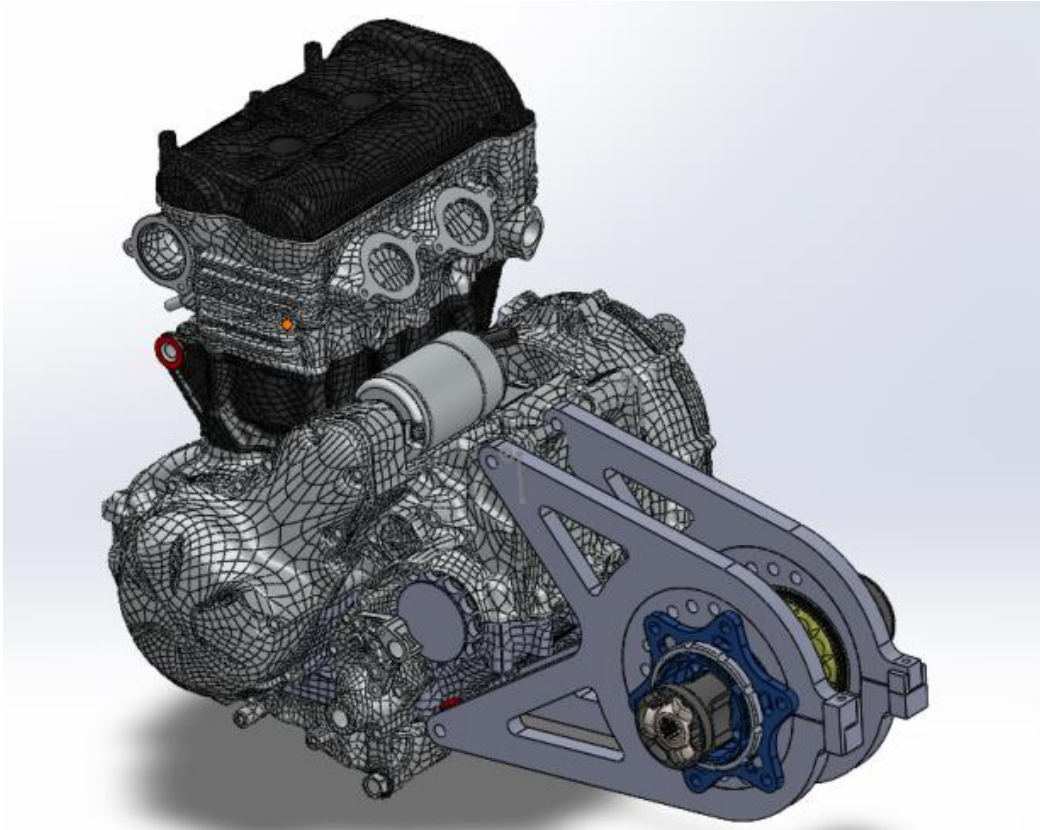


Figure 73 – Diff. Mount Attached to Engine

The mount was mirrored to the opposite side, and the Taylor differential aligned in the eccentric rings. Once the mounts were lined up to engine, I realized the spacing between bearings and ends of the engine mounting holes are not aligned. For the Final CAD model, the right mount will be modified to account for this, and a final FEA simulation will be performed on this piece and the engine mounting pieces for the frame.

6.3.2 Tulip CV Joint Analysis

This section will explore the decision between using a tripod and tulip constant velocity (CV) joint versus a traditional CV joint. Tripod and tulip joints tend to be more compact, stronger, and reduce friction in the drivetrain. Traditional CV joints do have more flexibility in application, though, as they can operate at steeper angles, allowing for more freedom when positioning drivetrain components in the frame. A finite element analysis will be performed on CAD files of each joint type, sourced from the Taylor Racing Engineering catalog [1], the manufacturer of the purchased differential for NAU FSAE's 2026 car.

To begin analysis, any and all assumptions must be defined. To account for worst case scenario conditions, we will assume that the differential is completely locked and is assuming the entire maximum torque load of the system, encountered in first gear after the final sprocket drive. While physical data testing has not been performed yet, we can assume that the factor engine brake torque of 47 lb.-ft is accurate,

We will also assume no mechanical losses in the driveline system, as no physical data testing has been

conducted. By assuming no mechanical losses, we are overestimating the torque acting on the system, thus ensuring an overly-safe design. The tulip CV joint is made from 6061 alloy aluminum with steel inserts.

This torque is transferred by the tulip housing to the tripod, where the center of the bearing's outer ring assumes the resultant loading. This both provides a shear force and bending moment to the tripod's spider. The load is equally distributed across three symmetric bolt supports. The center of each bearing is located 0.74 inches from the center of the axle, allowing us to calculate a reaction force from the input torque. By using

The tulip housing receives this load equally and opposite, occurring on the inner faces of each circle. Taylor Racing Engineering specifies a steel insert is placed inside of each individual circle, effectively distributing the load across the entirety of the insert. For the sake of this analysis, the insert was not included in simulations, as it is cheap and easy to replace relative to the tulip housing.

The finite-element method was used by SolidWorks. A static load of 6,064 lbs. was applied across the faces of each circle in the tulip to represent the maximum possible force that the tulip may receive. A total of 38669 nodes were used, resulting in 22,390 elements. The mesh uses largely triangular elements to capture the round edges of the tulip while saving computing power.

The following tulip simulation shows the results of the specified loading conditions. Table 2 and Figure 3 show the developed Von Mises stresses in the tulip.

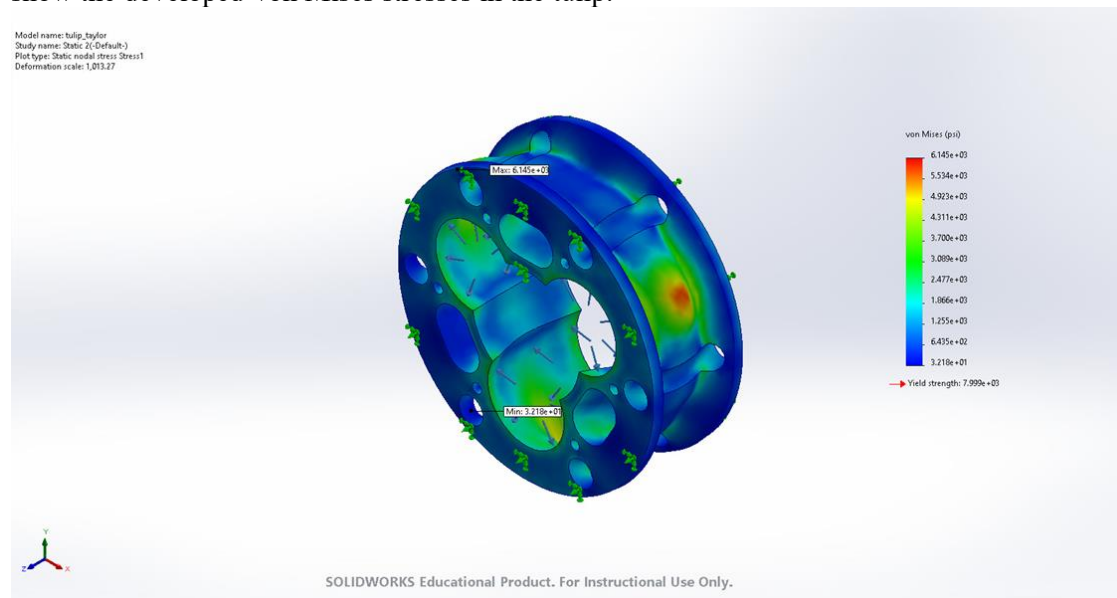


Figure 6-7: Von Mises Stress in Tulip Simulation (psi)

Table 2: Von Mises Stress in Tulip Simulation

Name	Type	Min	Max
Stress1	VON: von Mises Stress	3.218e+01psi	6.145e+03psi

Name	Type	Min	Max
		Node: 34828	Node: 1052

In Figure 3 and Table 2, we see a maximum stress of 6.145 kpsi developed at the approximate midpoint between the rails of the tulip at the height of each circle. This value is below the yield strength of 6061 alloy aluminum, which is listed at 7.99 kpsi. This means that in our worst case scenario, the tulip is operating at a safety factor of 1.3.

Figure 4 shows the displacements of the tulip after loading. Units are shown in millimeters instead of inches because of a computer error.

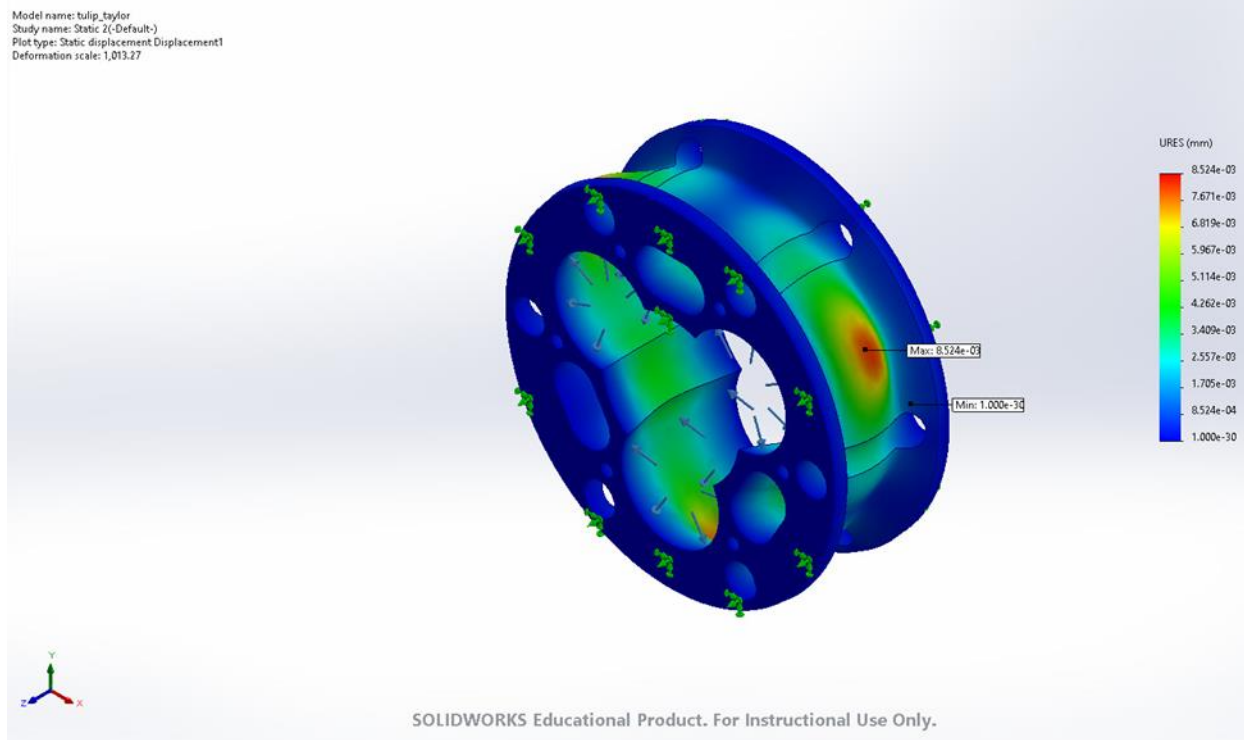


Figure 6-8: Displacement in Tulip Simulation (mm)

The maximum displacement experienced in the tulip is 8.524×10^{-3} mm, which is an acceptable displacement. This will not impact the functionality of the part. Because this deformation is occurring within the elastic range of the material, it will likely not be permanent either.

6.3.3 Radiator Fin Area

Objective

The performance of the radiator used to reject heat from the vehicle is important to ensure that the coolant remains within safe limits during competition rules as defined in SAE. The SAE's regulations permit only

using water as a coolant in the radiator, so the radiator must reject enough energy during the endurance race to prevent the vehicle from overheating. The present analysis estimates the reduction in coolant temperature and how much heat-transfer surface area will be needed to satisfy the engine's cooling requirements.

Model

The model used in MATLAB to simulate the radiator is a typical fin-and-tube type of heat exchanger configured as a crossflow pattern. Inside the tubes of the radiator, water flows as a liquid and outside the tubes air meets the fins on the radiator and will flow across the finned surfaces of the radiator fins to remove heat. Heat moves through the tube walls from the coolant to the ambient air by way of convection and conduction.

The calculations performed follow steady-state, one-dimensional assumptions. Thermal performance evaluations will include the coolant and air's heat capacities, the amount of heat that will be transferred under ideal conditions, the heat exchanger effectiveness, the number of heat-transfer units (NTU's), and the required heat-transfer surface area will confirm that the radiator can reject the engine's heat load during competition.

Assumptions:

- SAE Rules: Pure water is used to comply with competition rules
- Steady-state operation
- Constant properties of water and air
- Heat transfers outside the radiator are neglected
- Crossflow Radiator: Water is unmixed and air is the mixed fluid
- Air velocity changes are neglected across the radiator
- Single overall heat transfer coefficient of 500 W/m²·K.

Governing Equations:

To calculate how much heat moves from an engine's combustion process into its coolant we'll use the following equation:

$$\dot{Q}_{motor} = P_{engine} \cdot f$$

Equation 3-16 – Coolant Heat Transfer

where \dot{Q}_{motor} is the amount of combustion heat absorbed, P_{engine} is the power of the engine $f = 0.3$ is how much of the engine's power is rejected into the coolant.

The temperature of the coolant entering the radiator is defined as:

$$T_{in,coolant} = T_{out,coolant} - \frac{\dot{Q}_{motor}}{\dot{m}_{coolant} c_{p,coolant}}$$

Equation 3-17 – Coolant Temperature into Radiator

where $\dot{m}_{coolant}$ is the mass flow rate and $c_{p,coolant}$ is the heat capacity of the coolant. This relationship confirms that the temperature drop of the coolant across the radiator matches the amount of heat absorbed by the water inside the engine.

For both the coolant and the air, the total heat capacity rates are expressed as follows:

$$C_h = \dot{m}_{coolant} c_{p,coolant}, C_c = \dot{m}_{air} c_{p,air}$$

Equation 3-18 – Heat Capacity Rates

where \dot{m}_{air} and $c_{p,air}$ are the air's mass flow rate and heat capacity. C represents the energy that each type of fluid has to offer per degree of difference in temperature.

The minimum and maximum heat capacity rates are used to define the heat capacity ratio:

$$C_{min} = \min(C_h, C_c), C_{max} = \max(C_h, C_c), C_r = \frac{C_{min}}{C_{max}}$$

Equation 3-19 – Minimum and Maximum Heat Capacity Rates

The heat capacity ratio, C_r is based on the maximum/minimum heat capacity rates. This is an important quantity for determining the effectiveness of a heat exchanger, since the maximum heat transfer that can occur is limited by the maximum/minimum heat capacity rate of the fluids that make up the heat exchanger system.

The theoretical maximum heat transfer is denoted:

$$\dot{Q}_{max} = C_{min}(T_{hot,in} - T_{air,in})$$

Equation 3-20 – Theoretical Maximum Heat Transfer

Thus, for the maximum heat transfer to take place, the coolant fluid, $T_{hot,in}$, entering the radiator and the air, $T_{air,in}$, entering the radiator must be in thermal contact with each other through the heat exchange surface area of the heat exchanger.

The actual heat transfer is:

$$\dot{Q} = C_h(T_{hot,in} - T_{hot,out})$$

Equation 3-21 – Actual Heat Transfer

where $T_{hot,out}$ is the coolant temperature leaving the radiator. The actual heat transfer will always be somewhat less than the theoretical maximum due to finite heat transfer surface area and convective

limitations.

The Effectiveness of a heat exchanger is defined as the ratio of actual heat transfer to the theoretical maximum heat transfer:

$$\varepsilon = \frac{\dot{Q}}{\dot{Q}_{max}}$$

Equation 3-20 – Effectiveness Ratio

This is a dimensionless quantity and indicates how well the heat exchanger is performing in terms of its capacity to transfer heat.

Different calculations apply to the determination of NTUs, therefore, the number of NTUs for a Cross Flow Heat Exchanger will vary depending on which fluid has the lowest capacity rate. The following derive the NTUs for Cross Flow Heat Exchangers from the Fluid with the lower capacity:

$$\begin{aligned} \text{If coolant is } C_{\min}: NTU &= -\ln \left(1 + \frac{1}{C_r} \ln (1 - \varepsilon C_r) \right) \\ \text{If air is } C_{\min}: NTU &= -\frac{1}{C_r} \ln (1 + C_r \ln (1 - \varepsilon)) \end{aligned}$$

Equation 3-20 – NTU Calculation

The heat transfer area required to achieve the desired effectiveness is given by the following:

$$A = \frac{NTU \cdot C_{\min}}{U}$$

Equation 3-20 – Required Fin Area

Where U is the Overall heat transfer coefficient, this equation determines the minimum radiator surface area required to remove the engine heat load while providing the desired temperature drop for the coolant.

Results

The analysis predicts that the total effective heat transfer area of the radiator will be 0.427m². This surface area will reject the 70 hp engine heat load where 30% will be absorbed by the coolant, while the outlet temperature will be below the boiling point of water. The temperature drop of the coolant and heat rejection rate agrees with what would be expected under vehicle airflow while travelling at 55 mph.

6.3.4 Exhaust Manifold Analysis

A steady incompressible internal flow simulation was conducted in SimScale with a 50 m/s velocity inlet condition to reflect target exhaust flow rates.

The boundary conditions applied to the model are:

- Velocity input into both runners.
- Pressure output from the collector is defined as ambient pressure.

Model Description

The method uses steady state, non-transient fluid flow through the manifold to determine pressure zones inside the manifold. Although this method does not realistically model the exhaust flow of a running engine, insights are given into geometry optimization of the runner paths and bends.

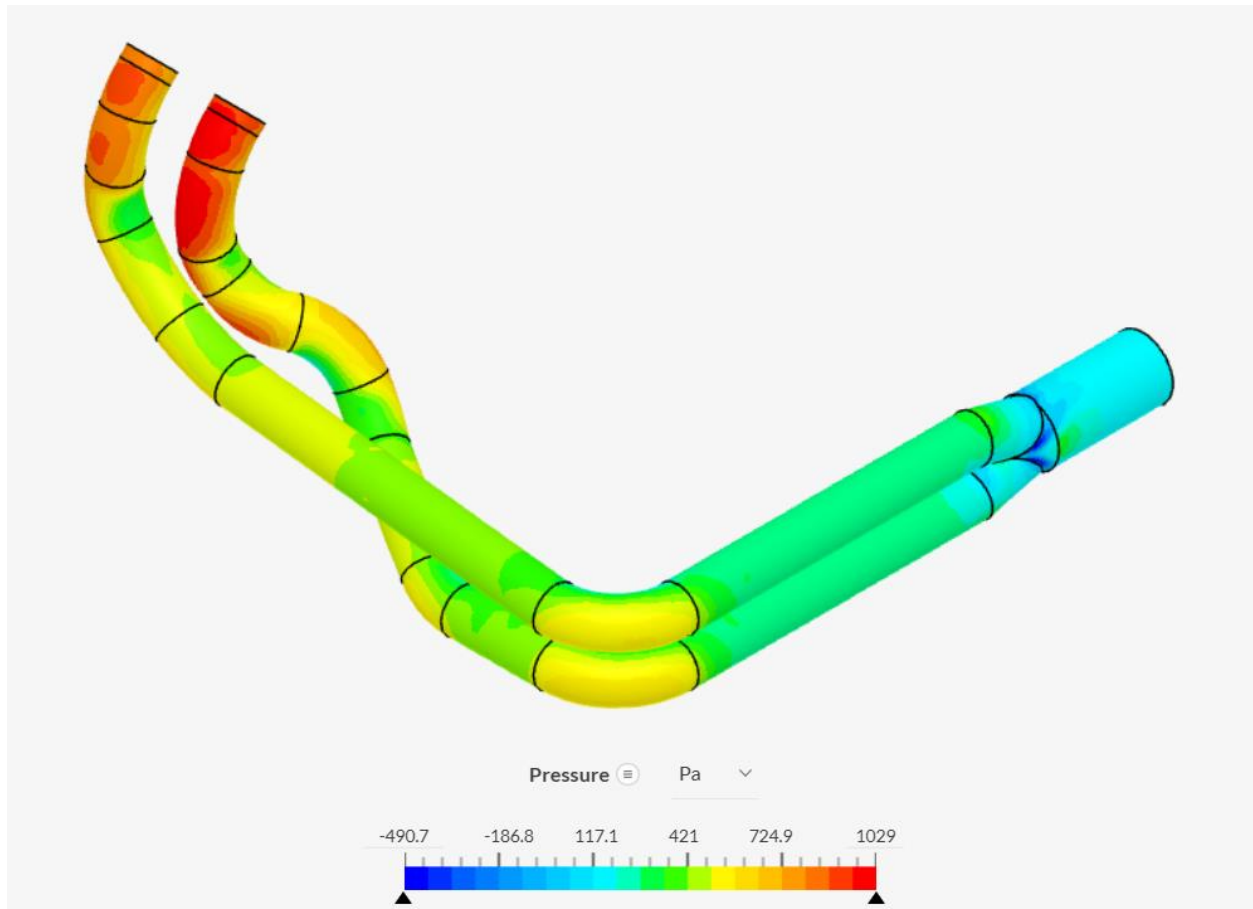


Figure 6 – Steady State Manifold Pressure

Results and Discussion

The results indicate that pressure in the field varies from approximately negative 490 Pa to just over 1029 Pa. These values are small relative to cylinder peak pressures. The spatial field of pressure indicates features of interest surrounding flow performance that will directly impact scavenging quality and pumping losses. Large pressure peaks occur just downstream of the exhaust flange and in the early bends of one of the runners. This area represents flow stagnation due to flow impingement on tube curvature, which suggests increased resistance to flow locally. In contrast, low-pressure zones exist around the collector throat and immediately downstream of the merge of the runners, suggesting local velocity acceleration and the potential for pressure recovery. These low-pressure areas are advantageous during valve overlap as they assist in drawing residual gas out of the cylinder into the collector, assisting with charge renewal. The current geometry also develops minor recirculation structures across the collector merge, indicating that the two gas streams are not fully aligned as they enter the collector. The pressure peaks within the one runner are stronger than the other runner, suggesting that geometric asymmetry, or bend radii and net effective length of the runners may lead to unbalanced pressure behavior. Consequently, scavenging behavior may vary slightly from cylinder to cylinder.

6.3.5 Camshaft Profile

The first step in making a realistic simulation of an intake manifold is to accurately represent the cycling of the intake valves. Intake valves are actuated by the lobes on the camshaft, which gives a unique motion to the opening and closing of the valve. This allows for the engine to have an air induction event that is finely calibrated to take in air for a period of time while also opening enough to take in a certain amount of air. These qualities are measured in terms of duration and lift. Duration is the amount of degrees of a crankshaft rotation that the intake valve is open for. Lift is the magnitude of length that the valve opens to. Both of these values are capable of increasing the total amount of air going into the cylinder, but each will affect the way the engine runs through its entire RPM range. This also indicates the need for an intake manifold that will work symbiotically with the camshaft profile. The camshaft profile is designed specifically for a certain running condition for the engine, and if the intake manifold can't supply air to the valvetrain in a way that complements that running condition, the engines' performance will go down.

The relationship between camshaft profile and intake manifold reinforces the idea that CFD simulations would be incomplete without factoring in camshaft profile. Camshaft profile comes directly from the geometry of the camshaft lobes, which is generally documented by the manufacturer of the engine. In the case of the chosen engine for Lumberjack's Racing, the Kawasaki Versy's 650 camshaft profile is documented in terms of duration, lift, time of opening, and time of closing [1].

Valve Timing:		Camshafts	
Inlet:		Cam Height:	
Open	25° (BTDC)	Exhaust	35.343 ~ 35.457 mm (1.3915 ~ 1.3959 in.)
Close	54° (ABDC)	Inlet	35.843 ~ 35.957 mm (1.4111 ~ 1.4156 in.)
Duration	260°		

Figure 6-9-Camshaft Profile Specifications

Based on these specifications a close approximation of the camshaft profile can be made. This starts with first laying out the valve timing for each cylinder. The specifications in figure 2 only give a general idea of when the valves open and close in relation to TDC. These must be expanded to a full four stroke cycle of 720 degrees to really understand when each valve is opening. You start with TDC of the induction stroke. This represents TDC of the first stroke in the cycle for cylinder #1, which represents 0° of crank rotation. Opening will be -25° and BDC is 180° beyond TDC so closing is $180+54=234^\circ$. This is then proven by taking the magnitude of these two numbers, coming to 259° , the same as our duration of 260° . With this information we now know that the intake valve of the first cylinder opens at -25° and closes at 234° in the 720° cycle. To then find the open and close of the second cylinder you must apply the firing order of the crankshaft. The Kawasaki Versy's 650 is a 180° twin, meaning that the second cylinder fires 180° after the first cylinder. This just means that the opening and closing of the valves for the second cylinder happen 180° after the first cylinder. Applying this you get an opening at $-25^\circ+180^\circ=155^\circ$ and a closing at $234^\circ+180^\circ=414^\circ$. With this information, the opening and closing of each intake valve is in one 4 stroke cycle.

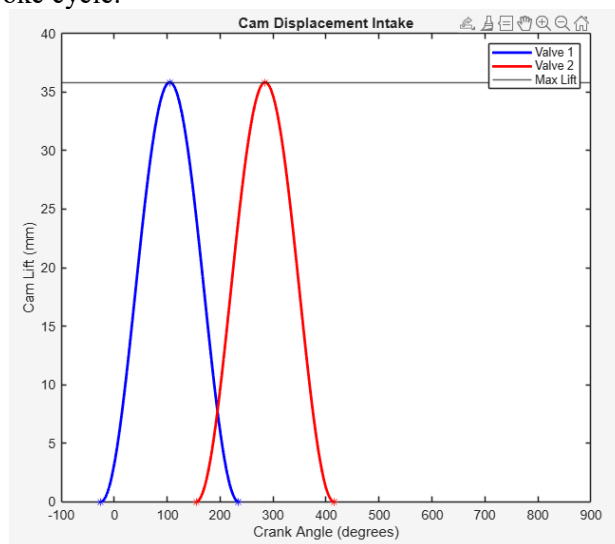


Figure 6-10- Camshaft Profile

As shown in Figure 3, a complete camshaft profile can be constructed based on the opening and closing points. Because camshaft lobes are symmetric, unless there is variable valve timing, the max lift of the camshaft will occur exactly halfway between the opening and closing of the valves. With that there is three known points in time for the action of the valve, opening, closing, and peak. Now, because there isn't any more given information, the rest of the curve that connects the 3 dots must be approximated. A simple quadratic function could suffice in showing the basic profile of the cam but doesn't simulate the opening and closing of a valve well. At open and close the valve slowly eases into the change, rather than a harsh instantaneous jerk that a quadratic relation would imply. With the lack of more geometrical information, higher order functions also cannot be used. This brings us to the Harmonic Position Function.

Harmonic Position

$$s(\theta) = \frac{h}{2} \left[1 - \cos \left(\frac{\pi\theta}{\beta} \right) \right]$$

Figure 6-11-Harmonic Position Function

Using the Harmonic function shown in Figure 4 produces graphs that have a much more realistic opening and closing profile, while retaining the realistic peak that a quadratic function has, shown in Figure 3. The beauty of this function is that it doesn't require any more information than the quadratic function but has a far more realistic profile. One thing to note is that this is a gross approximation. It does not replace measuring the physical geometry of the camshaft but acts as a placeholder until the camshaft can be measured properly, as there is a multitude of different functions that could still satisfy the three known points on the profile.

Now with a complete profile of valve lift with respect to degrees of the crankshaft, the action of the valves can be accurately predicted with respect to the crankshaft. To use this profile in CFD efficiently the crank angle needs to be converted into time. This is simply done by relating engine rpm to crank angle. We know that 1 rpm is 360° and by using this conversion you can obtain a lift vs time graph, that utilizes the exact profile already found, seen below in Figure 5.

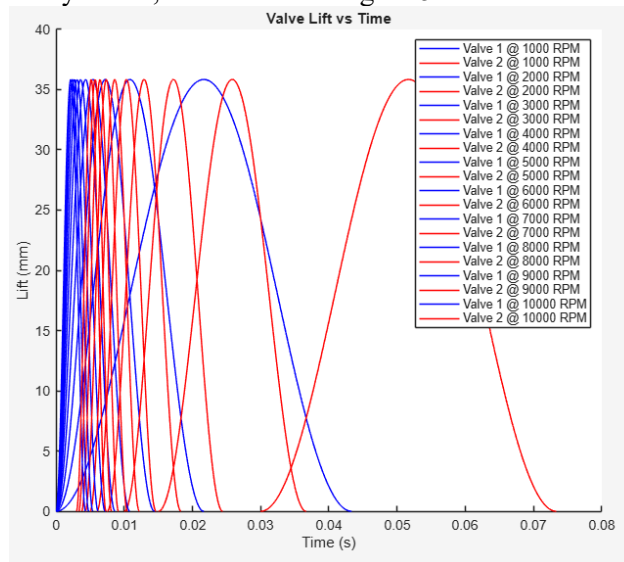


Figure 6-12- Valve Lift vs. Time

Figure 5 accurately represents the valve opening and closing with respect to time, which allows for use of the data in calculations. For CFD, a further transformation to pressure must be done, in order to use pressure drop to emulate valves opening and closing. This time, the valve lift must be transformed into pressure. This begins by making an assumption that the inlet of the intake manifold will be at atmospheric pressure. When a valve opens, there will be a subsequent pressure drop, pulling air into the plenum and through the port. This better simulates the action of the engine sucking air through the intake, rather than the intake pushing air into the engine. This assumption implies that a closed valve is atmospheric pressure, 101,325 Pa, and an open valve is less than that. A typical pressure drop from a valve opening through an intake is a 10% drop [3], implying that at max lift of the valve, the pressure will

be 10% less than atmospheric pressure. This will allow SolidWorks CFD to recognize a change in boundary condition. By equating the 0mm axis to 101,325 Pa and the max lift to $101,325 \times 0.1 = 91,192.5$ Pa from Figure 5, you can transform the graph into a Pressure vs. time graph.

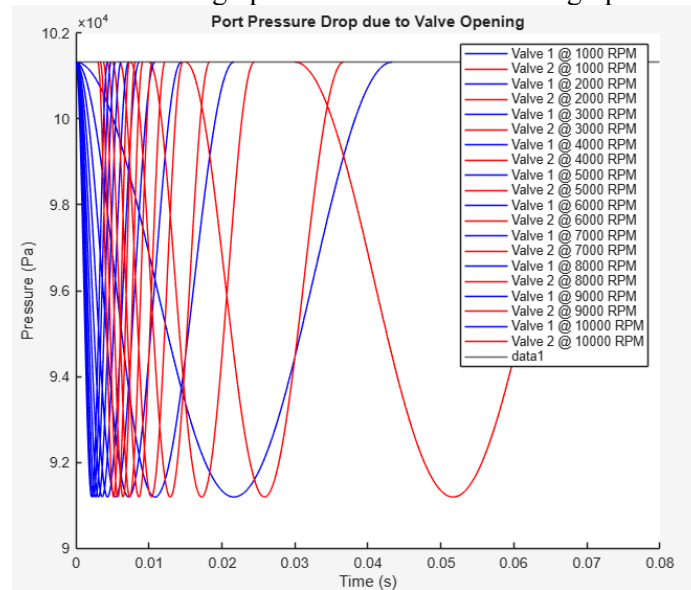


Figure 6-13- Pressure vs. Time Profile

Figure 6 represents the identical profile found at the beginning, transformed and reflected (to aid in visual understanding), showing the pressure drop from atmospheric pressure due to the valve, at exactly the time for each rpm value.

6.3.6 SolidWorks Internal Flow Simulation

By exporting the data from the graphs in Figure 6, you can run a simulation on any intake geometry for a given rpm. The data is used to represent the boundary condition of each outlet port, so that the simulation can capture the opening and closing of the valves within the intake geometry. By nature, this simulation is transient, since the boundary conditions change with time. By importing the raw table data into SolidWorks, you can assign each outlet the boundary conditions shown in the graph, allowing for a more realistic simulation.

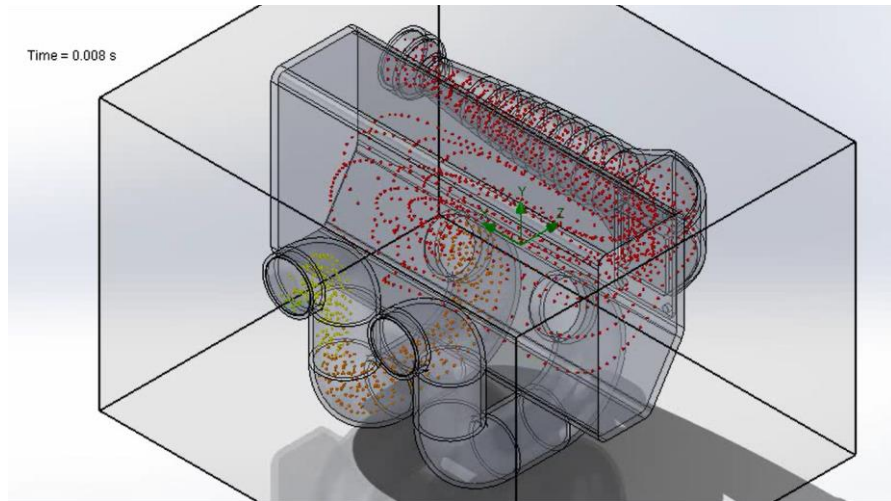


Figure 6-14- SolidWorks CFD Simulation

Videos of the dynamic simulations are seen in Figure 7 (just click or copy and paste to observe). These videos show the flow of air through the intake change from one to the other, indicating that the changing boundary conditions, are present and working. This kind of model allows the user to observe the movement of particles through the intake to get an idea of how the intake flows. It allows the user to find possible flaws in the geometry that could cause unwanted vortices and flow reversal that could hinder performance. This simulation is based on the 1000 rpm data, and it shows a very turbulent flow inside of the plenum, which could indicate a need to increase the plenum size. This is especially important to note, since the flow at higher rpm should have an even more turbulent nature, further exaggerating the geometry issue. Another key takeaway from the videos is that the bends and odd geometry of this model seem to excite the particles extensively, so it may be imperative that some geometry be adjusted to give it a straighter flow path.

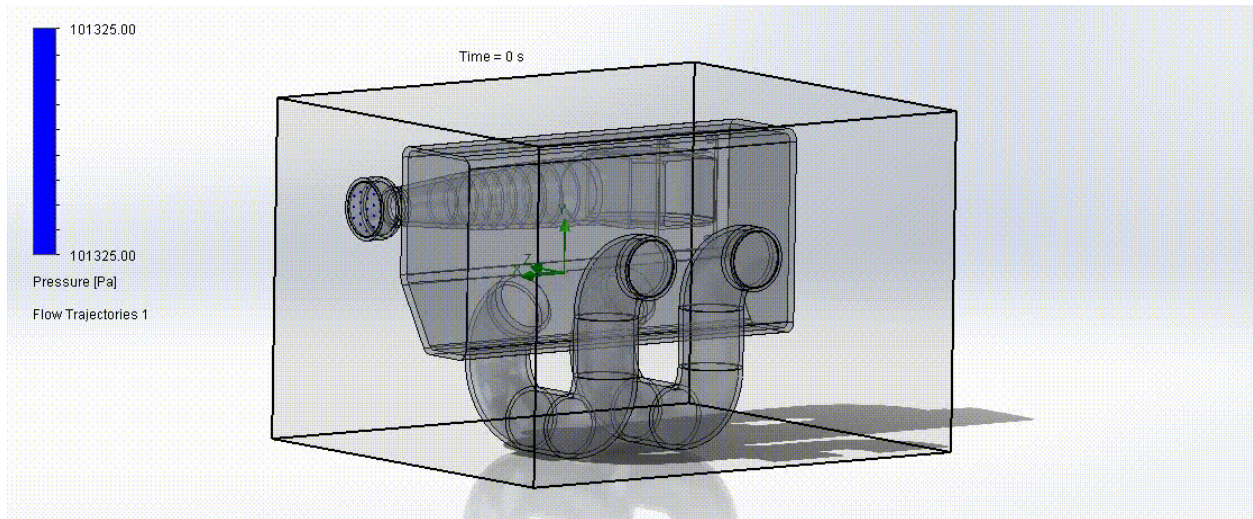


Figure 6-15- CFD isometric view

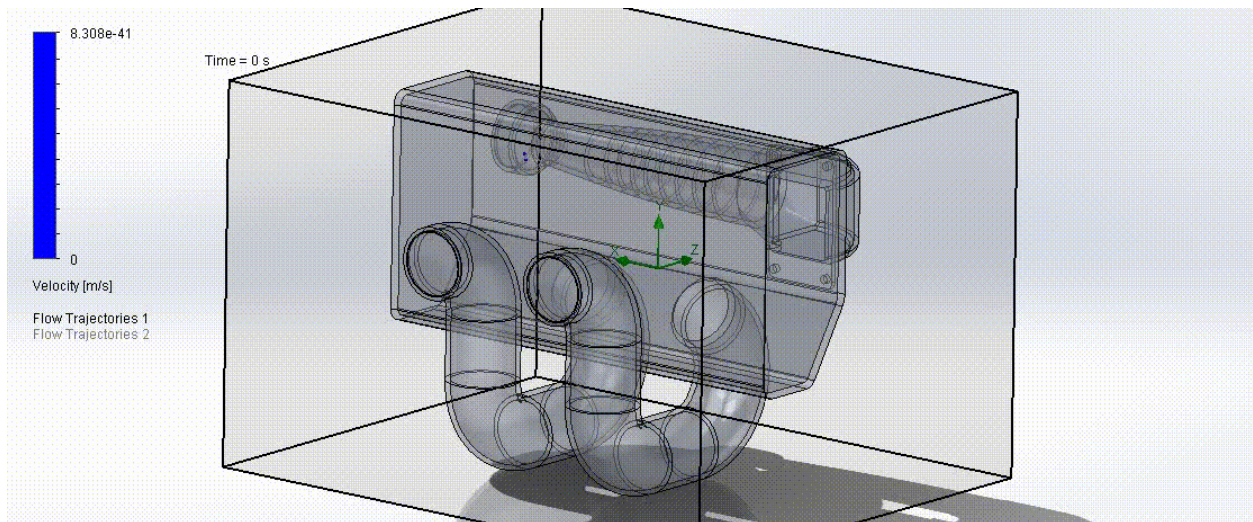


Figure 6-16- CFD isometric reversed view

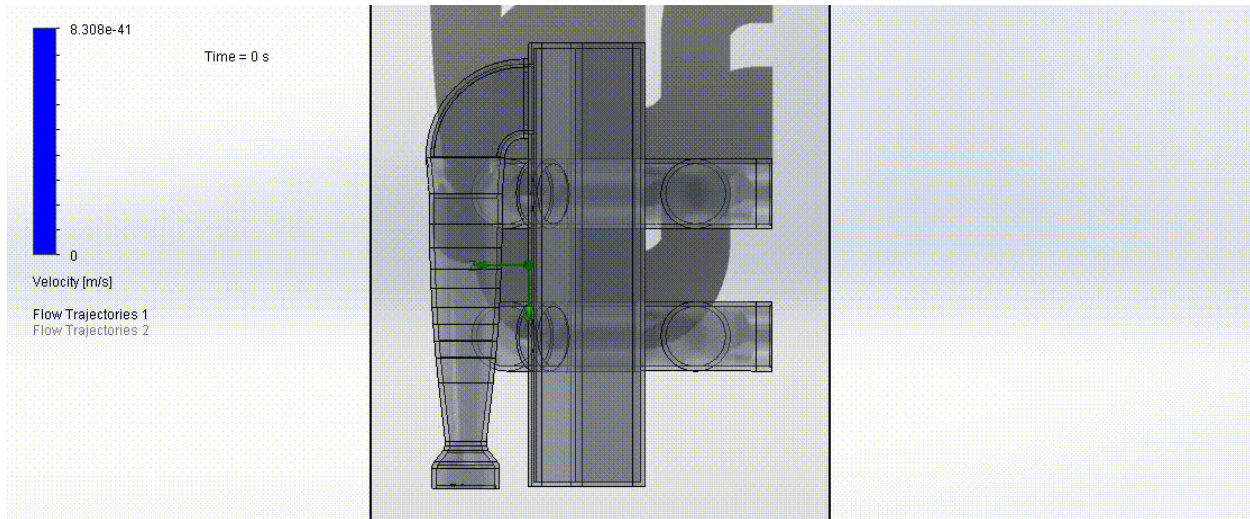


Figure 6-17- CFD top view

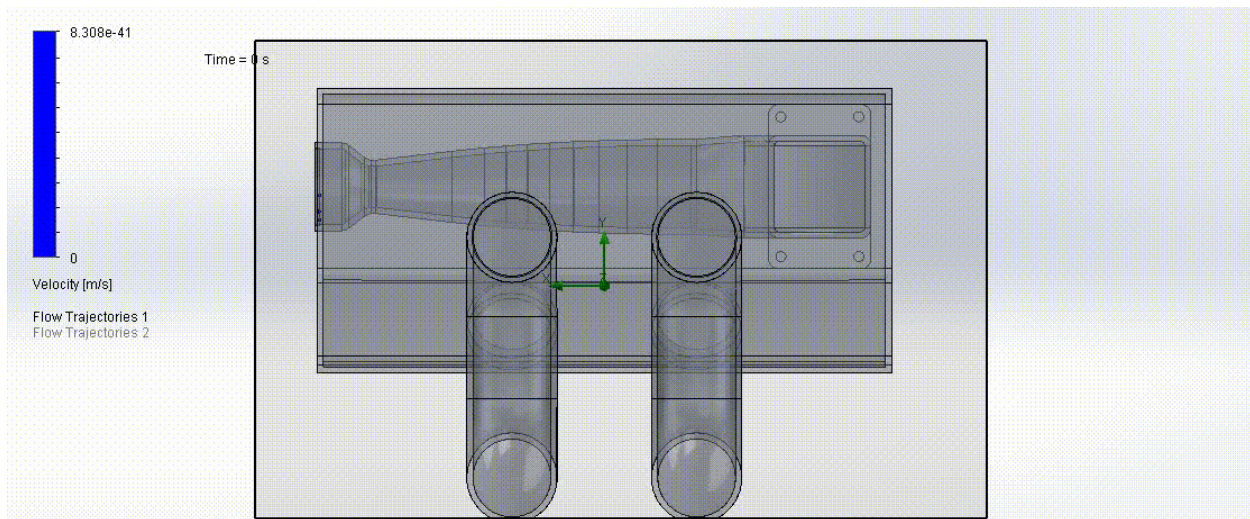


Figure 6-18- CFD side view

6.3.7 Motor Mount Tube Thickness

The thickness of tubing required to hold up the engine was to be calculated so that failure during use would not occur. The engine will be supported within the frame by four supports connected to the frame. One set of supports will be connected by a through bolt, whereas the other two will connect to the engine independently. Using this geometry, the moment induced by the engine hanging by one set of motor mounts was calculated. This moment was greater in magnitude than the moment of all four motor mounts working as intended with the torque of the engine included. The torque of the engine was not included in the hanging scenario, as the motor mount connections can be idealized as hinges. After acquiring the moment on the two supports, shear in one was found by dividing by two. The shear on one mount was calculated as $V = 93.75 \text{ lbf}$. Shear stress was found using the formula

Where V is the shear, A is the area defined by thickness, t and width, w. Solving the above equation for thickness, the following table was created with standardized tubing thicknesses.

	Shear Stress Alum (psi)	23,094	6061-T6
	Shear Stress Chromoly (psi)	28,290	A36 mild struc
	Shear (lbf)	93.75	
	w (in)	t (in)	FOS
Factory	0.031	0.1250	1.17
Chromoly	0.5	0.0066	
Chromoly	1	0.0033	
Chromoly	1.5	0.0022	
Aluminum	0.5	0.0081	
Aluminum	1	0.0041	
Aluminum	1.5	0.0027	
Selected Al	0.5	0.12	15

Figure 321 – Motor Mount Thicknesses vs OEM

Seen in the highlighted portion, Aluminum construction with a tube thickness equaling 0.5 in and a FOS of 15 was selected. This selection was made to reflect restraints on construction while saving weight. If the tube was thinner than selected, inexperienced students would likely have a hard time welding the pieces together. The material was chosen to be aluminum because it is lighter than chromoly, while remaining cost effective.

6.4

7 REFERENCES

- [1] “Honda CBR600F4 Motorcycle Specifications,” *MotorcycleSpecs.co.za*, [Online]. Available: <https://www.taylor-race.com/products/mk2-tre-quaife-atb-chain-drive-single-center-drive-no-sprocket-adapter?variant=54134113632547>. Accessed: Oct. 20, 2025.
- [2] “Kawasaki Ninja 650R,” *Wikipedia, The Free Encyclopedia*, [Online]. Available: https://en.wikipedia.org/wiki/Kawasaki_Ninja_650R. Accessed: Oct. 20, 2025.
- [3] “2014 Yamaha YZ450F Specifications,” *Motorcycle.com*, [Online]. Available: <https://www.motorcycle.com/specs/yamaha/off-road/2014/yz/450f/detail.html>. Accessed: Oct. 20, 2025.
- [4] Taylor Race, “MK2 · TRE Quaife ATB Chain Drive Differential for FSAE — Centre Drive and No Sprocket Adapter (Mk2.5 Adjustable Preload),” *Taylor Race Engineering*, [Online]. Available: <https://www.taylor-race.com/products/mk2-tre-quaife-atb-chain-drive-single-center-drive-no-sprocket-adapter?variant=54134113632547>. Accessed: Oct. 20, 2025.
- [5] Drexler Adjustable FSAE Differential V2/V3, “Drexler Automotive”, [Online]. Available: <https://autotech.com/i-30499382-drexler-adjustable-fsae-differential-v2-v3.html>. Accessed: Oct. 20, 2025.
- [6] Fab Heavy Parts, “ATV Front Differential Reducer Gearbox Q830-310000-10000 Fits for CFMOTO 500 600 800 1000 2017 2019,” *Fab Heavy Parts*, [Online]. Available: <https://www.fabheavyparts.com/products/atv-front-differential-reducer-gearbox-q830-310000-10000-fits-for-cfmoto-500-600-800-1000-2017-2019>. Accessed: Oct. 20, 2025.
- [7] R. G. Budynas and J. K. Nisbett, Shigley’s Mechanical Engineering Design, 11th ed. New York, NY, USA: McGraw-Hill, 2019. ISBN 978-0-07-339821-1.
- [8] SAE International, Formula SAE Rules 2025-v1, IC.1: “General Requirements”, VE.3: “Driver Equipment”, 31 Aug, 2025.
- [9] T. D. Gillespie, S. Taheri, C. Sandu, and B. L. Duprey, *Fundamentals of Vehicle Dynamics*. Warrendale, PA: SAE International, 2021.
- [10] “2015 Kawasaki Ninja 650 6,” *Scribd*, 2015. <https://www.scribd.com/document/776296988/2015-Kawasaki-Ninja-650-6> (accessed Sep. 14, 2025).
- [11] K. Lutenbacher, B. Mayeaux, and J. Waller, “FSAE Engine Selection: Four or One Cylinder.” Available: https://korilutenbacher.weebly.com/uploads/5/4/9/9/5499743/klutenbacher_bmayeaux_jwaller_me4633_fsa_report.pdf
- [12] MotorTrend Channel, “BIG Power from Small Block Engines! | Engine Masters | MotorTrend,” *YouTube*, Jul. 15, 2023. <https://www.youtube.com/watch?v=WAwXPMUe9JE> (accessed Sep. 10, 2025).
- [13] “Formula SAE 2025 Overall Results.” Accessed: Sep. 10, 2025. [Online]. Available: https://www.fsaeonline.com/CompResources/2025/c796a916-c2e8-4ce6-bae3-c79f36776556/FSAE_2025_MI5_results.pdf

- [14] [1]B. Singh, “- Race Car Vehicle Dynamics Milliken Milliken,” *Scribd*, 2025.
<https://www.scribd.com/document/858209436/Race-Car-Vehicle-Dynamics-Milliken-Milliken>
- [15] G. Blair, *Design and simulation of Four-Stroke Engines*. SAE International, 1999.
- [16] A. Graham. Bell, *FOUR-STROKE PERFORMANCE TUNING: 4th Edition*. 2022.
- [17] Y. Otobe, O. Goto, H. Miyano, M. Kawamoto, A. Aoki, and T. Ogawa, “Honda Formula One Turbo-charged V-6 1.5L engine,” *SAE Technical Papers on CD-ROM/SAE Technical Paper Series*, Feb. 1989, doi: 10.4271/890877.
- [18] V. Sharma, S. Hittalamane, P. Gunjal, and G. Edison, “Exhaust header designing for Formula SAE car,” 2017. <https://www.semanticscholar.org/paper/Exhaust-Header-Designing-for-Formula-SAE-Car-Sharma-Hittalamane/91196fd70b1747deae37f32b22c61aad7fcb1764>
- [19] Mr. Damien Kennedy¹ Dr. Gerry Woods², “Development Of A New Air Intake And Exhaust System For A Single Seat Race Car” ITRN 2011
- [20] Shubhamkumar Mangukiya¹ Mr. Ripen Shah², ”Enhancing The Performance Of Single Cylinder Motorcycle Engine For Formula Student Vehicle By Optimizing Intake And Exhaust System”, JETIR Volume 5, Issue
- [21] Arbaaz Sayyed, “Air Flow Optimization through an Intake System for a Single Cylinder Formula Student (FSAE) Race Car” IJERT Vol. 6 Issue 01.
- [22] J. B. Heywood, “Chapter 14: Modeling Real Engine Flow and Combustion Processes,” in *Internal Combustion Engine Fundamentals*, 2nd ed, Mcgraw Hill Education, 2018
- [23] SAE International, Formula SAE Rules 2026-Draft, IC.2: “Air Intake System” , 11 Aug, 2025
- [24] F. Leach, “The scope for improving the efficiency and environmental impact of internal combustion engines - sciencedirect,” ScienceDirect,
<https://www.sciencedirect.com/science/article/pii/S2666691X20300063> (accessed Sep. 18, 2025).
- [25] “Mass flow choking,” NASA, <https://www.grc.nasa.gov/www/k-12/airplane/mflchk.html> (accessed Sep. 18, 2025).
- [26] R. Stone, “Chapter 6: Induction and Exhaust Processes,” in *Introduction to Internal Combustion Engines*, 2nd ed, SAE Inc., 1993, pp. 231–274
- [27] D. Willy, “Formula SAE Restrictor Power Calculations.” Northern Arizona University, Flagstaff, 2024
- [28] R. Nakka, “Solid Rocket Motor Theory -- Nozzle Theory,” Richard Nakka’s Experimental Rocketry Site, https://www.nakka-rocketry.net/th_nozz.html (accessed Sep. 18, 2025).

- [29]“Figure 4: Drag and Lift coefficients of a FSAE car with different...,” *ResearchGate*, 2024. https://www.researchgate.net/figure/Drag-and-Lift-coefficients-of-a-FSAE-car-with-different-aerodynamic-packages_fig13_320556659
- [30]Caleb's Engineering Projects, “Calculate Top Speed and 0-60 of an Electric Racecar (FSAE),” *YouTube*, Sep. 08, 2020. <https://www.youtube.com/watch?v=pkWBeQO-0A8> (accessed Sep. 18, 2025).
- [31]Martin, “Engineering SPROCKET ENGINEERING DATA.” Available: <https://www.martinsprocket.com/docs/catalogs/engineering/engineering%20catalog/sprocket-engineering-data.pdf>
- [32]Tsubaki, “The Complete Guide to Chain.” Available: <https://www.ustsubaki.com/wp-content/uploads/the-complete-guide-1.pdf>
- [33]E. Neumann, “Power Limited,” *hpwizard.com*. <https://hpwizard.com/accelerating-power-limit.html>
- [34]FSAE, “FSAE Rulebook 2026 T5,” *Fsaeonline.com*, 2025. <https://www.fsaeonline.com/cdswb/gen/DownloadDocument.aspx?DocumentID=7ac1fb19-75d1-42d7-983d-ba9cd87fd092>
- [35]E. Oberg, F. Jones, H. Horton, H. Ryffel, C. Mccauley, and N. York, “Machinery’s Handbook 29 th Edition INDUSTRIAL PRESS,” 2012. Available: <https://dl.icdst.org/pdfs/files4/80364b03673ba30eb5ccf1e27e119ffc.pdf>
- [36]“Shop High Quality Kawasaki Engine Piston Kit With 83.00 MM Bore,” *JE Pistons*, Sep. 18, 2025. <https://www.jepistons.com/product/je-kawasaki-83-00-mm-bore-2-cyl-kit-3/?srsltid=AfmBOoruZq64dvVvlvqhQOSDH0Jlv9AFFL2r34nmp1iq-LF7enJ4JDTc>
- [37] Compression versus octane chart. good read! | Ski-Doo Snowmobiles Forum, <https://www.dootalk.com/threads/compression-versus-octane-chart-good-read.1322249/>
- [36]“Engine - fswiki.us,” *Fswiki.us*, 2022. https://fswiki.us/Engine#Motorcycle_engines (accessed Sep. 18, 2025).
- [37]M. Streeter, “The Suzuki RE-5 Was Supposed To Be The Future Of Motorcycles, Now It’s An Example Of A Past Failure - The Autopian,” *The Autopian*, May 04, 2023. <https://www.theautopian.com/the-suzuki-re-5-was-supposed-to-be-the-future-of-motorcycles-now-its-an-example-of-a-past-failure/> (accessed Sep. 16, 2025).
- [38]World Nuclear Association, “Heat Values of Various Fuels - World Nuclear Association,” *world-nuclear.org*, 2020. <https://world-nuclear.org/information-library/facts-and-figures/heat-values-of-various-fuels>
- [39]M. J. Moran, H. N. Shapiro, D. D. Boettner, and M. B. Bailey, *Fundamentals of engineering thermodynamics*, 8th ed. Hoboken, Nj: Wiley, 2014.
- [40] SAE International, *Formula SAE Rules 2026-Draft, T.5: “Powertrain”*, 29 Aug, 2025

- [41] F. M. White and H. Xue, Fluid Mechanics, 9th ed. New York, NY, USA: McGraw-Hill, 2021.
- [42] R. G. Budynas and J. K. Nisbett, Shigley's Mechanical Engineering Design, 11th ed. New York, NY, USA: McGraw-Hill, 2019. ISBN 978-0-07-339821-1.
- [43] A. Pandit and V. K. Chawla, "Design and manufacturing of a fuel tank for formula SAE vehicle," Materials Today: Proceedings, vol. 43, pt. 1, pp. 148–153, 2021, doi: 10.1016/j.matpr.2020.11.251.
- [44] "Engine - fswiki.us," Fswiki.us, 2022. https://fswiki.us/Engine#Motorcycle_engines (accessed Sep. 18, 2025).
- [45] M. Streeter, "The Suzuki RE-5 Was Supposed To Be The Future Of Motorcycles, Now It's An Example Of A Past Failure - The Autopian," The Autopian, May 04, 2023. <https://www.theautopian.com/the-suzuki-re-5-was-supposed-to-be-the-future-of-motorcycles-now-its-an-example-of-a-past-failure/> (accessed Sep. 16, 2025).
- [46] World Nuclear Association, "Heat Values of Various Fuels - World Nuclear Association," world-nuclear.org, 2020. <https://world-nuclear.org/information-library/facts-and-figures/heat-values-of-various-fuels>
- [47] M. J. Moran, H. N. Shapiro, D. D. Boettner, and M. B. Bailey, Fundamentals of engineering thermodynamics, 8th ed. Hoboken, Nj: Wiley, 2014.
- [48] SAE International, Formula SAE Rules 2026-Draft, T.5: "Powertrain" , 29 Aug, 2025
- [49] F. M. White and H. Xue, Fluid Mechanics, 9th ed. New York, NY, USA: McGraw-Hill, 2021.
- [50] Kawasaki Versys Manual, Kawasaki Heavy Industries, 2007.
- [51] *Introduction to Cams, Mechanical Reference*, [Online]. Available: <https://www.mechref.org/md/Cams/>. [Accessed: 25-Nov-2025].
- [52] J. B. Heywood, *Internal Combustion Engine Fundamentals*, 2nd ed. New York, NY, USA: McGraw-Hill, 1988.
- [53] *SolidWorks Flow Simulation Transient Pressure Pulse, GoEngineer*, [Online]. Available: <https://www.goengineer.com/videos/solidworks-flow-simulation-transient-pressure-pulse>. [Accessed: 25-Nov-2025].
- [54] M. F. Harrison and A. Dunkley, "The acoustics of racing engine intake systems," *Journal of Sound and Vibration*, vol. 271, no. 3–5, pp. 959–984, Apr. 2004, doi: 10.1016/S0022-460X(03)00773-9.
- [55] S. P. R. Chennadi, "Design and tuning of intake manifold by inertial and acoustic resonance effects," *International Journal for Research in Applied Science and Engineering Technology (IJRASET)*, vol. 8, no. VIII, pp. 884–890, Aug. 2020, doi: 10.22214/ijraset.2020.30884.

8 APPENDICES

8.1 Appendix A: Figures

System QFD: Powertrain

Project: QFD
Date: 09/14/25

1	Engine noise less than 103 Dbc								
2	Reduce weight of muffler	+							
3	Remove mass from intake manifold								
4	Minimize mechanical loss testing	+		++					
5	Obtain LSD with smallest impact on budget								
6	Decrease distance from fuel fill to outermost frame rail								
7	Robust throttle cable with 50mm of adjustment				+				

Legend

- A 2001 CBR600 F4i
- B 2012 Kawi Ninja 650R
- C 2014 Yamaha YZ450f

		Technical Requirements								Customer Opinion Survey				
Customer Needs		Customer Weights (1-5)	Engine noise less than 103 Dbc	Reduce weight of muffler	Remove mass from intake manifold	Minimize mechanical loss testing	Obtain LSD with smallest impact on budget	Decrease distance from fuel fill to outermost frame rail	Robust throttle cable with 50mm of adjustment	1 Poor	2	3 Acceptable	4	5 Excellent
1	Pass Tech Inspection	5	9	1	1	9	1	1	9					ABC
2	Reliable/Durable	4	1	1	3	9	3	1	9					B AC
3	Safe	5	3	1	1	9	3	3	9			AB		C
5	Limited slip rear power delivery	3	1	1	1	9	9	1	1					ABC
6	Ease of maintenance	3	1	3	3	1	1	3	3			A	B	C
7	Drivability	3	1	3	3	3	9	1	9			AB		C
8	Standardized parts	4	3	1	1	1	3	1	3					ABC
10	Make filling up fuel more accessible	5	1	1	3	1	1	9	1			A		BC
11	Lightweight car	3	1	1	9	1	1	1	1			ABC		
Technical Requirement Units			dbc	kg	kg	hp	\$	mm closer	mm					
Technical Requirement Targets			5	4	2	8	###	100	50					
Absolute Technical Importance			93	47	89	177	109	91	185					
Relative Technical Importance			11.8%	6%	11.3%	22%	14%	12%	23%					

Figure 8-1 - QFD

Enter the max rpm value: 8500
Enter the number of teeth on the front sprocket: 17
Enter the number of teeth on the rear sprocket: 36
Top Speed in 1st gear: 78.37 mph
Top Speed in 2nd gear: 111.47 mph
Top Speed in 3rd gear: 143.33 mph
Top Speed in 4th gear: 171.97 mph
Top Speed in 5th gear: 197.79 mph
Top Speed in 6th gear: 224.25 mph

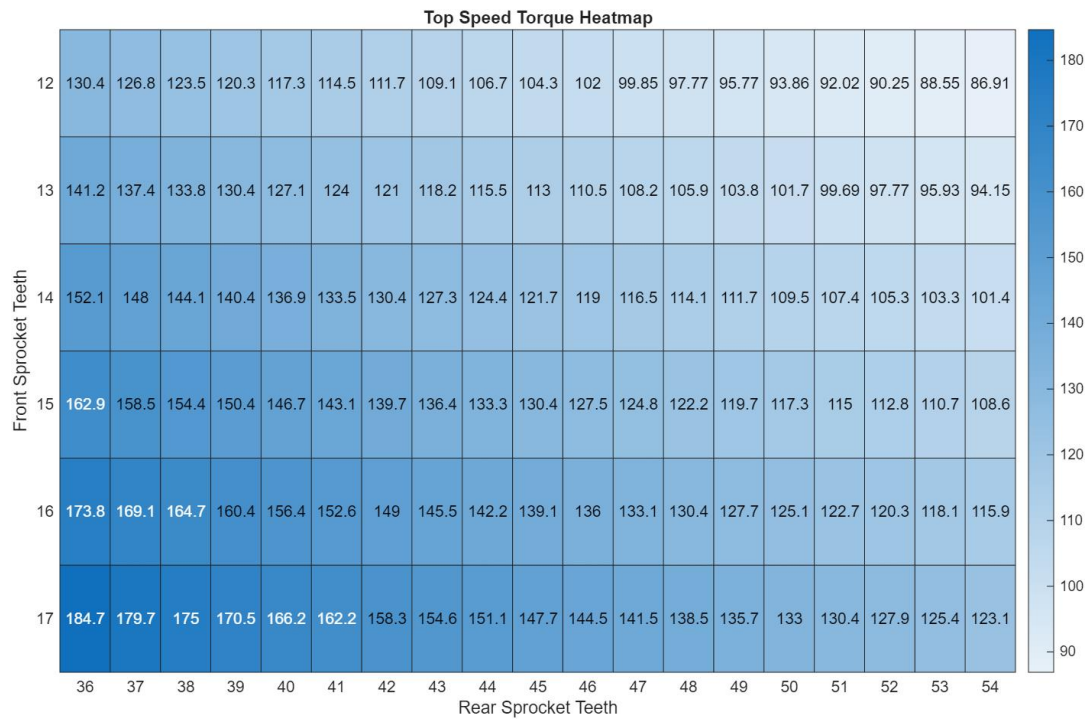


Figure 3-8-2: Theoretical Top Mechanical Speeds

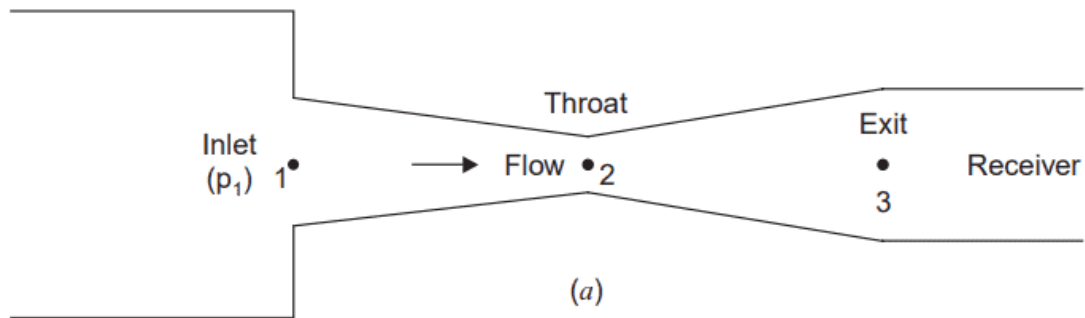


Figure 8-3 - Air Restriction Diagram

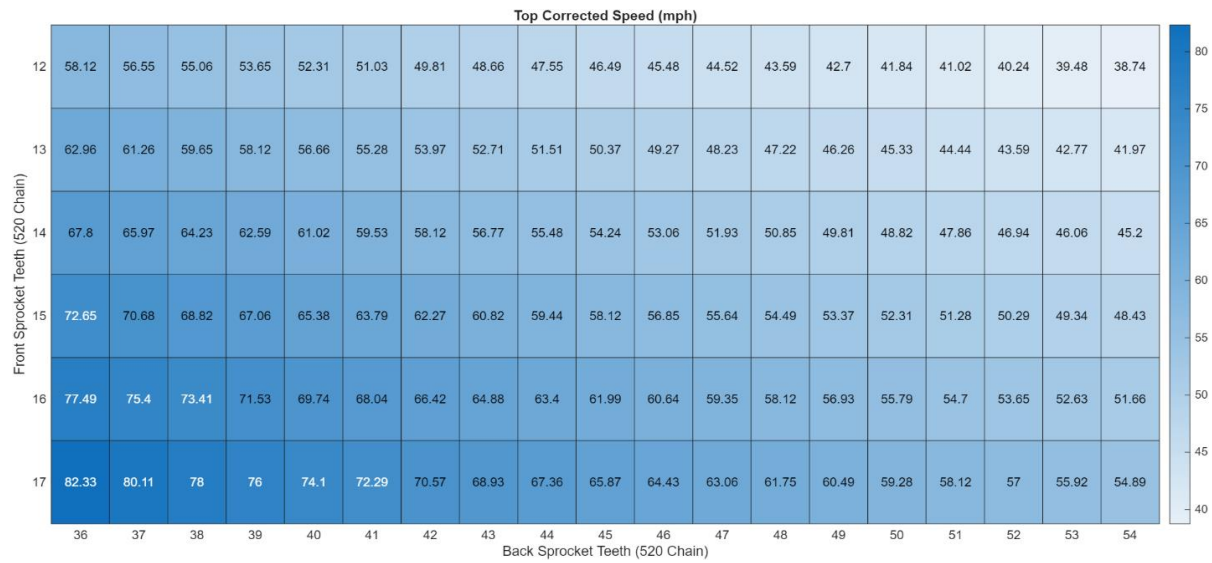


Figure 8-4: Top Corrected Speed in mph, with resistance

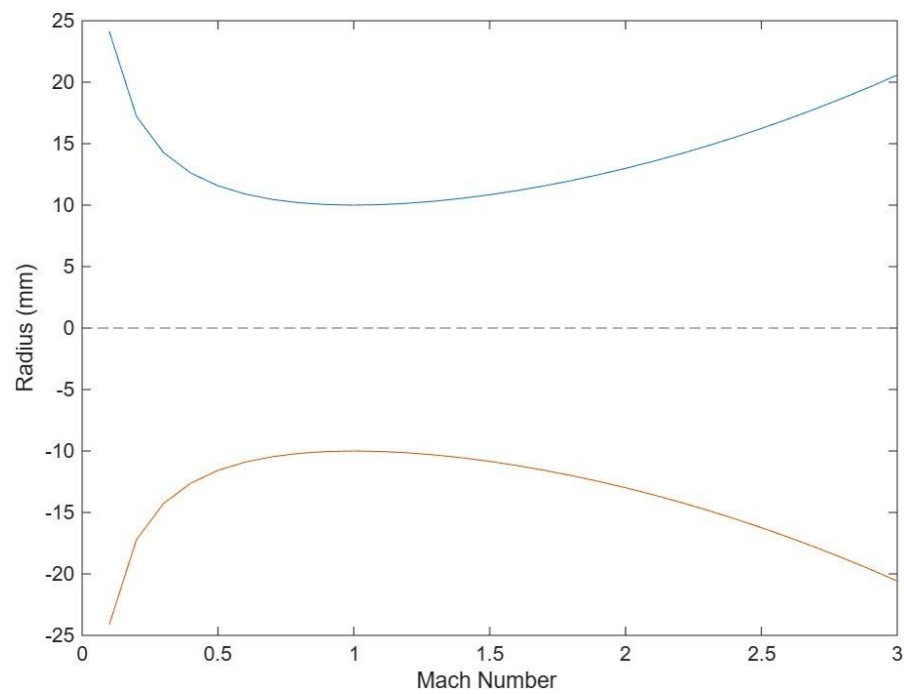


Figure 8-5 - Radius Vs. Mach Number

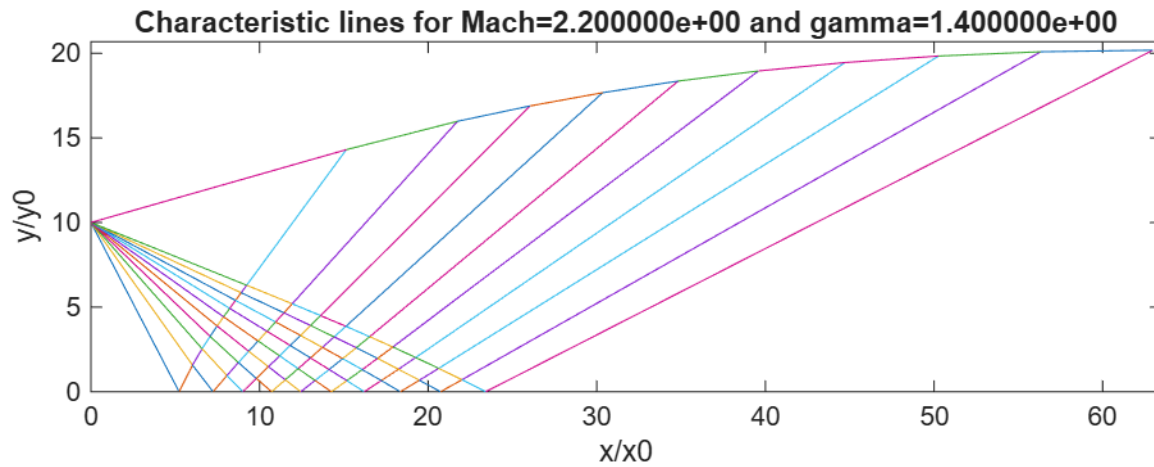


Figure 8-6 - Method of Characteristics Divergent Section

Aluminum alloy, wrought, 6061, T6

User defined name	Aluminum alloy, wrought, 6061, T6
State	Solid
Density	2710 kg/m ³
Viscosity	0 Pa·s
Thermal expansion coefficient	2.28e-5 1/°C
Isotropic thermal conductivity	155 W/m·K
Specific heat	0.916 kJ/kg.C
Description	Aluminum, 6061, T6, wrought Data compiled by Ansys Granta, incorporating various sources including JAHM and MagWeb. ANSYS, Inc. provides no warranty for this data.
Class	Metals - non-ferrous
Subclass	Aluminum alloys

Figure 8-7; Aluminum Parameters for Intake Simulation

User defined name	Air
State	Gas
Density	1.16 kg/m ³
Viscosity	1.83e-5 Pa·s
Thermal expansion coefficient	0.00333 1/°C
Isotropic thermal conductivity	0.0258 W/m·K
Specific heat	1.02 kJ/kg·C
Description	Gas, Air Data compiled by Ansys Granta, incorporating various sources including JAHM and MagWeb. ANSYS, Inc. provides no warranty for this data.
Class	Fluids
Subclass	Gases

Figure 8-8: Air parameters for intake simulations

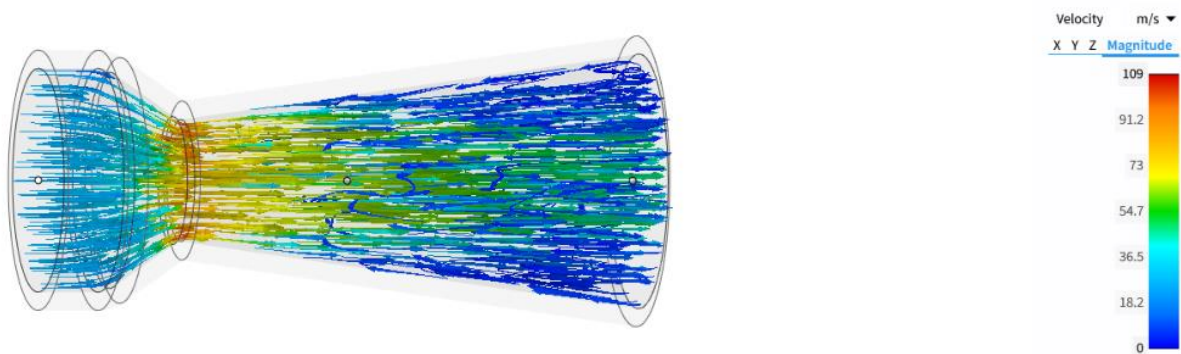


Figure 3-8-9; 77 mm de Laval Nozzle

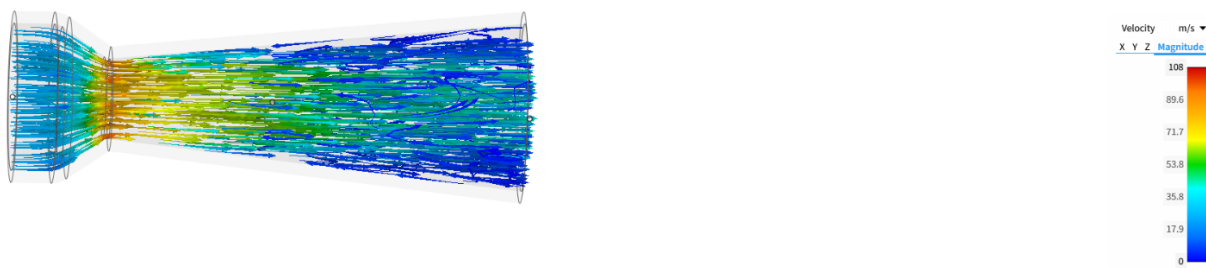


Figure 8-10; 89 mm de-Laval Nozzle

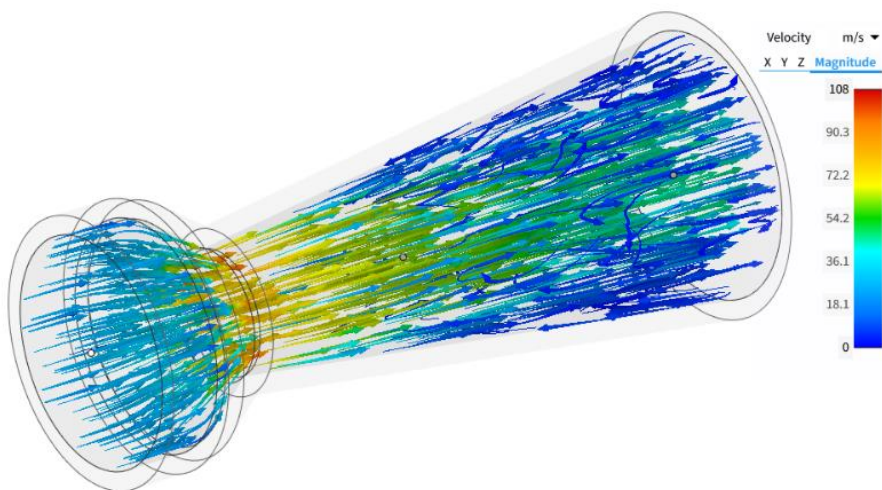


Figure 3-8-11; 104 mm de-Laval Nozzle

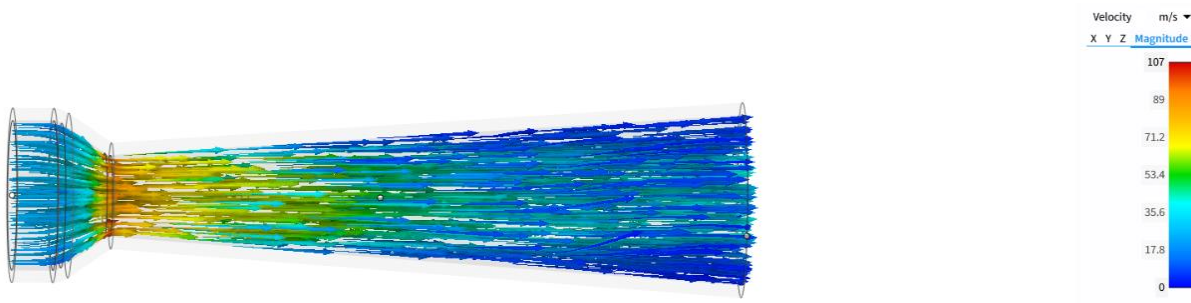


Figure 3-8-12; 153 mm de-Laval Nozzle

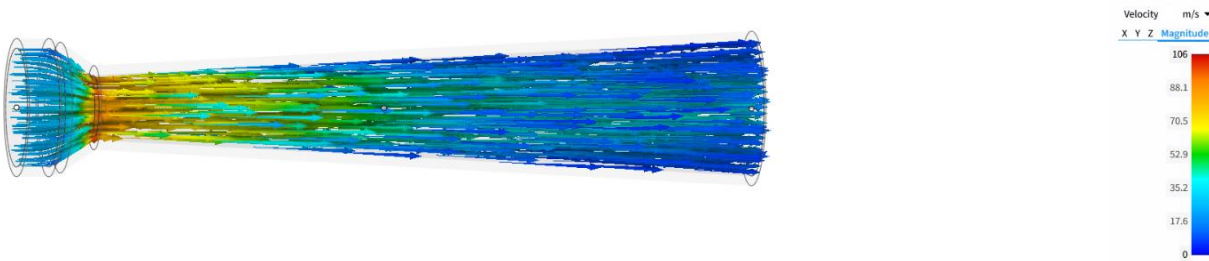


Figure 3-10; 208 mm de-Laval Nozzle

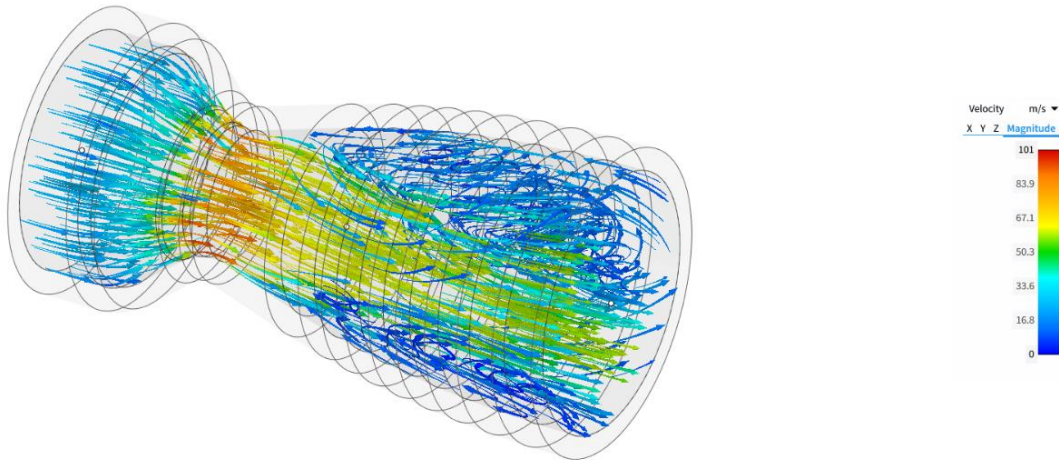


Figure 3-11; 63mm Bell Nozzle

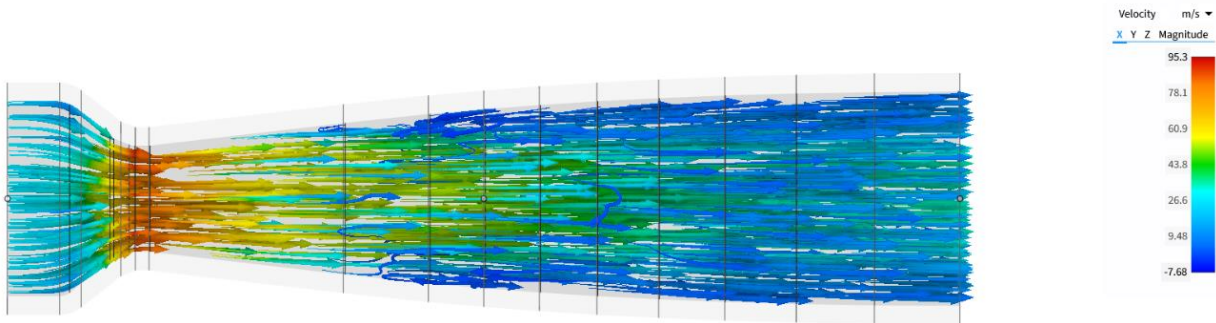


Figure 3-12; 153 mm Bell Nozzle

Command Window
 Limit reached at 75 HP
 Last valid mdotair = 0.073743 kg/s

Figure -13 - Horsepower Threshold

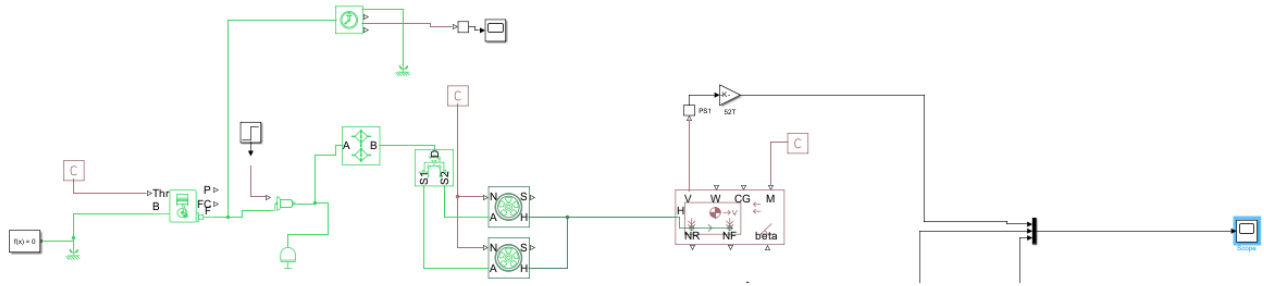


Figure 3-14 Vehicle Model in Simulink

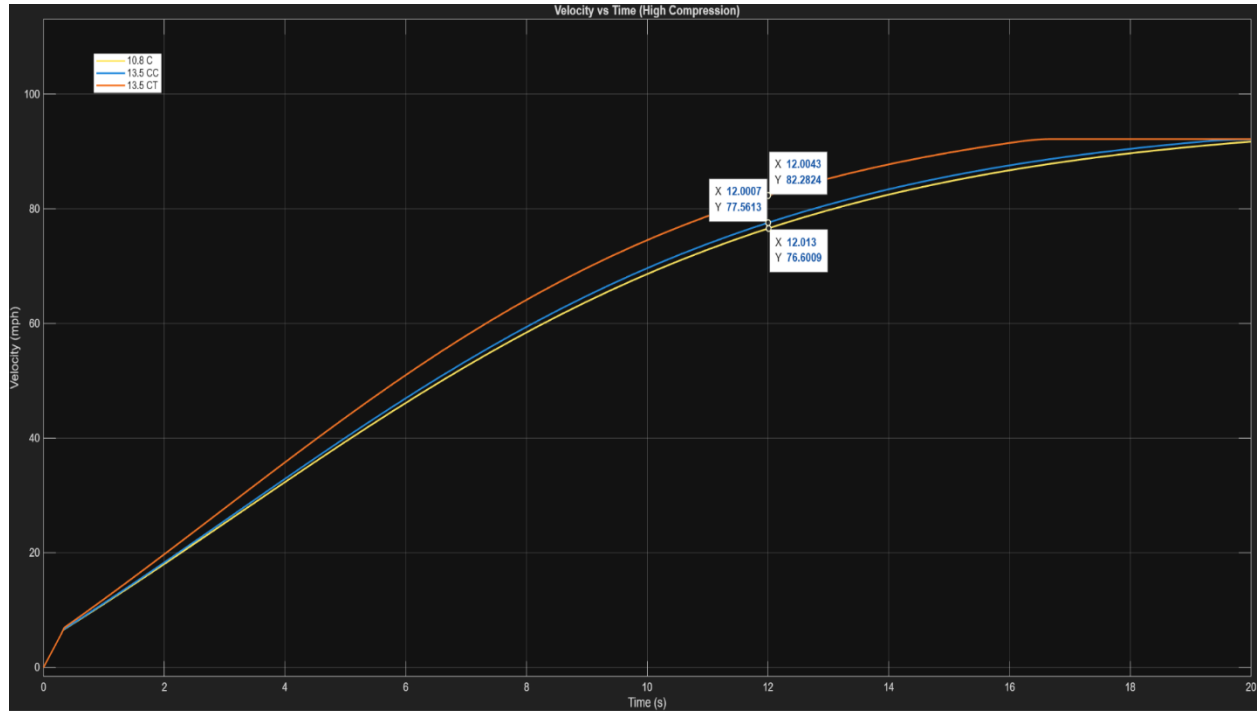


Figure 3-15 Velocity vs Time for Various Compression ratios

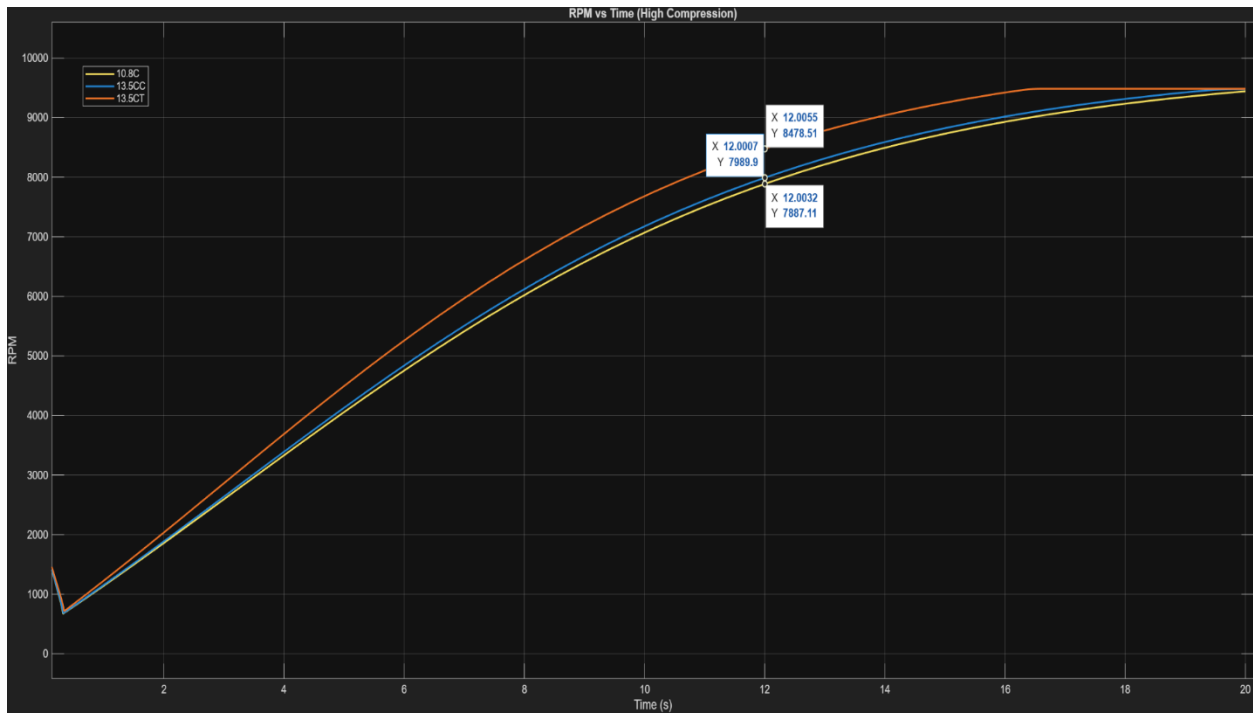


Figure 3-16 RPM vs Time for Various Compression ratios

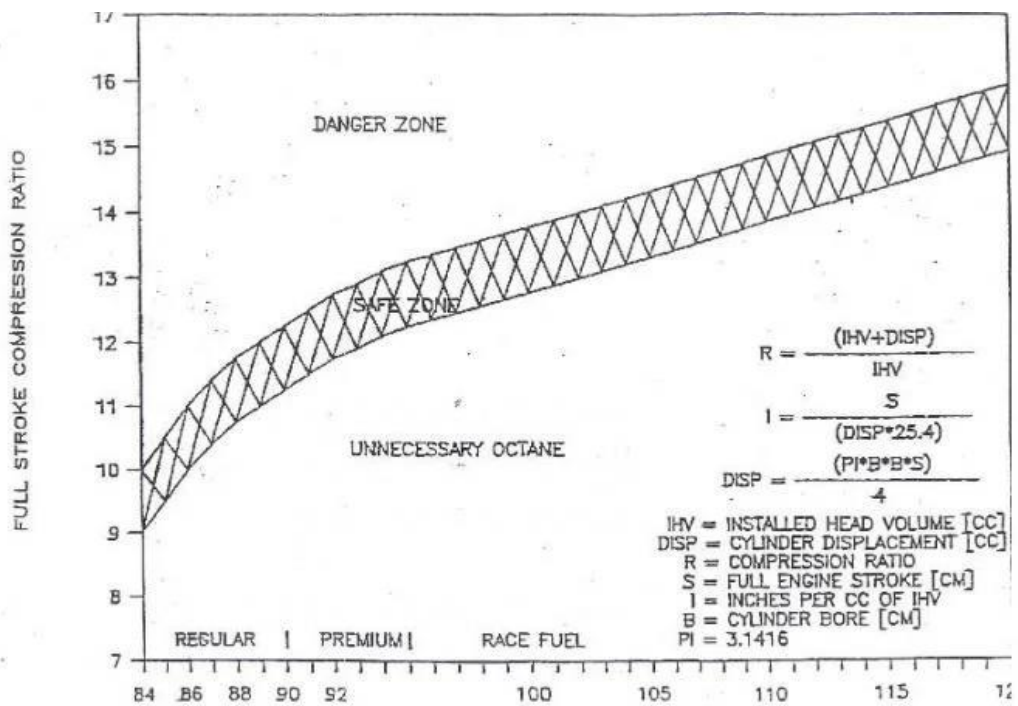


Figure -17 - Octane Vs. Compression Ratio

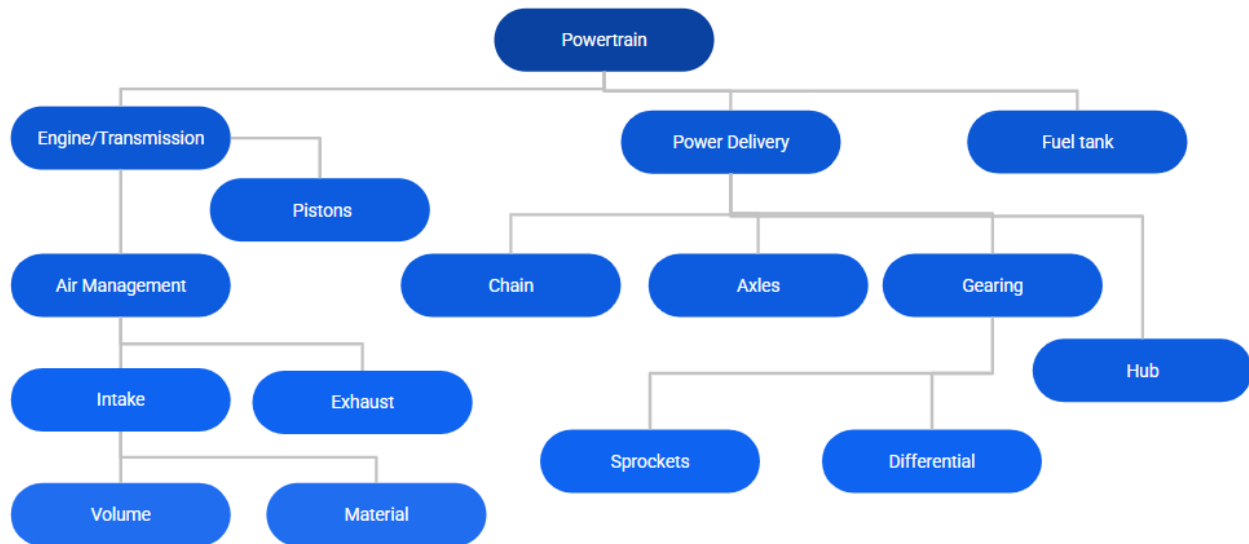


Figure 4-1







	Solution		
Subsystem	1	2	3
Engine			
	Yamaha 450F	Kawasaki 650R	Honda CBR 600
Differential			
	Drexler	Taylor V2	ATV OE




Figure 4-2: Morphological matrix of Engine and Differential Options

Motor Mounts	 A close-up photograph of a solid metal motor mount being installed into a larger metal structure.	 A person's hands are shown applying a red silicone sealant from a tube into a hole in a metal component.	 Three black, standard motor mounts are shown on a light-colored surface.
	Solid	High Stiffness Silicone	Standard
Cooling	 A black electric fan is mounted on top of a silver radiator.	 A black, perforated radiator cover is shown in front of a motorcycle.	 A side view of a go-kart with a red and white livery, featuring the text 'CARDIFF UNI' on its side panel.
	Fan over radiator	No fan	No Fan with aero Package

Figure 8-13 showing radiator and motor mount options

Intake Material			
	Aluminum	Plastic	Composite Printed Plastic w/ Strengthening
Fuel Tank			
	Stainless	Plastic	Aluminum

Figure 4-4; Intake and Fuel Tank Morphological Matrix

Exhaust			
	Side Exit	Rear Exit	Dual Side Exit

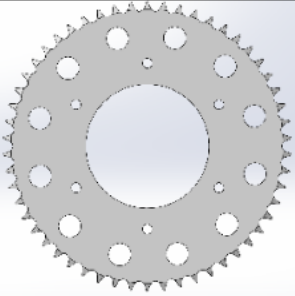
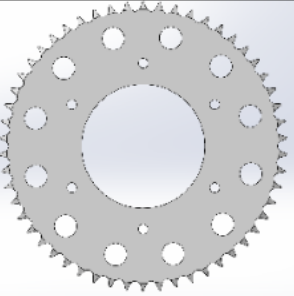
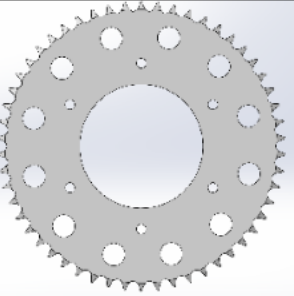
Rear Sprocket Count			
	36-42	42-48	48-54

Figure 4-2; Morphological Matrix with Every Part Choice

8.2 Appendix B: Tables

Engine	2001 Honda CBR600 F4i [1]	2012 Kawi Ninja 650R [2]	2014 Yamaha YZ450f [3]
<i>Stock Hp</i>	<i>110 Hp @ 12,500 rpm</i>	<i>72.1 Hp @ 8,500 rpm</i>	<i>58 Hp @ 9,900 rpm</i>
<i>Weight (lbs)</i>	<i>Heaviest</i>	<i>Medium</i>	<i>Lightest</i>
<i>Displacement (cc)</i>	<i>599</i>	<i>649</i>	<i>449</i>
<i>Peak Torque (lb-ft) (RPM)</i>	<i>48 lb-ft @ 10,500 rpm</i>	<i>48.6 lb-ft @ 7,000 rpm</i>	<i>35 lb-ft @ 7,300 rpm</i>

Table -1 - Engine Specifications

Differential	Taylor Race Engineering V2 [4]	Drexler V2/V3 [5]	Modified ATV [6]
<i>Cost</i>	\$2,450	\$3,656	~\$500
<i>Weight (lbs)</i>	8.9	5.9	11-21
<i>Further Drivetrain Support (Y/N)</i>	Y	Y	N

Table -2 - Differential Specifications

Name	Length of Divergent section (mm)	Type	Max Pressure Drop (Pa)
Strt_throat_1	104	De-Laval	466
Strt_throat_2	77	De-Laval	569
Strt_throat_3	89	De-Laval	532
Strt_throat_4	153	De-Laval	444
Strt_throat_5	208	De-Laval	471
MOC_throat_1	63	Bell	786
MOC_throat_2	153	Bell	412

Table -3

8.3 Appendix C: Equations

$$\omega_e = N_t * N_f * \omega_w \quad \frac{\omega_e}{(N_t * N_f)} = \omega_w$$

$$V_x = \omega_w * r$$

Equation 3-1 - Speed Equations

From equation (1) and **equation (1b) from the accelerating page**, we get: [\(more\)](#)

$$v_{max} = \sqrt[3]{\frac{q}{2} + \sqrt{\frac{q^2}{4} + \frac{p^3}{27}}} + \sqrt[3]{\frac{q}{2} - \sqrt{\frac{q^2}{4} + \frac{p^3}{27}}} \quad (9)$$

Where:

$$q = \frac{P_t}{0.5\rho (C_D A - f_r C_L A)} \quad (9.1)$$

$$p = \frac{f_r m g}{0.5\rho (C_D A - f_r C_L A)} \quad (9.2)$$

Equation 3-2- Top Speed with Resistance

$$\dot{m} = \frac{p_o A^*}{\sqrt{T_o}} \sqrt{\frac{\gamma}{R} \left[\frac{2}{\gamma + 1} \right]^{\left(\frac{\gamma + 1}{\gamma - 1} \right)}}$$

Equation 3-4 - Choked Flow Rate Formula

$$\frac{A}{A^*} = \frac{1}{M} \left(\frac{1 + \frac{k-1}{2} M^2}{1 + \frac{k-1}{2}} \right)^{\frac{k+1}{2(k-1)}}$$

Equation 3-5 - Area Ratio for Rocket Nozzle

$$\dot{m}_{fuel} = \frac{Power}{LHV * \eta_{thermal}}$$

Equation - - Power Formula

$$Q_{t,intake} = \frac{V_T \cdot N}{2 \cdot 60} \cdot V_E$$

Equation 3-7 - Intake Volumetric Flow Rate-

$$\rho_i = \frac{P}{R \cdot T_i}$$

Equation -8 – Intake Air Density

$$\dot{m}_{air} = \rho_i \cdot Q_{t,intake}$$

Equation 3-9 – Intake Mass Flow Rate

$$Q_{t,exhaust} = \frac{\dot{m}_{air} \cdot R \cdot T_e}{P}$$

Equation 3-10 – Exhaust Volumetric Flow Rate

$$Q_{c,exhaust} = \frac{Q_{t,exhaust}}{n_{cyl}}$$

Equation 3-11 – Volumetric Flow Rate per Cylinder Runner Area

$$A_r = \frac{Q_{c,exhaust}}{v_{target}}$$

Equation 3-12 –

$$\phi = \frac{AFR_{stoich}}{AFR}$$

Equation 3-13 – AFR Equivalency Ratio

$$y_i = \frac{n_i}{\sum n_i}, \quad i = CO_2, H_2O, O_2, N_2, CO$$

Equation 3-14 – Mole Fraction of Exhaust

$$C_{p,mix} = \sum_i y_i \cdot C_{p,i}(T)$$

Equation 3-15 – NASA Glenn's polynomials

$$R_{mix} = \frac{R_u}{MW_{mix}}$$

Equation 3-16 – Gas Constant

$$\gamma = \frac{C_{p,mix}}{C_{p,mix} - R_{mix}}$$

Equation 3-17 – Specific Heat Ratio

$$a = \sqrt{\gamma \cdot R_{mix} \cdot T}$$

Equation 3-18

$$L = \frac{a \cdot 120}{N}$$

Equation 3-19

$$\sqrt{\left(\frac{\sigma_x - \sigma_y}{2}\right)^2 + \tau_{xy}^2}$$

Equation 3-20

8.4 Appendix D: Matlab

```
%%%%%%%%%%%%%%%%%%%%%%%%%%%%%%%%%%%%%%%%%%%%%%%%%%%%%%%%%%%%%%%%%%%%%%%%%%%%%%
%% Written by: Liam O'Connor %%%%%%%%%
%%% Title: Max Restrictor Flow calculation and Max horsepower before Choked
%%% Flow
%%%%%%%%%%%%%%%%%%%%%%%%%%%%%%%%%%%%%%%%%%%%%%%%%%%%%%%%%%%%%%%%%%%%%%%%%%%%%%5
%%%%%%%%%%%%%%%%%%%%%%%%%%%%%%%%%%%%%%%%%%%%%%%%%%%%%%%%%%%%%%%%%%%%%%%%%%%%%%
%           Restrictor maximum flow rate calulation
%%%%%%%%%%%%%%%%%%%%%%%%%%%%%%%%%%%%%%%%%%%%%%%%%%%%%%%%%%%%%%%%%%%%%%%%%%%%%%
clc
A=0.00031415; % m^2 x-section at throat
y=1.4; % specific heat at 294K
t=300; % Kelvin temp at inlet
p=101325; % Pascal Pressure at inlet
r=287; % gas constant
m=(p*A)/(sqrt(t));
n=(y/r)*((2/(y+1))^( (y+1)/(y-1) ));
m_max=m*(sqrt(n)); %maximum mass flow rate through restrictor (kg/s)
%%%%%%%%%%%%%%%%%%%%%%%%%%%%%%%%%%%%%%%%%%%%%%%%%%%%%%%%%%%%%%%%%%%%%%%%%%%%%%
%%%%%%%%%% Max Horsepower Before Choked Flow %%%%%%%%%%%
%%%%%%%%%%%%%%%%%%%%%%%%%%%%%%%%%%%%%%%%%%%%%%%%%%%%%%%%%%%%%%%%%%%%%%%%%%%%%%
LHV=44; % low heating value for 87-93 octane 44-46 MJ/kg
https://world-nuclear.org/information-library/facts-and-figures/heat-values-of-various-fuels
AFR=14.7; %% Air Fuel ratio
eth=0.25; %thermal efficiency
mdotair=NaN; %initializing mdotair
last_mdotair = NaN; %initializing last_mdotair
for HP=30:1:120 %Horsepower
    power=HP*0.0007457;%conversion from horsepower to MegaWatt
    mdotfuel=power/(LHV*eth); %calc mdotfuel
    mdotair=mdotfuel*AFR; % mass flow rate of air

    if mdotair>m_max
        fprintf('Limit reached at %d HP\n',HP);
        fprintf('Last valid mdotair = %.6f kg/s\n', last_mdotair);
        break
    end
    last_mdotair=mdotair;
end
```

```

%%%%%%%%%%%%%%%%%%%%%%%%%%%%%%%%%%%%%%%%%%%%%%%%%%%%%%%%%%%%%%%%%%%%%%%%%%%%%%
% Written by: Marshall Fritz
% Title: Exhaust Diameter Calculations Based on Ideal Gas Law
%%%%%%%%%%%%%%%%%%%%%%%%%%%%%%%%%%%%%%%%%%%%%%%%%%%%%%%%%%%%%%%%%%%%%%%%%%%%%%
%
% Exhaust Diameter Calculation
%%%%%%%%%%%%%%%%%%%%%%%%%%%%%%%%%%%%%%%%%%%%%%%%%%%%%%%%%%%%%%%%%%%%%%%%%%%%%%
clc; clearvars; close all;
% USER INPUTS
V_T_cc = input('Enter total engine displacement [cc]: ');
N = input('Enter target engine speed [rpm]: ');
VE = input('Enter volumetric efficiency (0-1): ');
v_target = input('Enter target mean runner velocity [m/s]: ');
n_cyl = input('Enter number of cylinders: ');
T_i = input('Enter Intake temp [C]:') + 273; % Convert to K
T_e = input('Enter Exhaust temp [C]:') + 273; % Convert to K
P_atm = input('Enter Air Pressure [atm]:');
% CONSTANTS
R = 287; % J/kg·K
P = P_atm * 101325; % Convert pressure from atm to Pa
% CALCULATIONS
V_T = V_T_cc * 1e-6; % Total engine displacement [m^3]
Qt_intake = (V_T * N / (2*60)) * VE; % Total intake flow [m^3/s]
rho_i = P / (R * T_i); % Density of Intake Air [kg/m^3]
m_dot_air = rho_i * Qt_intake; % Mass Flow Rate of Air [kg/s]
Qt_exhaust = (m_dot_air * R * T_e)/P; % Total exhaust volumetric flow [m^3/s]
Qc_exhaust = Qt_exhaust / n_cyl; % Per-cylinder exhaust volumetric flow [m^3/s]
A_r = Qc_exhaust / v_target; % Runner area [m^2]
d_r = sqrt(4*A_r/pi)*1000; % Runner diameter [mm]
A_col = n_cyl * A_r; % Collector area [m^2]
d_col = sqrt(4*A_col/pi)*1000; % Collector diameter [mm]
% OUTPUT
fprintf('\nExhaust Sizing Results\n');
fprintf('Runner Diameter: %.1f mm\n', d_r);
fprintf('Collector Diameter: %.1f mm\n', d_col);
fprintf('Total Exhaust Volumetric Flow Rate: %.3f m^3/s\n', Qt_exhaust);

```

```

% Kawasaki Ninja 650
% peak torque occurs at 7000 rpm
% peak power occurs at 8500 rpm
% input for new bikes
RPM = input('Enter the max rpm value: '); % rev/min
% input for sprocket size
fsprocket = input('Enter the number of teeth on the front sprocket: ');
rsprocket = input('Enter the number of teeth on the rear sprocket: ');
FR = rsprocket/fsprocket; %final drive ratio
g1 = 2.438;
g2 = 1.714;
g3 = 1.333;
g4 = 1.111;
g5 = 0.966;
g6 = 0.852;
rear_r = 16/2; % rear radius in inches (Wheel+tire)
% Calculate the wheel rotational speed for each gear
% first gear
g1wheel = ((RPM*2*pi)/60)/(g1*FR);
g2wheel = ((RPM*2*pi)/60)/(g2*FR);
g3wheel = ((RPM*2*pi)/60)/(g3*FR);
g4wheel = ((RPM*2*pi)/60)/(g4*FR);
g5wheel = ((RPM*2*pi)/60)/(g5*FR);
g6wheel = ((RPM*2*pi)/60)/(g6*FR);

%convert wheel speed to ground speed using wheel radius and convert units to
% mph
speed1 = ((g1wheel * rear_r)/12)*(3600/5280);
speed2 = ((g2wheel * rear_r)/12)*(3600/5280);
speed3 = ((g3wheel * rear_r)/12)*(3600/5280);
speed4 = ((g4wheel * rear_r)/12)*(3600/5280);
speed5 = ((g5wheel * rear_r)/12)*(3600/5280);
speed6 = ((g6wheel * rear_r)/12)*(3600/5280);

% Display the calculated speeds for each gear
fprintf('Top Speed in 1st gear: %.2f mph\n', speed1);
fprintf('Top Speed in 2nd gear: %.2f mph\n', speed2);
fprintf('Top Speed in 3rd gear: %.2f mph\n', speed3);
fprintf('Top Speed in 4th gear: %.2f mph\n', speed4);
fprintf('Top Speed in 5th gear: %.2f mph\n', speed5);
fprintf('Top Speed in 6th gear: %.2f mph\n', speed6);

```

```

%%%%%%%%%%%%%%%%%%%%%%%%%%%%%%%%%%%%%%%%%%%%%%%%%%%%%%%%%%%%%%%%%%%%%%%%
%%PROGRAM: TOPSPEED
%%PROGRAMMER: TRENT GREENE
%%%%%%%%%%%%%%%%%%%%%%%%%%%%%%%%%%%%%%%%%%%%%%%%%%%%%%%%%%%%%%%%%%%%%%%%
clear all ; clc;
%PARAMETERS
output_torque = 48.679; %lb-ft, dependent on motor
max_torque_rpm = 7000; %rpm
engine_horsepower = 72.1;% dependent on motor
engine_kW = engine_horsepower / 1.34102; %in kW
engine_torque_standard = 47.2 %lb-ft

engine_torque_standard =
47.2000

engine_torque_metric = engine_torque_standard / 1.34102;
max_horsepower_rpm = 8500; %rpm
front_sprocket_teeth = [12:1:17]; %cycles through available sprocket sized from
taylor fsae catalog
back_sprocket_teeth = 36:1:54; %same as above, this goes on diff
tire_diameter = 16; %inches, this is up for debate; from Hoosier catalog for FSAE
trans_gear_ratio = 0.852; %in final gear (6th for 6 speed)
%%%%%%%%%%%%%%%%%%%%%%%%%%%%%%%%%%%%%%%%%%%%%%%%%%%%%%%%%%%%%%%%%%%%%%%%
%EQUATIONS
tire_circumference = pi * tire_diameter / 12; %tire circumference in feet
topspeed_torque = zeros(length(front_sprocket_teeth), length(back_sprocket_teeth));
topspeed_power = zeros(length(front_sprocket_teeth), length(back_sprocket_teeth));

% Theoretical top mechanical speed @ max hp and torque rpms
for i = 1:length(front_sprocket_teeth)
    for j = 1:length(back_sprocket_teeth)
        topspeed_torque(i,j) = max_torque_rpm / [(back_sprocket_teeth(j) /
front_sprocket_teeth(i)) * trans_gear_ratio] * tire_circumference * 60 / 5280;
%miles per hour
        topspeed_power(i,j) = max_horsepower_rpm / [(back_sprocket_teeth(j) /
front_sprocket_teeth(i)) * trans_gear_ratio] * tire_circumference * 60 / 5280;
    end
end
figure(1)
heatmap(back_sprocket_teeth, front_sprocket_teeth, topspeed_torque);

```

```

g = -9.801; %m/s^2
vehicle_mass = 250; %kg, rough ballpark
rolling_resistance = 0.02 * vehicle_mass * g * 4; %ballpark standard for fsae
%%%%%%%%%%%%%%%%%%%%%%%%%%%%%%%%%%%%%%%%%%%%%%%%%%%%%%%%%%%%%%%%%%%%%%%%%%%%%%
%%%top speed calculation
for i = 1:length(front_sprocket_teeth)
    for j = 1:length(back_sprocket_teeth)
        torque_tires(i,j) = engine_torque_metric * (back_sprocket_teeth(j) /
front_sprocket_teeth(i)) * trans_gear_ratio;
    end
end
q = tire_power_kW/ (0.5 * air_density * (drag_coeff - rolling_resistance *
lift_coeff));
p = rolling_resistance * vehicle_mass * g / (0.5 * air_density * (drag_coeff -
rolling_resistance * lift_coeff));
topspeed_friction = ((q / 2 + (q^2 / 4 + p^3 / 27)^(1/2))^(1/3) + (q / 2 - (q^2 / 4
+ p^3 / 27)^(1/2))^(1/3)) * 2.236936; %converted to hp at end
correction_factor = topspeed_friction ./ max(topspeed_power,[],'all');
topspeed_corrected = correction_factor .* topspeed_power;
figure(3)
heatmap(back_sprocket_teeth, front_sprocket_teeth, topspeed_corrected);

```

```

%%%%%%%%%%%%%%%%%%%%%%%%%%%%%%%%%%%%%%%%%%%%%%%%%%%%%%%%%%%%%%%%%%%%%%%%
%           Restrictor maximum flow rate calulation
%%%%%%%%%%%%%%%%%%%%%%%%%%%%%%%%%%%%%%%%%%%%%%%%%%%%%%%%%%%%%%%%%%%%%%%%
clc
A=0.00031415; % m^2 x-section at throat
gamma=1.4; % specific heat at 294K
T=300; % Kelvin temp at inlet
P=101325; % Pascal Pressure at inlet
R=287; % gas constant
m=(P*A)/(sqrt(T));
n=(gamma/R)*((2/(gamma+1))^(gamma/(gamma-1)));
m_max=m*(sqrt(n)); %maximum mass flow rate through restrictor (kg/s)
%%%%%%%%%%%%%%%%%%%%%%%%%%%%%%%%%%%%%%%%%%%%%%%%%%%%%%%%%%%%%%%%%%%%%%%% Hp calcs
LHV=44; % low heating value for 93 octane 44-46 MJ/kg
AFR=14.7; %% Air Fuel ratio
eth=0.25; %thermal efficiency
mdotair=NaN; %initializing mdotair
last_mdotair = NaN; %initializing last_mdotair
for HP=30:1:100 %Horsepower
    power=HP*0.0007457;%conversion from horsepower to MegaWatt
    mdotfuel=power/(LHV*eth); %calc mdotfuel
    mdotair=mdotfuel*AFR; % mass flow rate of air

    if mdotair>m_max
        fprintf('Limit reached at %d HP\n',HP);
        fprintf('Last valid mdotair = %.6f kg/s\n', last_mdotair);
        break
    end
    last_mdotair=mdotair;
end
%amount of fuel
fprintf('\n Amount of Fuel\n')
power=75*0.0007457;%conversion from horsepower to MegaWatt
mdotfuel=power/(LHV*eth) %calc mdotfuel [kg/s]
fprintf('Kg/s\n\n')
FOS = 1.1;
Time = 23.15 * 60 * FOS; %1st place time convert to sec * Factor of slowness
fuelInKgs = Time * mdotfuel;
fuelInGal = fuelInKgs * 2.2 /6.3 %gallons
fprintf('Gallons\n')
%{
FSAE fuel tanks typically range from about 5 to 10 liters
(approximately 1.3 to 2.6 US gallons)
%}

```



```

##### Solid Shaft #####
%initialize variables
iter = 1;
d = 2;%mm
%Constants
%material: medium steel
FOS = 1.5; % Factor of safety
Sy = 450e6; % Yield strength of medium steel in MPa
T= 66;%MNm @6,900 RPM
M = T/.3302 * 0.508; %Tangent force in tire (Torque/ 13" overall tire) * lever
arm(20" axle with 3deg shaft misalignment)
%Calcs
StressAllow = Sy/FOS;
dm = d*1e-3; %convert d to m
J = pi()*dm^4/32; %Polar moment of inertia
I = pi()*dm^4/64; %Area moment of inertia
c = dm/2; % Outer radius m
ShearS = T*c/J;
BendingS = M*c/I;
Stress = sqrt(3*ShearS^2+BendingS^2); % Calc Von Mises Stress
while (Stress > StressAllow)
d = d+0.1;
dm= d*1e-3; %m
iter = 1+iter;
J = pi()*dm^4/32; %Polar moment of inertia
I = pi()*dm^4/64; %Area moment of inertia
c = dm/2; % Outer radius m
ShearS = T*c/J;
BendingS = M*c/I;
Stress = sqrt(3*ShearS^2+BendingS^2);
end

```

```

%%%%%%%%%%%%%%%%%%%%%%%%%%%%%%%%%%%%%%%%%%%%%%%%%%%%%%%%%%%%%%%%%%%%%%%%%%%%%%
% Written by: Marshall Fritz %
% Exhaust Runner Length Based on Specific Heat Ratio of Exhaust Gas %
%%%%%%%%%%%%%%%%%%%%%%%%%%%%%%%%%%%%%%%%%%%%%%%%%%%%%%%%%%%%%%%%%%%%%%%%%%%%%%
% Runner Length Calculation %
%%%%%%%%%%%%%%%%%%%%%%%%%%%%%%%%%%%%%%%%%%%%%%%%%%%%%%%%%%%%%%%%%%%%%%%%%%%%%%
% Inputs
T_C = input('Enter exhaust gas temperature [°C] (625-825°C): ');
AFR = input('Enter air-fuel ratio: ');
rpm = input('Enter engine speed [RPM]: ');
T = T_C + 273.15; % Convert to Kelvin
% Stoichiometry
AFR_stoich = 14.7; % Stoichiometric AFR
phi = AFR_stoich / AFR; % Equivalence ratio
% 93 Octain Gasoline Composition
nC = 8; nH = 18;
nO2_stoich = nC + nH/4;
nO2_actual = nO2_stoich / phi;
nN2 = nO2_actual * 3.76;
% Determine combustion products
if phi <= 1
    n_species = [nC, nH/2, nO2_actual-nO2_stoich, nN2, 0]; % [CO2, H2O, O2, N2, CO]
else
    n_species = [nC/phi, nH/2, 0, nN2, nC - nC/phi]; % [CO2, H2O, O2, N2, CO]
end
species = {'CO2','H2O','O2','N2','CO'};
MW = [44.01, 18.02, 32.00, 28.01, 28.01]; % g/mol
% Mole fractions
y = n_species / sum(n_species);
% NASA TP-2002 High-Temp Coefficients
a.CO2 = [3.85746 0.004414 -0.000002215 5.2349e-10 -4.7208e-14];
a.H2O = [3.034 0.002177 -1.641e-07 -9.7042e-11 1.682e-14];
a.O2 = [3.283 0.001483 -7.580e-07 2.095e-10 -2.167e-14];
a.N2 = [2.953 0.001397 -4.926e-07 7.860e-11 -4.608e-15];
a.CO = [3.048 0.001352 -4.858e-07 7.885e-11 -4.698e-15];
R_u = 8.3145; % J/mol·K
% Compute Cp for each species
Cp = zeros(1,5);
for i = 1:5
    coeffs = a.(species{i});
    Cp(i) = R_u * (coeffs(1) + coeffs(2)*T + coeffs(3)*T^2 + coeffs(4)*T^3 + coeffs(5)*T^4);
end
% Mixture Properties
Cp_mix_mol = sum(y .* Cp);
MW_mix = sum(y .* MW);
R_mix = R_u / (MW_mix / 1000); % J/kg·K
Cp_mix_mass = Cp_mix_mol / (MW_mix / 1000);
gamma = Cp_mix_mass / (Cp_mix_mass - R_mix);
% Speed of Sound
a_sound = sqrt(gamma * R_mix * T); % m/s
% Runner Length
a_ft = a_sound * 3.28084; % convert to ft/s
L_in = (a_ft * 120)/rpm; % inches
L_m = L_in * 0.0254; % meters
% Results |
fprintf('Speed of sound: %.1f m/s\n', a_sound);
fprintf('Runner Length: %.4f m\n', L_m);

```

```

%%%%%%%%%%%%%%%%%%%%%%%%%%%%%%%%%%%%%%%%%%%%%%%%%%%%%%%%%%%%%%%%%%%%%%%%
% Written by: Marshall Fritz
% Title: RADIATOR SURFACE AREA BASED ON NTU
%%%%%%%%%%%%%%%%%%%%%%%%%%%%%%%%%%%%%%%%%%%%%%%%%%%%%%%%%%%%%%%%%%%%%%%%
clc; clearvars; close all;
% INPUTS
HP = 70; % Engine power [hp]
GPM = 10; % Coolant flow rate [gal/min]
Tout = 90; % Coolant outlet temperature [°C]
rho_coolant = 980; % Coolant density [kg/m³]
cp_coolant = 4186; % Coolant specific heat [J/kg·K]
percent_heat_to_coolant = 0.30; % Fraction of engine heat removed by coolant
U = 500; % Overall heat-transfer coefficient [W/m²·K]
cp_air = 1030; % Air specific heat [J/kg·K]
rho_air = 1.2; % Air density [kg/m³]
V_air_mph = 55; % Air velocity [mph]
T_air_in_C = 20; % Air inlet temperature [°C]
A_frontal = 0.05; % Frontal area [m²]
tolerance = 1e-6; % Convergence tolerance
max_iter = 100; % Max iterations for area convergence
% UNIT CONVERSIONS
V_air = V_air_mph * 0.44704; % mph → m/s
T_air_in = T_air_in_C + 273.15; % °C → K
% COOLANT MOTOR INLET TEMPERATURE
Q_motor = HP * 745.7 * percent_heat_to_coolant; % Heat rejected to coolant [W]
V_dot = GPM * 3.78541e-3 / 60; % Coolant volumetric flow [m³/s]
mdot_coolant = rho_coolant * V_dot; % Coolant mass flow [kg/s]
T_coolant_in = Tout - Q_motor / (mdot_coolant * cp_coolant);
% HEAT EXCHANGER LOOP
T_hot_in = Tout + 273.15; % Coolant out (hot) in K
T_hot_out = T_coolant_in + 273.15; % Coolant in (cold) in K
A_heat = 1.0; % Initial guess [m²]
mdot_air = rho_air * V_air * A_frontal; % Air mass flow [kg/s]
for iter = 1:max_iter
    % Heat capacity rates
    C_h = mdot_coolant * cp_coolant;
    C_c = mdot_air * cp_air;
    % which is Cmin/Cmax
    if C_h <= C_c
        C_min = C_h; C_max = C_c;
        flip = false; % coolant = Cmin
    else
        C_min = C_c; C_max = C_h;
        flip = true; % air = Cmin
    end
    C_r = C_min / C_max;
    % Actual and maximum possible heat transfer
    Q = C_h * (T_hot_in - T_hot_out);
    Q_max = C_min * (T_hot_in - T_air_in);
    epsilon = Q / Q_max;
    % Compute NTU
    if ~flip

```

```

    % Case: Cmax mixed, Cmin unmixed
    inner = 1 - epsilon * C_r;
    arg = 1 + (1 / C_r) * log(inner);
    if inner <= 0 || arg <= 0
        warning('Invalid epsilon/Cr combination; using small-Cr approx.');
```

$$NTU = -\log(1 - \epsilon); \quad \% \text{ fallback}$$

```

    else
        NTU = -log(arg);
    end
else
    % Case: Cmin mixed, Cmax unmixed
    term = 1 + C_r * log(1 - epsilon);
    if term <= 0
        warning('Invalid epsilon/Cr combination; using small-Cr approx.');
```

$$NTU = -\log(1 - \epsilon);$$

```

    else
        NTU = -(1 / C_r) * log(term);
    end
end
% Update heat transfer surface area
A_new = NTU * C_min / U;

if abs(A_new - A_heat) < tolerance
    A_heat = A_new;
    break;
end
A_heat = A_new;
end
% 5. OUTPUT RESULTS
% fprintf('\nHeat Exchanger Design Results\n');
% fprintf('Cmin = %.2f W/K, Cmax = %.2f W/K\n', C_min, C_max);
% fprintf('Flip occurred: %d (1 = yes, 0 = no)\n', flip);
% fprintf('Heat exchanger effectiveness: %.4f\n', epsilon);
% fprintf('NTU: %.4f\n', NTU);
% fprintf('Air mass flow rate: %.4f kg/s\n', mdot_air);
fprintf('Required heat transfer area: %.4f m²\n', A_heat);
% fprintf('Frontal area used for airflow: %.4f m²\n', A_frontal);

```